GENETIC NETWORK REGULATING VARIATION IN VEGETATIVE PHASE CHANGE IN MAIZE

BY

WEI ZHANG

DISSERTATION

Submitted in partial fulfillment of the requirements
for the degree of Doctor of Philosophy in Biology
with a concentration in Physiological and Molecular Plant Biology
in the Graduate College of the
University of Illinois at Urbana-Champaign, 2010

Urbana, Illinois

Doctoral Committee:

Associate Professor Stephen P. Moose, Chair
Associate Professor Matthew E. Hudson
Professor Lila O. Vodkin
Professor Mary A. Schuler

Abstract

Vegetative phase change in maize is characterized by the transition from waxy juvenile leaves to pubescent, glossy adult leaves. In maize, mutants that alter the timing of vegetative phase change are valuable resources to identify the responsible factors. Also, continuous variation of leaf identity traits in diverse genetic mapping populations indicates the feasibility to use quantitative trait locus (QTL) analyses to find underlying genes.

I demonstrate here that *Glossy15 (Gl15)* is the most important gene controlling leaf identity traits in maize. Decreased level of *Gl15* mRNA in various *gl15* mutant alleles promoted the transition from juvenile to adult leaf identity in all genetic backgrounds tested. Additionally, the *Gl15* gene appears as the most significant QTL for leaf identity traits in multiple genetic mapping populations, where variation in both its DNA sequence and mRNA expression could explain phenotypic differences among population of diverse maize inbred lines.

Building on studies of the genetic network controlling vegetative phase change in the model plant species Arabidopsis, *microRNA156* (*miR156*) and its target the SQUAMOSA PROMOTER BINDIND LIKE PROTEIN (SPL) genes also control leaf identity traits in maize. The *miR156g* and SBP_5 genes are found within other large-effect QTLs that controlling leaf identity traits, and the relative expression levels of these genes correlates with the timing of vegetative phase change. The unique and easily visible leaf identity traits in maize offer advantages to characterizing the effects of many other regulators as well. I found that the activities of GAs, an upstream component of the genetic network regulating vegetative phase change, promote adult leaf identity by

influencing the antagonistic interactions of *miR156* and *miR172;* whereas *Gl15* conditions changes in epicuticular wax composition between juvenile and adult leaves by activating aldehyde reductase and suppressing aldehyde decarbonylase.

Acknowledgements

I would like to take this opportunity to thank many people who gave me guidance, support, help and assistance during my study here in University of Illinois at Urbana.

First, I wish to thank my advisor, Dr. Stephen P. Moose, for inspiring me with bright ideas and encouraging me with his future vision and positive feedbacks. He shows the example of a passionate and diligent scientist; a patient, knowledgeable and supporting mentor. I hope I could become a professor like him in the future. I also thank to my thesis committee Dr. Matthew E. Hudson, Dr. Lila O. Vodkin and Dr. Mary A. Shuler for their advices and support in my research and future career development.

I also thank Prof. Hans J. Bohnert for his always willingness to talk to me and give me ideas. I am very grateful to Shawn Carlson, Prof. Jack Widholm, Weiqun Zhang and many other people who have given me help and assistance in plant transformation.

My project would not be finished without the excellent support and assistance from many people. Han Zhao and Yuhe Liu were extremely helpful in QTL analysis and marker design. I am also grateful to Jeff Church and Devin Nichols for advice with quantitative PCR analysis and for not getting bothered by a starter in the lab. I am indebted to Micheal Zinder, Marti Schneerman and Ellen Taylor for making lab and field work organized, and for their readily assistance when needed. I would like to acknowledge Wes Barber, Kranthi Varala and Ying Li for collaborating with small RNA sequencing analysis. I also thank Jing Lu and many other undergraduates who helped and assisted lab and field work.

I appreciate the friendship and moral support of Yinghong Pan, Ying Yin, Anton Arkhipov, Han Zhao, Tongfei Wang and Xia Wu, they made weekends and holidays meaningful. Best wishes to all of them.

I thank my parents and siblings for supporting all of my endeavors, past and present, without which I would never have attained this degree.

The last but the most important, I would like to express my gratitude to my husband Yu Fu for his sharing happiness and sadness, for encouraging during difficulties, for planning ahead and working hard for our future, and for giving endless love and support for my study.

Table of Contents

Chapter 1: Introduction and literature review……. 1

Chapter 2: Leaf identity mutants and the genetic network of vegetative phase change…….. 29

Chapter 3: Expression variation for genes regulating vegetative phase change mediates quantitative inheritance of the transition from juvenile to adult leaf identity in maize…...……... 80

Chapter 4: Sequence and expression variation of *Glossy15* and *miR156* among diverse maize inbred lines…….…… 119

Chapter 5: Transcriptome profiling comparisons of *gl15* mutant and wildtype shoot apices reveals potential downstream target genes of *Glossy15*…….. 142

Chapter 1:

Introduction and literature review

Plant shoot development is usually divided into vegetative and reproductive stages based on the capability of the shoot apical meristem for reproductive development. During the vegetative growth, many plant species produce juvenile and adult leaves that differ in a series of leaf identity characteristics. In Arabidopsis, adult leaves are bigger and elliptical compared to juvenile leaves, and possess serrated margins, higher photosynthetic efficiency and abaxial trichomes (Telfer et al., 1997 and Tanya et al., 2001). Maize (*Zea mays L.*), juvenile and adult leaf differ for a variety of traits which are summarized in Figure 1 (Poethig 1990, Moose and Sisco, 1994). The biochemical composition of juvenile epicuticular waxes gives these leaves a blue-gray appearance (Bianchi and Salamini, 1979), whereas adult leaves are glossy and green. Changes in cell wall composition of leaf epidermal cells is revealed by histochemical stains such as toluidine blue, which stains juvenile leaves purple and adult leaves blue. Adult leaves also produce specialized cell types such as bulliform cells and macrohairs. The transition from juvenile to adult leaf identity is the defining feature of vegetative phase change, which typically occurs following the production of six to eight juvenile leaves in maize.

Studies in trees, Arabidopsis, maize and other plants revealed that many of these leaf identity traits contribute to tolerance of environmental stresses and resistance to disease, insect pests, and herbivory (Kearsley and Whitham, 1989; Eigenbrode and Espelie, 1995; Abedon and Tracy, 1996; Williams et al., 2000, Riederman et al., 2008;

Riederman and Tracy, 2010). Thus, leaf identity traits contribute to environmental adaptation in natural populations and the performance of improved crop varieties (Brooks et al., 2005, Chandler et al., 2007b, Basso et al., 2008). In maize, the onset of adult leaf identity was shown to be correlated with flowering time, but was not strongly associated with other agronomic traits (Abedon et al., 1996).

Maize mutants that affect vegetative phase change

Molecular genetic studies of vegetative phase change have focused primarily on maize and Arabidopsis, due to the presence of distinct phenotypes for the juvenile and adult phases, mutations that alter the expression of phase-specific phenotypes, and the advantages of these two model plant systems for the isolation and functional analysis of genes. Mutations have been characterized in both Arabidopsis and maize that alter the relative timing and/or position of vegetative phase change, and some of these genes have been cloned. Figure 1 illustrates the phenotypic effects of the maize mutations that affect vegetative phase change.

Genes that specify or maintain juvenile development were first identified in maize and demonstrated that vegetative phase change is under genetic control. *Corngrass1* (*Cg1*), *Teopod1* (*Tp1*) and *Teopod2* (*Tp2*) are semi-dominant, gain-of-function mutations that each prolong the expression of the juvenile traits and slightly delay the onset of adult traits, indicating these genes act to promote juvenility (Galinat, 1966; Poethig, 1988). Each of these mutations produce narrow leaves, increase the number of nodes with tillers and prop roots, delay vegetative phase change, and condition the expression of vegetative characters in the inflorescence.

The *GLOSSY15 (Gl15*) gene plays a key role in specifying juvenile leaf identity. The *glossy15 (gl15)* mutation was initially described for its glossy leaf phenotype due to reduced production of juvenile leaf wax (Bianchi and Marchesi, 1960). It was subsequently found that *gl15* mutations condition the expression of other adult leaf identity traits beginning with the third leaf, but have no effect on reproductive development or other vegetative phase-transition traits (Evans et al., 1994; Moose and Sisco, 1994, Fig. 1). Analysis of a transposon-induced mutable allele of *gl15* demonstrated that *Gl15* acts to both coordinately activate juvenile and suppress adult leaf identity traits in a cell-autonomous manner. The *Gl15* gene encodes a putative transcription factor that belongs to the small sub-family of proteins that contain two APETALA2 domains, among which AINTEGUMENTA from Arabidopsis has been shown to bind DNA (Nole-Wilson and Krizek, 2001). *Gl15* mRNA expression is normally limited to juvenile leaves and the juvenile shoot apex (Moose and Sisco, 1996; Lauter et al. 2005). Transgenic maize lines with increased *Gl15* expression under the control of its native flanking sequences (*Gl15-TG*) complemented the *gl15* mutant phenotype and also increased the number of juvenile leaves, total nodes and days to flowering (Lauter et al., 2005).

The plant hormones GA and ABA regulate the transition from juvenile to adult leaf identity

The gibberellin (GA) class of phytohormones is one group of mobile factors that regulate leaf identity. Exogenous application of GA modulates vegetative phase change and flowering time in a number of plant species (Rogler and Hackett, 1975; Zimmerman

et al., 1985). GAs promote the precocious appearance of abaxial trichomes in Arabidopsis (Telfer et al., 1997) and mutations that are defective in either GA biosynthesis or perception delay the appearance of adult leaf identity in both Arabidopsis and maize (Telfer et al., 1997; Evans and Poethig, 1995). For example, mutation of the *dwarf1* (*d1*) gene required for GA biogenesis in maize (Spray et al., 1996) increases the number of leaves with juvenile traits and greatly reduces stem elongation, both of which can be reversed by exogenous GA application. GA application could also partially restore the *Teopod* phenotypes.

The action of GA is often antagonized by ABA, and mutations in the maize VIVIPAROUS8 (VP8) gene, which reduces ABA levels in developing embryos, also delay vegetative phase change (Evans and Poethig, 1997). The *VP8* gene encodes a putative peptidase most closely related to the Arabidopsis *ALTERED MERISTEM PROGRAM1* (*AMP1*) gene (Suzuki et al., 2008), mutations in which also affect vegetative phase change in Arabidopsis (Conway and Poethig, 1997).

Combining the *glossy15* mutation with each of the *Cg1, Tp1*, *Tp2 and d1* mutations led to the production of adult leaf epidermal traits beginning with leaf three, but did not influence other vegetative phase change characters such as leaf shape or the formation of tillers. These results show that *Glossy15* acts in the same genetic pathway, but downstream of *Cg1, Tp1*, *Tp2* and *d1* (Moose and Sisco, 1994). Further evidence for the downstream role of *Glossy15* is obtained when the gain-of-function *Gl15-TG* is crossed with each of the *Cg1, Tp1, Tp2, d1* and *early phase change1* (*epc1*) mutant backgrounds, which increases the number of leaves with juvenile leaf epidermal traits (Kampani, 2003).

Genes controlling small RNA biogenesis or function are important for vegetative phase change

Many of the Arabidopsis genes identified through mutant screens for accelerated vegetative phase change affect small RNA biogenesis and metabolism. The HASTY (HST) gene encodes the Arabidopsis exportin5/MSN5 protein that functions in export of pre-microRNAs from the nucleus to the cytoplasm, and mutation of HASTY accelerates vegetative phase change and alters shoot meristem size (Bollman et al., 2003; Park et al., 2005). Similarly, the EARLY PHASE CHANGE (*epc1)* mutation, which is the presumed maize ortholog of *HST*, reduces the number of juvenile but not adult leaves and exhibits pleiotropic effects on shoot meristem maintenance (Vega et al., 2002).

Loss of function mutations in SQUINT (SQN) also reduces the number of juvenile leaves without influencing flowering time. The SQUINT gene product is a cyclophilin40 protein that is conserved among mammals, yeast and Arabidopsis, and was recently shown to reduce the activity of ARGONAUTE1 (AGO1) (Berardini et al., 2001; Smith et al., 2009). AGO1 is a well known factor that associates with and mediates the biochemical activities of microRNAs and small interfering RNAs on their mRNA targets (Chen, 2009).

Mutation at ZIPPY, an Argonaute7 protein, causes premature appearance of adult leaf identity, but not reproductive competence of flowering time, indicating the role of normal ZIPPY is to maintain juvenility (Hunter et al., 2003). Similarly, mutations in the RNA-DEPENDENT POLYMERASE6(*rdr6*) and SUPPRESSOR OF GENE SILENCING3 (*sgs3*) genes also condition early adult leaves, both proteins function in post-transcriptional gene silencing via siRNAs (Peragine et al., 2004). In addition,

mutation at DICER LIKE 4 (DCL4) lacks 21-nt trans-acting siRNAs and possesses elevated levels of their targets, and exhibits accelerated vegetative phase change phenotypes that are similar to those observed in *rdr6* mutants (Xie et al., 2005). Phenotypic and molecular analysis indicates that mutations at *SGS3, RDR6, AGO7* or *HST* have higher levels of *miR166*, suggesting they act in the same developmental pathway (Peragine et al., 2004 and Xu et al., 2006).

The above mutant studies in Arabidopsis and maize suggest that microRNAs or trans-acting small interfering RNAs regulate key aspects of vegetative phase change (reviewed in Willmann and Poethig, 2005). The importance of trans-acting small RNA is validated through studies of mutant screens that could counteract the *zippy* mutation, which found the trans-acting siRNA *TAS3* could reduce the expression of auxin-related transcription factors ARF3 and ARF4 (Hunter et al., 2006) and suppress the juvenile to adult transition. Production of *TAS3*, is dependent on *microRNA390* (Axtell et al., 2006), *AGO7, RDR6* and *DCL4* (Fahlgren et al., 2006).

miR172 and miR156 are important for vegetative phase change

An important regulatory role for specific miRNAs in promoting phase change was first documented in Arabidopsis for *miR172* (Aukerman et al., 2003). *MiR172* expression progressively increases during vegetative shoot development to promote flowering, via complementary binding to mRNAs of APETALA2 (AP2)-like genes such as *TOE1, TOE2, APETALA2, SMZ* and *SNZ* (Aukerman et al., 2003; Chen, 2004; Schmid et al., 2003, Mathieu et al., 2009). The interactions between *miR172* and its AP2-like targets appear to be highly conserved between Arabidopsis and maize,

because both species contain five *miR172* loci that could produce mature *miR172*. The maize genome contains four dual AP2-domain genes that contain predicted *miR172* target sites, including *Glossy15* (Moose et al., 1996). *MiR172* downregulates the expression of *Gl15* transcripts to promote adult leaf identity (Lauter et al., 2005). The onset of detectable *miR172* expression corresponds to the period when *Gl15* mRNA expression declines, the first adult leaves are initiated, and their identity is specified (Orkwiszewski and Poethig, 2000).

Two other AP2-like genes in maize, *INDETERMINATE SPIKELET1 (IDS1)* and its close relative *SISTER OF INDETERMINATE SPIKELET1 (SID1)* regulate the determinacy of spikelet pair meristems in the inflorescence meristem and floral organ identity. The functional importance of *miR172* in regulating *IDS1* and *SID1* is illustrated by the *tasselseed4* mutation where expression of miR172e is reduced, which phenocopies the *Tasselseed6* mutation in the *miR172* binding site of *IDS1* (Chuck et al., 2007, Chuck et al., 2008). In both of the tasselseed mutations, carpels develop in the tassels and inflorescence branching increases due to loss of determinacy in spikelet pair meristems. Altered regulation of expression for *Rap2.7,* another AP2-like gene from maize, appears to control a major QTL for flowering time, which is confirmed by delayed flowering in transgenic lines that overexpress *Rap2.7* and early flowering in RNAi lines that target *Rap2.7* (Salvi et al., 2007).

MiR172 has also been shown to be involved in the photoperiodic induction of flowering in Arabidopsis (Jung et al., 2007) and control of tuber growth in potato (Martin et al., 2009). Photoperiod is sensed through the light receptor protein phytochrome B, and in both Arabidopsis and potato, *miR172* expression is increased in *phyB* mutants

relative to wild-type plants. Genetic analyses place miR172 downstream of GIGANTEA, upstream of FLOWERING LOCUS T and independent of CONSTANS in the Arabidopsis regulatory network for flowering time (Jung et al., 2007). In potato, *miR172* works downstream of PHYB and upstream of BEL5, both of which are well known factors for photoperiodic responses (Martin et al., 2009).

In contrast to *miR172* that promotes phase change, *miR156* functions to delay both vegetative and reproductive phase change by repressing expression of SQUAMOSA BINDING PROTEIN-LIKE (SPL) genes. SPL proteins interact with promoter elements in MADS-box genes such as *SQUAMOSA* from *Antirrhinum* and *APETALA1* of Arabidopsis. In Arabidopsis, 10 of the 16 *SPLs* were predicted (Rhoades et al., 2002) and later validated to be *miR156* targets via their target mRNA cleavage and their inverse transcription pattern relative to *miR156*: *SPL2, SPL3, SPL4, SPL5, SPL6, SPL9, SPL10, SPL11, SPL13 and SPL15* (Wu and Poethig, 2006, Schwarz et al., 2008, Wang et al., 2008, Wu et al., 2009, Shikata et al., 2009, Usami et al., 2009). The 10 *SPLs* regulated by *miR156* how largely overlapping expression levels and patterns that is consistent with their genetic redundancy in controlling shoot maturation; however, specific phenotypic effects of mutations in individual SPL genes or mutant combinations are also observed (Wang et al., 2009). The *SPL3/4/5* appear to be more important in regulating both vegetative phase change and flowering time (Wu and Poethig, 2006). The*SPL10/11/2* genes influence lateral organ development throughout shoot maturation, mutation of these three genes leads to more trichomes on cauline leaves and flowers (Shikata et al., 2009). The*SPL9/15* genes affect plastochron (leaf initiation rate) length, with the *SPL15* mutation in Arabidopsis also increasing cell number and

reducing cell size (Wang et al., 2009 and Usami et al., 2009). In Arabidopsis, *miR156* overexpression results in delayed vegetative phase change and flowering time (Wu and Poethig, 2006), whereas titration of *miR156* by an artificial microRNA promotes the onset of adult traits (Wang et al., 2008 and Wu et al., 2009).

The *miR156-SPLs* regulatory pathway appears to be evolutionarily conserved in monocot grasses. In domesticated rice, *miR156b/c* activity contributes to its bushy grass phenotype and juvenile leaf identity (Wang et al., 2007); overexpression of *miR156b* gives rice more tillers and late flowering (Xie et al., 2006). The SPL family has expanded from 13 genes in Arabidopsis to 19 genes in the rice genome, and 13 of them (*OsSPL2, OsSPL3, OsSPL4, OsSPL7, OsSPL11, OsSPL12, OsSPL13, OsSPL14, OsSPL16, OsSPL17, OsSPL18*) harbor a *miR156* target site (Xie et al., 2006). Recently, the rice*OsSPL14* gene has been shown to be the basis for the strongest QTL for panicle branching and tiller number, which are important agronomic traits in rice (Jiao et al., 2010 and Miura et al., 2010).

The maize *Cg1* mutation greatly delays vegetative phase change, is highly tillered with a bushy phenotype, and harbors inflorescence abnormalities. The *Cg1* mutation overexpresses *miR156* due to the insertion of a retrotransposon in the upstream region of *miRNA156b/c.* In addition, transgenic maize plants overexpressing *miR156b/c* controlled by the CaMV35S promoter exhibit the *Cg1* phenotype (Chuck et al., 2007a). In maize, at least 13 *SPL* genes are predicted to be targeted by *miR156* (Chuck et al., 2007), mutations in two of these maize *SPL* genes have been characterized. The *teosinte glume architecture1* (*tga1*) gene is critical for glume growth, lignification, and silica deposition (Wang *et al.*, 2005), and *TGA1* expression is

repressed in the *Cg1* mutant that overexpresses *miR156* (Chuck et al.,2007). The *tasselsheath4* (*tsh4*) locus encodes another *SPL* gene that regulates bract development and establishes meristem boundaries, based on the phenotype of *tsh4* mutants that cause altered phyllotaxy, fewer lateral meristems and the production of ectopic leaves at the expense of meristems. Expression analysis indicates that the *Tsh4* gene is expressed at the base of lateral meristems in a pattern that is complementary to that observed for *miR156* (Chuck et al., 2010).

The complementary expression patterns of *miR156* and *miR172* during both Arabidopsis and maize shoot development, as well as their opposing effects on the timing of vegetative phase change, indicates these two miRNAs might be working in the same regulatory pathway. *MiR156* mainly controls juvenile leaf identity and expresses at very early stages in vegetative growth, whereas *miR172* expression is higher in adult leaves and is repressed by overexpressing *miR156* (Wu and Poethig, 2006; Chuck et al., 2007). Research in Arabidopsis recently showed that SPL9/10 proteins are key to the interaction between these two miRNAs: SPL9/10 could bind promoter regions in *miR172b*, and promote the transcription of *pre-miR172b* and the mature *miR172* level (Wu et al., 2009). Recently, researchers were able to demonstrate that feedback regulation is involved in both the *miR172-AP2* and *miR156-SPL* interactions, via the binding of AP2 and SPL proteins to the regulatory regions of that encode them (Mathieu et al., 2009, Wu et al., 2009). The above findings suggest a number of complex interactions influence the regulation of shoot maturation via *miR156* and *miR172*.

Another maize miRNA related to *miR156, miR529,* (Zhang et al., 2009), shares 14-16 nucleotides of homology with *miR156* and is highly expressed in tassels, whereas

miR156 mainly expresses in juvenile shoots. Target prediction analysis indicates that both *miR156* and *miR529* target *SPL* genes (Zhang et al., 2009), which was validated through 1) cleavage analysis by 5'RACE and 2) complementary pattern of *miR156/miR529* with the SPL gene *TSH4* (Chuck et al., 2010). Although both miRNAs target SPLs, *miR156* mainly functions in vegetative phase change and *miR529* mainly functions in tassel development (Zhang et al., 2009 and Chuck et al., 2010).

Maize genes that specify leaf identity traits

The most visually obvious trait that distinguishes juvenile from adult leaf identity in maize is the production of leaf epicuticular waxes. Juvenile leaves exhibit a blue-gray coating of epicuticular wax that is lost upon transition to the adult phase (Fig. 1). Adult leaves thus appear shiny or "glossy". A total of 18 distinct genetic loci have been identified where mutations interfere with juvenile epicuticular wax production, leading to a glossy seedling leaf phenotype (reviewed in Schnable et al., 1994). Comparisons of biochemical changes in leaf wax production among maize *glossy* mutants and wild-type seedlings, as well as the analogous *eceriferum* (*cer*) mutations in Arabidopsis and barley, have established a general pathway for epicuticular wax production in plants. Fatty acid precursors (18 carbons in length, C_{18}) are sequentially elongated in 2-carbon steps to very long chain fatty acids ($>C_{24}$) that can subsequently be reduced to aldehydes then alcohols, decarbonylated to alkanes, or conjugated to alcohols to form wax esters (reviewed in Avato, 1987; Samuels et al., 2008). Maize juvenile leaves produce a greater amount of wax relative to adult leaves, which consists nearly entirely of the C_{32} primary alcohol dotriacontanol (Bianchi et al., 1984; Blaker and Greyson,

1988). In contrast, adult leaf wax is a complex mixture of alkanes and esters. Many of the maize *glossy* mutants can be placed at defined steps within the wax biosynthetic pathway, and at least four of these genes have been cloned. *Glossy1* encodes a putative membrane-bound decarbonylase (Sturaro et al., 2005) and *Glossy8* a beta-keto acyl reductase/elongase (Xu et al., 1997; Xu et al., 2002). *Glossy2* is homologous to the Arabidopsis CER2 acyltransferase, which is required for the C_{30}-C_{32} elongation step. Glossy4 was recently cloned, this gene shares 60% similarity to Arabidopsis CUT1 gene (Liu et al., 2009), which encodes a condensing enzyme involved in the synthesis of very- long-chain fatty acids (Miller et al., 1999).

A distinguishing feature of maize adult leaves is the formation of a number of specialized cell types, the most prominent being the visible macrohairs. The *macrohairless1 (mhl1)* mutation specifically blocks macrohair initiation in the leaf blade (Moose et al., 2004). Double mutant analysis with *dwarf1* and *gl15*, which maps only 5cM from *mhl1*, demonstrated that *mhl1* acts downstream of these genes, suggesting that the *MHL1* gene product is likely to be repressed by *Gl15* and stimulated by GAs.

Juvenile and adult maize leaves also differ in the staining reaction of epidermal cells with toluidine blue. Juvenile epidermal cells stain purple, whereas adult cells stain blue. These staining differences are believed to reflect biochemical differences in cell wall composition, most likely resulting from the higher degree of transesterification among glucoarabinoxylans in adult compared to juvenile leaves (Moose, 1994). Genetic screens conducted by the Moose laboratory have identified the *epidermal cell wall1(ecw1)* mutation, which causes adult leaf epidermal cells to stain violet instead of aqua with toluidine blue without altering the expression of leaf waxes or hairs. A second

transposon-induced allele of *ecw1* has been characterized by Guri Johal's laboratory at Purdue University, which they have named *Corn rootworm sensitive1* (*Crs1*) because of the associated phenotype of increase susceptibility to leaf feeding by insects such as the corn rootworm beetle (*Diabrotica* spp.).

Quantitative trait variation for vegetative leaf identities

Beyond the mutant screens for altered timing or patterns of leaf identity traits, the number of leaves expressing juvenile leaf waxes and adult macrohairs also varies as a quantitative trait in maize populations (e.g., Revilla et al., 2000 and 2002). Divergent phenotypic selection for the number of leaves with visible epicuticular wax was effective in producing genotypes with early or late transitions from juvenile to adult leaf identity (Revilla et al., 2002). Moreover, vegetative phase change related traits show significant additive variance, high heritability (>65%) and limited interaction with environment (Revilla et al., 2004). The quantitative nature and the high heritability of phase transition traits suggest that quantitative trait loci (QTL) mapping approaches may offer insights into the regulation of leaf identity phenotypes. Chandler and Tracy (2007) recently used a sweet corn population of 130 S_3 lines to identify a single significant QTL controlling the first leaf with adult glossy and the last leaf with juvenile wax, which mapped to the genomic region on chromosome 9 containing *Glossy15*.

The development and use of a high resolution genetic map for maize using the intermated B73×Mo17 recombinant inbred lines (IBMRILs) population (Lee et al., 2002; Sharopava et al., 2002) has made QTL mapping a viable tool for gene discovery. The IBMRILs are a high resolution mapping population developed by crossing B73 and

Mo17, followed by 4 cycles of random mating to increase the potential for recombination before developing inbred lines (Lee et al., 2002). The IBMRILs have become the premier resource for genetic mapping in maize. The genetic map contains over 3000 markers, including 1051 novel simple sequence repeat (SSR) markers developed by the Missouri Maize Project (Sharapova et al., 2002) and 1329 novel indel polymorphism (IDP) markers developed by the Schnable laboratory at Iowa State University (Fu et al., 2006). Balint-Kurti et al. (2007) mapped QTL for resistance to southern leaf blight in both the IBMRILs population and a conventional recombinant inbred line population derived from the same parents, B73 and Mo17. They found that for the QTL detected in both populations, the IBMRILs population provided between 5 and 50 times greater resolution in the position of the QTL than the conventional population.

The Moose laboratory has used the IBMRILs population to quantitatively map genes for nitrogen use efficiency (Nichols, 2008), shoot maturation traits (Lauter et al., 2008) and leaf identity traits (Lauter et al., unpublished). Four major QTLs controlling shoot maturation in the IBMRILs have been identified using composite interval mapping and three years of replicated phenotypic data (Lauter et al., 2008). The same study also found four significant QTLs controlling either the first leaf producing macrohairs or the last leaf expressing juvenile wax, three of which were coincident. Each of the three major effect QTLs controlling both juvenile wax and adult macrohair production are localized to small chromosomal intervals that contain candidate genes expected to influence vegetative phase change.

The Moose laboratory has also developed the NC61 X W23 recombinant inbred mapping population. The parental lines NC61 and W23 exhibit extreme and distinctive

phenotypes for the timing of vegetative phase change, with W23 showing adult macrohairs at leaf three, whereas NC61 producing adult macrohairs beginning with leaf eight and juvenile waxes through leaf 12. Although the IBMRILs could provide higher genetic mapping resolution in maize, NC61 and W23 may offer a broader distribution of phenotypes and potentially stronger allelic effects that may facilitate detection of QTLs controlling leaf identity.

Maize core collection of diversity inbreds

QTL analysis to study quantitative trait usually only considers variation among offspring of relatively few genotypes and relies solely on recombination events observed in their progeny, only allelic variation in parental genotypes can be evaluated. Association mapping is an alternative approach to characterize the genetic architecture and genomic loci affecting phenotypic traits. Association mapping in maize typically considers t both the population structure and the linear association of allelic variation with phenotypic variation (Flint-Garcia et al., 2005, Yu et al., 2006). The success of association mapping is based on capturing as many genotypes as possible for the tested locus. Molecular markers such as restriction length polymorphisms (RFLPs), simple sequence repeats (SSRs) or microsatellites were widely used to estimate the relationship among a large collection of diverse inbred lines. Core sets of maize inbred lines representing the maximum proportion of diversity observed in the larger collection were found through marker analysis, which greatly reduces the number of lines required to achieve adequate sampling of alleles (Liu et al., 2003 and Yan et al., 2009). In one study, 94 microsatellite markers were used to capture 2039 alleles in 260 temperate

lines that represent much of the genetic diversity for important public temperate and some tropical germplasm sources, and a set of 25 core inbreds were identified to represent 80% of the allelic variation found among the original 260 lines (Liu et al., 2003). Single nucleotide polymorphisms (SNPs) may also be used to estimate genetic diversity, although their information content is about ten-fold lower compared to SSRs (Yu et al., 2009). A recent study to estimate relationships among inbreds using 1229 SNP markers generated1794 haplotypes within 327 loci which confirm the results of Liu et al., (2003), where the 25 core inbreds plus B73 and Mo17 captured 74.6% of all haplotypes (Yan et al., 2009). Thus, these 25 core inbred lines are appropriate to estimate allelic variations in all maize lines (25 core inbred lines are listed in Liu et al., 2003 and Yan et al., 2009).

Wider use of the core set of diverse maize inbreds was made possible by the development of Nested Association Mapping (NAM) populations, where each of the core inbreds were crossed with B73 to create a target population of 200 recombinant inbred lines, 3875 recombinant inbred lines were generated in total. The NAM population is designed to integrate the genetic diversity of the core set of inbred lines and the power of traditional linkage-based QTL analysis (Buckler et al., 2009).

microRNA quantification in plants

Since the importance of plant and animal microRNAs were discovered at the end of last century, the biogenesis of miRNAs are extensively studied in several research groups. Now many aspects of the miRNA biogenesis pathway are clear. In plants, miRNAs are usually transcribed by RNA polymerase II from intergenic regions; this

mRNA is called the primary miRNA (pri-miRNA). pri-miRNAs are processed by several proteins and cleaved into a stem-loop structure named pre-miRNAs, the loops of pre-miRNAs are then further processed to release the miRNA/miRNA* duplex. The miRNA/miRNA* are exported to the cytoplasm by HASTY, then methylated by HEN1. The functional strand from the miRNA/miRNA* is called the mature miRNA and is then incorporated by AGO protein to provide a guide function targeting specific mRNAs (reviewed by Voinnet, 2009 and Chen, 2009).

The mature miRNAs that are abundant in plant tissues are usually generated from more than one locus. Mature *miR156* accumulation in maize is potentially derived from 13 *miR156* loci and *miRNA172* from 5 loci (www.mirbase.org). Each of the miRNA loci could be transcribed differently in tissues and developmental stages, but the functional effect is through the accumulated mature miRNAs. An effective method to quantify mature miRNAs is through hybridization of Locked Nucleic Acid (LNA) probes to RNA-gel blots (Exiqon life sciences). LNA is defined as oligonucleotides containing at least one LNA monomer (2‘-*O*, 4‘-*C*-methylene-*β*-D-ribofuranosyl nucleotide). The sensitivity of the LNA modified probes in miRNA northern blots is increased dramatically in comparison to traditional miRNA probes, while simultaneously being very specific (Valoczi et al., 2004 and Varallyay et al., 2008).

Tracking the locus-specific effects of individual miRNAs can also be achieved by treating the pri-miRNAs as a regular mRNA, which may be detected through reverse transcription-PCR (RT-PCR); however, the detection of pri-miRNAs is complicated by their unstable nature and relatively lower expression levels (e.g., Schmittgen et al., 2004). Mature miRNAs are more stable and more abundant, but their small size

requires modification to established RT-PCR protocols. One such modification involves the initial addition of adaptors of known sequence to the end of the miRNAs, followed by amplification with a miRNA specific forward primer and adaptor-specific reverse primers to detect the abundance of miRNAs (Shi and Chiang, 2005). This method works well with animal but not plant miRNAs, because plant miRNAs are often methylated at their 3' hydroxyl groups (Yang et al., 2006) and thus not competent for adaptor ligation. Ambion (now part of Applied Biosystems) developed the stem-loop RT-PCR method to detect mature miRNAs, where an oligonucleotide which could form a stem-loop structure itself and part of it is complementary to the 3'portion of the miRNA is annealed to miRNAs, which is then amplified by primers specific to the 5' end of the miRNA and specific to the stem loop (Chen et al., 2005).

The concept of miRNA target mimics in plants and miRNA sponge in animals

The fact that mature miRNAs often derive from multiple genome loci and have functional redundancy makes it difficult to create genetic knockouts for miRNA, for example, all of the 11 *miR156* appear to be highly expressed in juvenile shoots in maize (Zhang et al., 2009). In mammalian systems, *C. elegans* and *Drosophila*, transfection of cell cultures with chemically modified antisense locked nucleic acid (LNA) oligonucleotides have been used to characterize effects of transient depletion of miRNAs (Cheng et al., 2007, Horwich et al., 2008, Hutbagner et al., 2004, Meister et al., 2004, Orom et al., 2006). However, this method is not useful for the study of plant shoot maturation, since the shoot development is a gradual tissue and organ-level process

In mammalian cells, artificial miRNA binding sites named “miRNA sponges” have been designed and delivered to cells to sequester miRNAs via competitive hybridization. The artificial miRNA binding site was designed by introducing several mismatches in the middle of the complementary sequence, thus producing a bubble when pairing with miRNAs. By introducing this artificial miRNA sponge, miRNA level could be reduced by several times compared to control (Ebert et al., 2007).

Franco-Zorrilla et al. (2007) found that a similar sequestration mechanism operates in Arabidopsis: a non-protein coding RNA called *IPS1* could sequester phosphate (P_i) starvation-induced *miR399* by near-complete complementary paring with *miR399*, except for the presence of a 4-bp mismatched loop in the middle of the duplex that interferes with mRNA target cleavage. Although *IPS1* is not cleaved, it sequesters *miR399* and decrease the availability of free *miR399*. Because of this, overexpression of *IPS1* results in the accumulation of *PHO2* mRNA that is normally targeted by *miR399.* Using the backbone of *IPS1* driven by a strong promoter, target mimicry successfully decreased the level of *miR156* and *miR319* in Arabidopsis, suggesting potential use of target mimics to other microRNAs (Franco- Zorrilla et al., 2007).

Research objectives

Molecular genetics and quantitative trait analyses, primarily in maize and Arabidopsis, have identified a number of factors that control leaf identity. However, detailed knowledge of the interactions that define the regulatory network for control of leaf identity in maize is still lacking. Studies focused on the genomic structure of key leaf identity genes, their contributions to variation in leaf identity phenotypes within

structured mapping populations, and functional confirmation of interactions predicted from observed expression patterns are necessary and are the focus of this dissertation. Several objectives to this research are addressed in the following chapters. The first objective examines the known leaf identity mutants and further investigates their role in altering vegetative phase change. The second objective analyzes quantitative trait locus of leaf identity factors and documents sequence and expression variations in leaf identity genes that are associated with identified QTLs and natural variation for vegetative phase change phenotypes in maize populations. The third objective is to see whether expression levels in *miR156, miR172* and *Glossy15* are heritable and could be used to predict leaf identity phenotypes. The fourth objective is to find potential downstream genes of *Glossy15* by microarray analysis.

References

Abedon, B.G., P. Revilla, and W.F. Tracy. 1996. Vegetative phase change in sweet corn populations: Genetics and relationship with agronomic traits (vegetative phase change in open-pollinated sweet corn). Maydica 41:77-82.

Abedon, B.G., R.D. Hatfield, and W.F. Tracy. 2006. Cell wall composition in juvenile and adult leaves of maize (Zea mays L.). Journal of Agricultural and Food Chemistry 54:3896-3900.

Aukerman, M.J., and H. Sakai. 2003. Regulation of flowering time and floral organ identity by a microRNA and its APETALA2-like target genes. Plant Cell 15:2730-2741.

Avato, P. 1987. Chemical genetics of epicuticular wax formation in maize. Plant Physiol. Biochem. 25: 179-190.

Axtell, M.J., C. Jan, R Rajagopalan and D.P. Bartel. 2006. A two-hit trigger for siRNA biogenesis in plants. Cell 127(3):565-77.

Balint-Kurti, P.J., J.C. Zwonitzer, R.J. Wisser, M.L. Carson, M.A. Oropeza-Rosas, J.B. Holland, and S.J. Szalma. 2007. Precise mapping of quantitative trait loci for resistance to southern leaf blight, caused by *Cochliobolus heterostrophus* Race O, and flowering time using advanced intercross maize lines. Genetics 176: 645-657.

Basso, C.F., M.M. Hurkman, E.S. Riedernan, and W.F. Tracy. 2008. Divergent selection for vegetative phase change in maize and indirect effects on response to Puccinia sorghi. Crop Science 48:992-999.

Berardini, T.Z., K. Bollman, H. Sun, and R.S. Poethig. 2001. Regulation of vegetative phase change in Arabidopsis thaliana by cyclophilin 40. Science 291:2405-2407.

Bianchi**,** A, and Marchesi, G. 1960**.** The surface of the leaf in normal and glossy maize seedling. Z Vererbungls, 91, 214219

Bianchi, G, P. Avato and F. Salamini. 1979. Glossy mutants of maize. Heredity 42 (3), 391-395.

Bianchi, G., Avato, P. and F. Salamini. 1984. Surface waxes from grain, leaves, and husks of maize (Zea mays L.). Cereal Chem. 61: 45-47.

Blaker, T.W. and R.I. Greyson. 1988. Developmental variation of leaf surface wax of maize, *Zea mays*. Can. J. Bot. 66: 839-846.

Bollman, K.M., M.J. Aukerman, M.Y. Park, C. Hunter, T.Z. Berardini, and R.S. Poethig. 2003. HASTY, the Arabidopsis ortholog of exportin 5/MSN5, regulates phase change and morphogenesis. Development 130:1493-1504.

Brooks, T.D., M.C. Willcox, W.P. Williams, and P.M. Buckley. 2005. Quantitative trait loci conferring resistance to fall armyworm and southwestern corn borer leaf feeding damage. Crop Science 45:2430-2434.

Buckler, E.S., J.B. Holland, P.J. Bradbury, C. B. Acharya, P.J. Brown, et al., 2009. The Genetic Architecture of Maize Flowering Time. *Science,* 325: 714-718.

Chandler, M.A., and W.F. Tracy. 2007. Identification of genomic regions affecting vegetative phase change in a sweet corn (Zea mays L.) population. Maydica 52:407-414.

Chandler, M.A., and W.F. Tracy. 2007. Vegetative phase change among sweet corn (Zea mays L.) hybrids varying for reaction to common rust (Puccinia sorghi Schw.). Plant Breeding 126:569-573.
Chen, C.F., D.A. Ridzon, A.J. Broomer, Z.H. Zhou, D.H. Lee, J.T. Nguyen, M. Barbisin et al., 2005. Real-time quantification of microRNAs by stem-loop RT-PCR. Nucleic Acids Research 33:-.
Chen, X.M. 2004. A microRNA as a translational repressor of APETALA2 in Arabidopsis flower development. Science 303:2022-2025.
Chen, X.M. 2009. Small RNAs and Their Roles in Plant Development. Annual Review of Cell and Developmental Biology 25:21-44.
Chuck, G., A.M. Cigan, K. Saeteurn, and S. Hake. 2007. The heterochronic maize mutant *Corngrass1* results from overexpression of a tandem microRNA. Nature Genetics 39:544-549.
Chuck, G., R. Meeley, E. Irish, H. Sakai, and S. Hake. 2007. The maize tasselseed4 microRNA controls sex determination and meristem cell fate by targeting Tasselseed6/indeterminate spikelet1. Nature Genetics 39:1517-1521.
Chuck, G., R. Meeley, and S. Hake. 2008. Floral meristem initiation and meristem cell fate are regulated by the maize AP2 genes ids1 and sid1. Development 135:3013-3019.
Chuck, G., C. Whipple, D. Jackson and S. Hake. 2010. The maize SBP-Box transcription factor encoded by tasselsheath4 regulates bract development and the establishment of meristem boundaries. Development 137: 1243-1250.
Clemens, J., R.E. Henriod, D.G. Bailey, and P.E. Jameson. 1999. Vegetative phase change in Metrosideros: Shoot and root restriction. Plant Growth Regulation 28:207-214.
Conway, L.J. and R.S. Poethig. 1997. Mutations of *Arabidopsis thaliana* that transform leaves into cotyledons. Proc. Natl. Acad. Sci. USA 94: 10209-10214.
Eigenbrode, S. D., and K. E. Espelie. 1995. Effects of plant epicuticular lipids on insect herbivores. *Annu. Rev. Entomol*, 40:171-194.
Evans, M.M.S., H.J. Passas, and R.S. Poethig. 1994. Heterochronic Effects of Glossy15 Mutations on Epidermal-Cell Identity in Maize. Development 120:1971-1981.
Evans, M.M.S., and R.S. Poethig. 1995. Gibberellins Promote Vegetative Phase-Change and Reproductive Maturity in Maize. Plant Physiology 108:475-487.
Evans, M.M.S., and R.S. Poethig. 1997. The viviparous8 mutation delays vegetative phase change and accelerates the rate of seedling growth in maize. Plant Journal 12:769-779.
Fahlgren, N., T. A. Montgomery, M. D. Howell, E. Allen, S. K. Dvorak, A. L. Alexander,and J. C. Carrington. 2006. Regulation of AUXIN RESPONSE FACTOR3 by TAS3 ta-siRNA affects developmental timing and patterning in Arabidopsis. Current Biology 16, 939–944.
Flint-Garcia, S.A., A.C. Thuillet, J.M. Yu, G. Pressoir, S.M. Romero, S.E. Mitchell, J. Doebley, S. Kresovich, M.M. Goodman, and E.S. Buckler. 2005. Maize association population: a high-resolution platform for quantitative trait locus dissection. Plant Journal 44:1054-1064.

Fu, Y., T. Wen, Y.I. Ronin, H.D. Chen, L. Guo, D.I. Mester, Y. Yang, M. Lee, A.B. Korol, D.A. Ashlock, and P.S. Schnable. 2006. Genetic dissection of intermated recombinant inbred lines using a new genetic map of maize. Genetics 174:1671-1683.

Galinat, W.C. **(**1966**)** The *corngrass* and *teopod* loci involve phase change. Maize Genet Coop. Newsl. 40**:**102-103.

Hunter, C., H. Sun, and R.S. Poethig. 2003. The Arabidopsis heterochronic gene ZIPPY is an ARGONAUTE family member. Current Biology 13:1734-1739.

Hunter, C., M.R. Willmann, G. Wu, M. Yoshikawa, M. de la Luz Gutierrez-Nava, and R.S. Poethig. 2006. Trans-acting siRNA-mediated repression of ETTIN and ARF4 regulates heteroblasty in Arabidopsis. Development 133:2973-2981.

Jiao, Y., Y. Wang, D. Xue, J. Wang, M. Yan, G. Liu, G. Dong, D. Zeng, Z. Lu, X. Zhu, Q. Qian and J. Li. 2010. Regulation of OsSPL14 by OsmiR156 defines ideal plant architecture in rice. Nature Genetics 42: 541-544.

Jung, J.H., Y.H. Seo, P.J. Seo, J.L. Reyes, J. Yun, N.H. Chua and C.M. Park. 2007. The GIGANTEA-regulated microRNA172 mediates photoperiodic flowering independent of CONSTANS in Arabidopsis. Plant Cell 19:2736 -2748.

Kampani, A.V. 2003. The generation and characterization of the maize Glossy15 transgenic line. M.S. thesis, University of Illinois at Urbana-Champaign.

Lauter, N., A. Kampani, S. Carlson, M. Goebel, and S.P. Moose. 2005. microRNA172 down-regulates glossy15 to promote vegetative phase change in maize. Proceedings of the National Academy of Sciences of the United States of America 102:9412-9417.

Lauter, N., M. J. Moscou, J. Habiger, and S. P. Moose. 2008**.** Quantitative Genetic Dissection of Shoot Architecture Traits in Maize: Towards a Functional Genomics Approach. The Plant Genome, 1(2): 99 – 110

Liu, K.J., M. Goodman, S. Muse, J.S. Smith, E. Buckler, and J. Doebley. 2003. Genetic structure and diversity among maize inbred lines as inferred from DNA microsatellites. Genetics 165:2117-2128.

Liu, S.Z., C.R. Dietrich, and P.S. Schnable. 2009. DLA-Based Strategies for Cloning Insertion Mutants: Cloning the gl4 Locus of Maize Using Mu Transposon Tagged Alleles. Genetics 183:1215-1225.

Lee, M., N. Sharopova, W. D. Beavis, D. Grant, M. Katt et al., 2002 Expanding the genetic map of maize with the intermated B73 × Mo17 (IBM) population. Plant Mol. Biol 48: 453–461.

Mathieu, J., L.J. Yant, F. Mürdter, F. Küttner and M. Schmid. 2009. Repression of Flowering by the miR172 Target SMZ. PLoS Biol 7(7): e1000148. doi:10.1371/journal.pbio.1000148.

Martin, A., H. Adam,M. D.Mendoza, M. Żurczak, N.D. González-Schain and P. Suárez-López. 2009. Graft-transmissible induction of potato tuberization by the microRNA miR172. Development 136:2873-2881

Miura, K., M. Ikeda, A. Matsubara, X. Song, M. Ito, K. Asano, M. Matsuoka, H. Kitano and M. Ashikari. 2010. OsSPL14 promotes panicle branching and higher grain productivity in rice. Nature Genetics 42: 545-549.

Moose, S.P., and P.H. Sisco. 1994. Glossy15 Controls the Epidermal Juvenile-to-Adult Phase-Transition in Maize. Plant Cell 6:1343-1355.

Moose, S.P., and P.H. Sisco. 1996. Glossy15, an APETALA2-like gene from maize that regulates leaf epidermal cell identity. Genes & Development 10:3018-3027.
Moose, S.P., N. Lauter, and S.R. Carlson. 2004. The maize macrohairless1 locus specifically promotes leaf blade macrohair initiation and responds to factors regulating leaf identity. Genetics 166:1451-1461.
Nichols, D. 2008. Genetic analysis of nitrogen use efficiency and related traits in the IBMRIL X IHP1 population of Maize. Ph.D. dissertation. University of Illinois at Urbana-Champaign.
Nole-Wilson, S., and B.A. Krizek. 2001. DNA binding properties of the Arabidopsis floral development protein AINTEGUMENTA (vol 28, pg 4076, 2000). Nucleic Acids Research 29:U6-U6.
Orkwiszewski, J.A.J., and R.S. Poethig. 2000. Phase identity of the maize leaf is determined after leaf initiation. Proceedings of the National Academy of Sciences of the United States of America 97:10631-10636.
Park, M.Y, G. Wu, A. Gonzalez-Sulser, H. Vaucheret, R.S. Poethig (2005) Nuclear processing and export of microRNAs in *Arabidopsis*. *Proc Natl Acad Sci USA* 102: 3691–3696.
Peragine, A., M. Yoshikawa, G. Wu, H.L. Albrecht, and R.S. Poethig. 2004. SGS3 and SGS2/SDE1/RDR6 are required for juvenile development and the production of trans-acting siRNAs in Arabidopsis. Genes & Development 18:2368-2379.
Poethig, R.S. 1988. Heterochronic mutations affecting shoot development in maize. Genetics 119: 959–973.
Poethig, R.S. 1990. Phase change and leaf morphogenesis in plants. Science 250:923-930.
Revilla, P., P. Velasco, R.A. Malvar, P. Soengas, and A. Ordas. 2000. Variability for phase transition among races of maize and related wild forms. Maydica 45:35-44.
Revilla, P., R.A. Malvar, A. Butron, W.F. Tracy, B.G. Abedon, and A. Ordas. 2002. Response to selection for the timing of vegetative phase transition in a maize population. Crop Sci. 42:1471–1474.
Riedeman, E.S., M.A. Chandler, and W.F. Tracy. 2008. Divergent recurrent selection for vegetative phase change and effects on agronomic traits and corn borer resistance. Crop Science 48:1723-1731.
Riedeman, E.S., and W.F. Tracy. 2010. Vegetative Phase Change Characteristics and Resistance to Common Rust of Corn Cultivars Developed in Different Eras. Crop Science 50:87-92.
Rogler, C.E. and Hackett, W.P. 1975. Phase change in Hedera helix: Induction of the mature to juvenile phase change by gibberellin A_3. Physiol. Plant. 34, 141–147.
Rhoades, M. W., B. J. Reinhart, L. P. Lim, C. B. Burge, B. Bartel and D. P. Bartel. 2002. Prediction of plant microRNAs targets. Cell 110 (4):513-520.
Salvi, S., G. Sponza, M. Morgante, D. Tomes, X. Niu, K.A. Fengler, R. Meeley, R. Tuberosa et al., 2007. Conserved noncoding genomic sequences associated with a flowering-time quantitative trait locus m maize. PNAS 104:11376-11381.
Samuels, L., Kunst, L. and R. Jetter. 2008. Sealing plant surfaces: cuticular wax formation by epidermal cells. Annu. Rev. Plant Biol. 59: 683-707.

Sharopova, N., Mcmullen, M.D., Schultz, L., S. Sschroeder, H. Sanchez-villeda et al., 2002. Development and mapping of SSR markers for maize. Plant. Mol. Biol. 48: 463–481.

Schmid, M., Uhlenhaut, N.H., Godard, F., Demar, M., Bressan, R., Weigel, D. and Lohmann, J. U. 2003. Dissection of floral induction pathways using global expression analysis. Development 130,6001 -6012.

Schmittgen, T.D., J.M. Jiang, Q. Liu, and L.Q. Yang. 2004. A high-throughput method to monitor the expression of microRNA precursors. Nucleic Acids Research 32:-.

Schnable, PS, PS Stinard, TJ Wen, S Heinen, D Weber, L Zhang, JD Hansen, BJ Nikolau. 1994. The genetics of cuticular wax biosynthesis. Maydica 39:279-287.

Schwarz, S., A.V. Grande, N. Bujdoso, H. Saedler, and P. Huijser. 2008. The microRNA regulated SBP-box genes SPL9 and SPL15 control shoot maturation in Arabidopsis. Plant Molecular Biology 67:183-195.

Scott, D.B., W. Jin, H.K. Ledford, H.S. Jung, and M.A. Honma. 1999. EAF1 regulates vegetative-phase change and flowering time in Arabidopsis. Plant Physiology 120:675-684.

Shi, R. and V.L. Chiang. 2005. Facile means for quantifying microRNAs expression by real-time PCR. Biotechniques 39:519-525.

Shikata, M., T. Koyama, N. Mitsuda, and M. Ohme-Takagi. 2009. Arabidopsis SBP-Box Genes SPL10, SPL11 and SPL2 Control Morphological Change in Association with Shoot Maturation in the Reproductive Phase. Plant and Cell Physiology 50:2133-2145.

Smith, M.R., M.R. Willmann, G. Wu, T.Z. Berardini, B. Moller, D. Weijers, and R.S. Poethig. 2009. Cyclophilin 40 is required for microRNA activity in Arabidopsis. Proceedings of the National Academy of Sciences of the United States of America 106:5424-5429.

Spray, C.R., M. Kobayashi, Y. Suzuki, B.O. Phinney, P. Gaskin and J. Macmillan. 1996. The dwarf-1 (dt) Mutant of Zea mays blocks three steps in the gibberellin-biosynthetic pathway. PNAS 93 (19): 10515-10518.

Sturaro, M., Hartings, H., Schmelzer, E., Velasco, R., Salamini, F. and M. Motto. 2005. Cloning and characterization of GLOSSY1, a maize gene involved in cuticle membrane and wax production. Plant Physiol. 138: 478-489.

Suzuki, M., Latshaw, S., Sato, Y., Settles, A.M., Koch, K.E., Hannah, L.C., Kojima, M., Sakakibara, H. and McCarty, D.R. 2008. The maize *Viviparous8* locus encoding a putative ALTERED MERISTEM PROGRAM1-like peptidase, regulates abscisic acid accumulation and coordinates embryo and endosperm development. Plant Physiol. 146: 1193-1206.

Telfer, A., K.M. Bollman, and R.S. Poethig. 1997. Phase change and the regulation of trichome distribution in Arabidopsis thaliana. Development 124:645-654.

Telfer, A., and R.S. Poethig. 1998. HASTY: a gene that regulates the timing of shoot maturation in Arabidopsis thaliana. Development 125:1889-1898.

Usami, T., G. Horiguchi, S. Yano, and H. Tsukaya. 2009. The more and smaller cells mutants of Arabidopsis thaliana identify novel roles for SQUAMOSA PROMOTER BINDING PROTEIN-LIKE genes in the control of heteroblasty. Development 136:955-964.

Vega, S.H., M. Sauer, J.A.J. Orkwiszewski, and R.S. Poethig. 2002. The early phase change gene in Maize. Plant Cell 14:133-147.
Voinnet, O. 2009. Origin, biogenesis and activity of plant microRNAs. Cell 136:669-687.
Walsh, J., and M. Freeling. 1999. The liguleless2 gene of maize functions during the transition from the vegetative to the reproductive shoot apex. Plant Journal 19:489-495.
Wang, H., T. Nussbaum-Wagler, B.L. Li, Q. Zhao, Y. Vigouroux, M. Faller, K. Bomblies, L. Lukens, and J.F. Doebley. 2005. The origin of the naked grains of maize. Nature 436:714-719.
Wang, S., Q.H. Zhu, X.Y. Guo, Y.J. Gui, J.D. Bao, C. Helliwell, and L.J. Fan. 2007. Molecular evolution and selection of a gene encoding two tandem microRNAs in rice. Febs Letters 581:4789-4793.
Wang, J.W., R. Schwab, B. Czech, E. Mica, and D. Weigel. 2008. Dual effects of miR156-targeted SPL genes and CYP78A5/KLUH on plastochron length and organ size in Arabidopsis thaliana. Plant Cell 20:1231-1243.
Williams, W.P., P.M. Buckley, and F.M. Davis. 2000. Vegetative phase change in maize and its association with resistance to fall armyworm. Maydica 45:215-219.
Willmann, M.R., and R.S. Poethig. 2005. Time to grow up: the temporal role of smallRNAs in plants. Current Opinion in Plant Biology 8:548-552.
Wu, G., and R.S. Poethig. 2006. Temporal regulation of shoot development in Arabidopsis thaliana by miR156 and its target SPL3. Development 133:3539-3547.
Wu, G., M.Y. Park, S.R. Conway, J.W. Wang, D. Weigel, and R.S. Poethig. 2009. The Sequential Action of miR156 and miR172 Regulates Developmental Timing in Arabidopsis. Cell 138:750-759.
Xie, Z., E. Allen, A. Wilken and J.C. Carrington. 2005. DICER-LIKE 4 functions in trans-acting small interfering RNA biogenesis and vegetative phase change in *Arabidopsis thaliana*. PNAS 102(36):12984–12989.
Xie, K., C. Wu and L. Xiong. Genomic organization, differential expression, and interaction of *SQUAMOSA promoter-binding-like* transcription factors and *microRNA156* in rice. *Plant Physiol.* 142, 280–293 (2006)
Xu, X., C.R. Dietrich, M. Delledonne, Y. Xia, T.J. Wen, D.S. Robertson, B.J. Nikolau, and P.S. Schnable. 1997. Sequence analysis of the cloned glossy8 gene of maize suggests that it may code for a beta-ketoacyl reductase required for the biosynthesis of cuticular waxes. Plant Physiol 115:501-10.
Xu, X., Dietrich, C.R., Lessire, R., Nikolau, B.J. and P.S. Schnable. 2002. The endoplasmic reticulum-associated maize GL8 protein is a component of the acyl-coenzyme A elongase involved in the production of cuticular waxes. Plant Physiol. 115: 501-510.
Xu, L., L. Yang, L.M. Pi, Q.L. Liu, Q.H. Ling, H. Wang, R.S. Poethig, and H. Huang. 2006. Genetic interaction between the AS1-AS2 and RDR6-SGS3-AGO7 pathways for leaf morphogenesis. Plant and Cell Physiology 47:853-863.
Yan, J.B., T. Shah, M.L. Warburton, E.S. Buckler, M.D. McMullen, and J. Crouch. 2009. Genetic Characterization and Linkage Disequilibrium Estimation of a Global Maize Collection Using SNP Markers. Plos One 4:-.

Yang, Z.Y., Y.W. Ebright, B. Yu, and X.M. Chen. 2006. HEN1 recognizes 21-24 nt small RNA duplexes and deposits a methyl group onto the 2 ' OH of the 3 ' terminal nucleotide. Nucleic Acids Research 34:667-675.

Yu, J.M., G. Pressoir, W.H. Briggs, I.V. Bi, M. Yamasaki, J.F. Doebley, M.D. McMullen, B.S. Gaut, D.M. Nielsen, J.B. Holland, S. Kresovich, and E.S. Buckler. 2006. A unified mixed-model method for association mapping that accounts for multiple levels of relatedness. Nature Genetics 38:203-208.

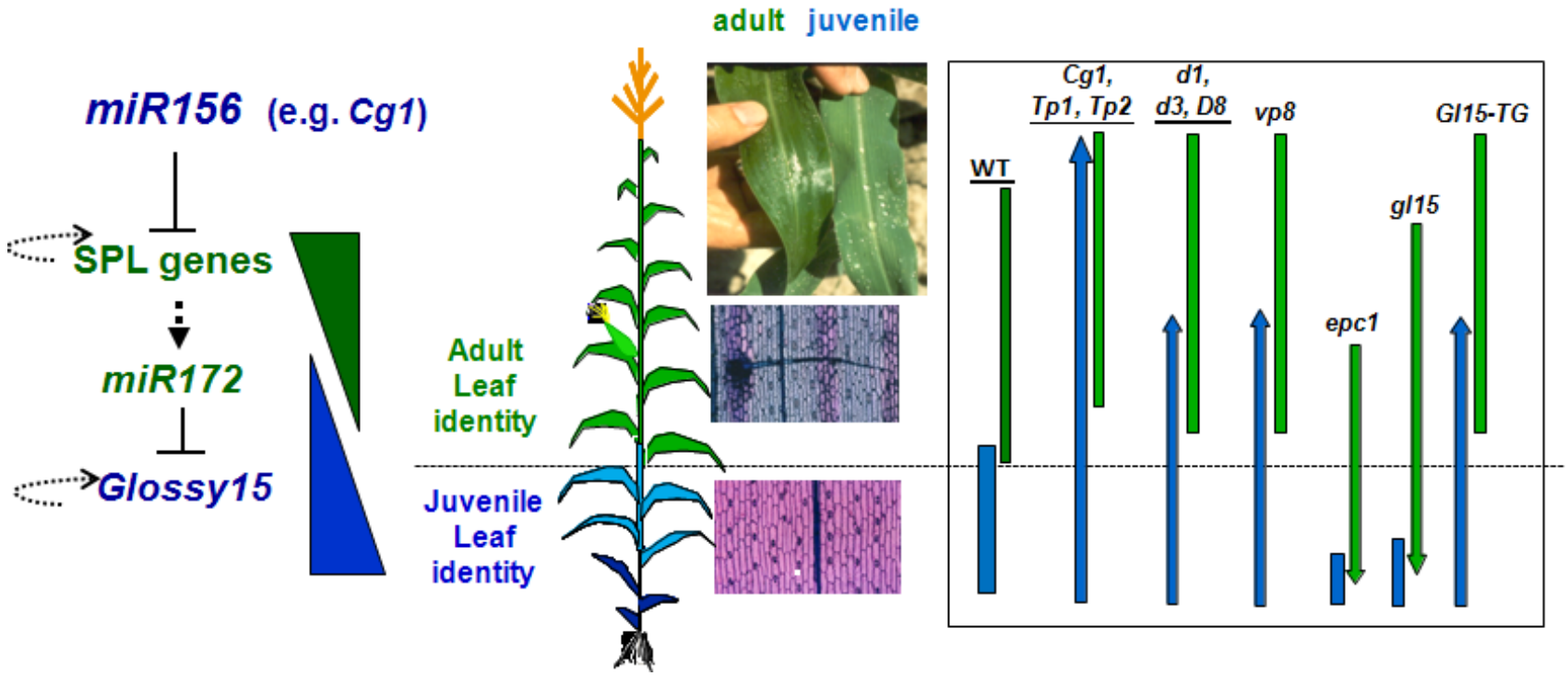
Yu, J.M., Z. Zhang, C. Zhu, D.A. Tabanao, G. Pressoir, et al. (2009) Simulation appraisal of the adequacy of number of background markers for relationship estimation in association mapping. The Plant Genome 2: 63–77.

Zhang, L.F., J.M. Chia, S. Kumari, J.C. Stein, Z. Liu, A. Narechania, C. A. Maher, K. Guill, M.D. McMullen and D. Ware. 2009. A genome wide characterization of microRNAs genes in maize. Plos genetics 5 (11): e1000716

Zhao, L., Y. Kim, T. Dinh, and X. Chen. 2007. miR172 regulates stem cell fate and defines the inner boundary of APETALA3 and PISTILLATA expression domain in Arabidopsis floral meristems. Plant J. 51,840 -849.

Zimmerman, R.H., Hackett, W.P. & Pharis, R.P. 1985 Hormonal aspects of phase change and precocious flowering. In: *Hormonal Regulation of Development III: Role of Environmental Factors (Encyclopedia of Plant Physiology New Series)*, Vol. 11 (Pharis, R.P. & Reid, D.M.. Berlin: Springer-Verlag, pp. 79–11.

Figure 1.1: **Maize leaf identity traits and known regulatory factors.** Phenotypes distinguishing juvenile and adult leaf identity include leaf waxes, macrohairs and bulliform cells (purple cell files in adult leaves), and differences in cell wall biochemistry visualized by staining with toluidine blue. Transition leaves exhibit juvenile then adult phenotypes in a proximal-distal pattern. The dashed line marks the boundaries that typically define the transitions from juvenile to adult leaf identity in wild-type (WT). The relative expression of juvenile (blue) and adult (green) leaf identities in WT and mutant genotypes is indicated by the position and height of the colored bars, mutants are described in detail in the following text. The cartoon at left depicts known or predicted features of the regulatory network for vegetative phase change, where the expression of juvenile factors (blue triangle) progressively declines and adult factors (green triangle) increases during shoot development.



Chapter 2:

Leaf identity mutants and the genetic network of vegetative phase change

Abstract

Vegetative phase change in maize is characterized by the transition from waxy juvenile leaves to pubescent, glossy adult leaves. Molecular genetic studies in maize and Arabidopsis have identified important factors for the general process of phase change, including genes that function in small RNA biogenesis and metabolism, small RNAs, transcription factors and growth regulators (GA and ABA). Detailed analysis of molecular interactions within the vegetative phase change pathway has clarified the functional relationships among some of these regulatory factors. Analysis of mutations affecting vegetative phase change indicates that the observed antagonistic effects of *miR156* and *miR172* converge to regulate *Glossy15*. Experiments involving exogenous GA application and GA-deficient mutants demonstrate that GA both represses *miR156* and promotes *miR172* expression, but acts more strongly on *miR172*.The effects of GA on phase change can be reversed by increasing *Glossy15* expression, supporting the view that vegetative phase change is regulated by the relative activities of GAs that promote and *Glossy15* that inhibits shoot maturation, which are mediated by the antagonistic interactions between *miR156* and *miR172*.

Introduction

Vegetative phase change in maize is well characterized by the transition of juvenile leaves to adult leaves, where juvenile leaves are covered with a layer of visible wax and adult leaves develop epidermal bulliform cells and macrohairs (Moose and Sisco, 1994). Maize has been used as a model plant system to study phase change, due to the presence of distinct phenotypes for juvenile and adult phases, mutations that alter the expression of phase-specific phenotypes, and the advantages of this plant system for the isolation and functional analysis of genes.

Maize genetic mutants have been identified that later the timing of juvenile-to-adult transition. *Corngrass1* (*Cg1*), *Teopod1* (*Tp1*) and *Teopod2* (*Tp2*) are semi-dominant gain-of-function mutations that each prolong the expression of the juvenile phase and slightly delay the onset of adult traits (Galinat, 1966; Poethig, 1988, Dubley and Poethig, 1993). In addition, GA-deficient *dwarf (an1, d1, d3, d5* and *D8*) and ABA-deficient *vivaparous8* (*vp8*) are loss of function mutations that also prolong the transition of juvenile-to-adult leaves (Evans and Poethig, 1995, Evans and Poethig, 1997). In contrast to the above mutations, recessive, loss-of-function mutations of *glossy15* accelerates the expression of adult epidermal traits. Phenotypes of double mutants between *glossy15* and the above mutations indicate that wild-type *Glossy15* is required to maintain juvenile leaf identity and *Glossy15* acts downstream of *Tp1, Tp2, Cg, Vp8* and gibberellins (Moose and Sisco, 1994, Evans and Poethig, 1994). *Glossy15* encodes a protein with two repeated *APETALA2* binding domains and is

predicted to function as a transcription factor (Moose and Sisco, 1996). Vega et al. (2002) also identified a recessive mutant, *early phase change1 (epc1),* that could promote adult leaf identity traits as early as the first leaf and also influences broader aspects in shoot and root development. The *epc1* gene is predicted to be the Arabidopsis ortholog of *HASTY (HST)*, which encodes the exportin5/MSN5 protein that functions in nucleocytoplasmic export of pre-microRNAs and when HST function is lost by mutation, reduces the number of juvenile leaves (Telfer and Poethig, 1998, Bollman et al., 2003).

microRNA172 (*miR172*) and *microRNA156* (*miR156*) were recently documented as important factors in the vegetative phase change pathway via repression of *Glossy15* mRNA by *miR172* (Lauter et al., 2005) and *SPL* mRNA targets by *miR156* (Wu and Poethig, 2006; Chuck et al., 2007). Importantly, *miR172* accumulation is not affected in either increased (*Gl15-TG*) or decreased (*gl15* mutants) *Gl15* activity, providing additional genetic evidence that *GL15* is a downstream molecular target of *miR172* (Lauter et al., 2005). Wu and Poethig (2006) have demonstrated that *SPL* genes in Arabidopsis could promote vegetative phase change, a function that could be repressed by *miR156*. The interaction of *miR156* and *SPL* genes is conserved in maize. The *Cg1* mutation, which delays vegetative phase change and has a bushy phenotype, results from *miR156b/c* overexpression due to the insertion of a retrotransposon element upstream of the *miRNA156b/c* transcribed region. This conclusion was supported by the fact that maize plants overexpressing *miR156b/c* under control of the strong 35S promoter mimics *Cg1* phenotypes (Chuck et al., 2007). The maize

genome contains 11 predicted *miR156* genes and approximately 20 SPL genes with *miR156* binding sites (maize B73 RefGen_v2), all of the 11 *miR156* genes are more highly expressed in juvenile tissues compared to the inflorescence (Zhang et al., 2009). Seven SPL genes are shown to be greatly reduced by overexpressing *miR156* (Chuck et al., 2007; Chuck et al., 2010).

Research from Arabidopsis and maize shows that *miR156* and *miR172* have complementary expression patterns during shoot development. Overexpression of *miR172* in Arabidopsis leads to early flowering and flower organ defects (Aukerman and Sakai, 2003). On the contrary, overexpression of *miR156b/c* in *Cg1* maize results in delayed flowering (Chuck et al., 2007). The opposite expression patterns and phenotypic effects of *miR156* and *miR172* raises the possibility that these two miRNAs work in an opposing manner within the same regulatory pathway. Recently, Wu et al. (2009) demonstrated that in Arabidopsis, *miR156* reduces accumulation of SPL9 and possibly SPL10 protein, which binds to the promoter regions of *miR172b* and increases the levels of *miR172b* precursor as well as mature *miR172*. These results indicate the importance of the *miR156-SPL9-miR172-AP2* pathway during Arabidopsis vegetative phase change (Wu et al., 2009).

Prior work in the Moose laboratory has shown that overexpression of *Gl15* increases the number of juvenile leaves and delays the onset of adult leaf identity. *Glossy15* transgenic plants also have delayed reproductive development, as measured by the total number of leaves and days to 50% anthesis (Lauter et al., 2005). The delayed flowering in *Glossy15* transgenic lines

indicate two scenarios that may explain the phenotype: the first is that additional *Glossy15* mRNA may sequester *miR172*, thus increasing the relative activities of *Glossy15* and other AP2 genes or delaying the accumulation of active *miR172* above a threshold critical to downregulate other AP2 genes and hence AP2-like proteins, which could bind to their targets and delay flowering. The second hypothesis is that greater production of GLOSSY15 protein, functionally substitutes for other related AP2 proteins that normally delay flowering. A solution to differentiate the two scenarios is to specifically reduce *miR172* activity and observe whether the resulting phenotypes could mimic *Gloss15* transgenic plants.

The fact that mature miRNAs often derive from multiple genome loci and have functional redundancy makes it difficult to create genetic knockouts for miRNA. For example, all of the 11 *miR156* are highly expressed in juvenile shoots in maize (Zhang et al., 2009). In mammalian cells, artificial miRNA binding sites named “miRNA sponges” have been designed and delivered to cells to soak up miRNAs. The artificial miRNA binding site was designed by introducing several mismatch in the middle of the complementary sequence, thus produce a bubble when pairing with miRNAs. By introducing this artificial miRNA sponge, miRNA level could be reduced by several times compared to control (Ebert et al., 2007).

In addition to the altered vegetative phenotypes in GA-deficient dwarf mutants, the importance of GAs as one group of mobile factors that regulate leaf identity relies on the leaf identity effect brought by exogenous GA application.

Exogenous application of GA modulates vegetative phase change in a number of plant species (Telfer et al., 1997, Rogler and Hackett, 1975). GAs promote the precocious appearance of abaxial trichomes in Arabidopsis (Telfer et al., 1997) and exogenous GA could restore dwarf mutant phenotypes of fatter leaves and limited internode elongation and partially restore vegetative phase change in *Tp* mutants (Evans and Poethig, 1995).

Put together, the regulatory network for vegetative phase change involves genes that function in small RNA biogenesis and metabolism (Arabidopsis *HST1/*maize *epc1*), microRNAs (*miR156* and *miR172*), transcription factors (*Glossy15* and *SPL* genes) and growth regulators (GA and ABA). We use genetic as well molecular methods to define the interactions among these factors within the vegetative phase change pathway of maize. We demonstrate here that antagonistic regulatory interaction between microRNAs (*miR156* and *miR172*) and their corresponding targets is the regulatory center in the pathway. Our results support the idea that GA is involved in the transition of juvenile to adult leaf identity by regulating *miR156* and *miR172* accumulation and that antagonistic effects of *miR156* and *miR172* converge to regulate *Glossy15*.

Materials and Methods

Genetic stocks

All plants were grown in Crop Sciences Research and Education nursery in Champaign, IL or a controlled environment greenhouse. Each of the *Cg1, Tp1, Tp2* and *d1* mutants (Maize Genetics Cooperation Stock Center, Urbana, IL)

were introgressed into the W64A inbred background by at least six backcrosses to W64A followed by selfing for *d1* to produce homozygous lines. The e*pc1* mutant in the W23 inbred background was described by Vega et al. (2002). *Glossy15*-transgenic plants were generated by microprojectile bombardment in H99 inbred background (Lauter et al., 2005) and introgressed into W64A by five backcrosses. W64A:*Gl15-TG* plants were crossed twice to *gl15,* W64A:*Cg1*, W64A:*Tp1*, W64A:*Tp2* and W64A:*d1*, seeds were grown in the following year for phenotypic segregation. Plant genotypic classes (plus or minus *Gl15-TG* in mutant backgrounds) were differentiated by their phase change phenotypes as measures by last leaf with visible juvenile waxes, with the mutant plus *Gl15-TG* genotypes confirmed by independent segregation of transgenic and mutant phenotypes in their progeny the following year.

The *gl15-m1*, *gl15-H, gl15-L* and *gl15-S* alleles were described previously (Moose and Sisco, 1994; Moose and Sisco, 1996). The *gl15-91642* and *gl15-94317* alleles are derived from *gl15-m1*, where the *dSpm* insertion transposed and generated heritable stable *gl15* mutant phenotypes. The *gl15-956, gl15-63, gl15-46* and *gl15-98* alleles were generated from a targeted Mutator transposon-tagging experiment where active *Mutator* in a Q60/Q66 background (gift from Pat Schnable, Iowa State University) was crossed to a *wx1, gl15-H, mhl1-R* stock and *gl15* mutant phenotypes recovered (Moose et al., 2004). The *gl15-C256A* was identified in segregating families from EMS-mutagenized population of *ra1-RS* as described by Gallavotti et al. (2010). Two additional *gl15* mutations were identified from the Illinois long-term selection experiment for low grain protein

(ILP) concentration (Moose et al., 2004b) and the inbred line LH82. Each of the *gl15* mutant alleles were confirmed by testcrossing to *gl15-H* and *gl15-m1*, and were introgressed into the W64A background, except for the *gl15-LH82* allele.

Tissue sampling and RNA isolation

Plants were grown to desired developmental stages as appropriate to each experiment, to represent shoots entirely in the juvenile phase, undergoing vegetative phase change, or entirely in the adult phase based on the timing of vegetative phase change in the normal W64A inbred. Leaf identity mutants and plants for the GA treatment experiment were grown in a summer nursery. The other plants were grown in a greenhouse under 16 hour day length, 28°C day/20°C night temperatures. Shoot apexes were sampled by dissecting leaves that were >5cm in length and keeping the basal 2cm of leaf tissue which enclosed the shoot apical meristem. Leaf 5 and leaf 10 samples were taken at V7 stage. At least 3 plants from each genotype were sampled and pooled as a sample. Leaf blade, vein/midrib and sheath tissues were dissected from B73 leaves grown for 48 days in the greenhouse. Samples were instantly frozen in liquid nitrogen and stored at -80°C until RNA isolation. TRIZOL was used for RNA isolation followed by isopropyl alcohol precipitation and wash with 75% ethanol. RNA is then dissolved in water and treated with DNAse at 37ºC, followed by Qiagen RNAse Easy clean up. The concentration, yield and quality of purified RNA was estimated using a NanoDrop spectrophotometer.

PCR

PCR primers (GI15_1245 and GI15_4504) were designed based on *Glossy15* sequences in maize inbreds W64A (accession AY714877) and B73. Expanding long template PCR system was purchased from Roche and used to amplify *Glossy15* sequences from genomic DNA isolated from leaf tissue of lines homozygous for each *glossy15* mutant allele. The PCRs included 500ng DNA, 17.5 um dNTP, 15 nm primer1, 15 nm primer 2, 1 ul DMSO and 0.75 ul Taq polymerase in a 50 μl final volume. PCR amplification used the following thermal cycling profile: initial denaturation at 94°C for 2 min; 11 cycles of 94°C for 15 sec, 60°C for 30 sec, 68°C for 6 minutes and 20 sec; 16 cycles of 94°C for 15 sec, 60°C for 30 sec, 68°C for 6 minutes and 30 sec; followed by 4 additional cycles where elongation time increase from 6 minutes and 30 sec by 20 sec in each cycle, and a final extension at 68 °C for 7min. PCR products was then purified by Qiagen PCR purification kit and sent to Roy J. Carver Biotechnology Center for sequencing using the *Glossy15* sequencing primers.

GA treatment

25μg or 50μg GA/plant was applied as a 1mg/mL solution in water by pipetting into leaf whorls at 12 days after planting. Twenty replicate plants were treated and phenotypes measured for H99 and its isogenic *GI15-TG* line, 10 replicate plants were treated and phenotypes measured for *d1* and its isogenic *GI15-TG* line. Treatments and data collection were conducted in each of two years in the summer nursery. Shoot apical meristem RNA samples were taken 4

days after GA application and samples for microRNA assays were taken 2 days after GA application.

Phenotypic measurements

Three phenotypes were used as markers for the duration of juvenile and onset of adult leaf identities. Both first glossy leaf and first leaf with macrohairs were used as markers for the onset of adult leaf identity, and were scored as the number of leaves that completely lacked these traits plus the proportion of the length of the leaf that lacked these traits within the leaf where they first appeared. For example, a phenotypic value of 2.5 for either glossy or macrohairs indicates that the first two leaves and half of the length of the third leaf lack these traits, or conversely, adult traits appeared after the development of 2.5 leaves. The last leaf wax (LLW) is a marker for the maximum duration of the juvenile phase, and was scored as the last leaf blade where visible epicuticular wax was present, typically at the tip of the leaf blade. L5 Width was measured at the widest part of leaf 5 and total nodes were recorded at flowering. Error bars indicate standard errors of the mean from at least 10 replicate plants in each genotypic class.

mRNA profiling

The *miR172* sequence was used in BLASTN searches of the maize B73 genome sequence to identify five predicted *miR172* loci. These sequences were used to design primers that specifically amplify individual *pre-miR172* sequences. Reverse transcription reactions were performed on 1µg total RNA at 42°C in 20µl

reaction volume by oligo(dT) and reverse transcription kit (New England Biolabs). Real time PCR primers were tested for primer dimers and robust melting curves in a MJ Research Opticon2 real time PCR machine. Real-time PCR reactions were performed by mixing 2X SYBR-green mastermix from BioRad with 10 pmol primers and diluted cDNA, followed by PCR cycles with 94°C for 15 sec, 63°C for 30 sec and extension at 72 °C for 30 sec. The $\Delta\Delta C_t$ method (Livak et al., 2001) was used to measure expression of *miR172* precursors relative to Actin mRNA as internal standard. ΔC_t method was used for *GAPDH* mRNA levels in the W23 and *epc1* mutant samples.

microRNA quantitation

The *miR156a, miR172a* and *miR166a* TaqMan assays were purchased from Applied Biosystems (ABI). *sRc1* is a putative miRNA observed from Illumina deep sequencing analysis of small RNAs from 11 days after sowing shoot apices to show no difference in accumulation among genotypes (Barber et al., unpublished). Custom designed (by ABI) *sRc1* and *ZmmiR168a* assays were used along with the other assays. Reverse transcription and real-time PCR preparation were performed according to Taqman miRNA assay protocol except that the reverse primers of *miR156a, miR172a* and *miR168a* were combined in a multiplex reaction for reverse transcription to minimize experimental error. Multiplex reaction was performed using 20ng RNA, 100U RT, 3ul each primer, 0.25ul RNAse inhibitor and 0.4ul dNTP (100mM) in a 20ul reaction. Relative expression levels of *miR156* and *miR172* in mutants and GA treatment studies

were calculated relative to *miR168a* using the $\Delta\Delta C_t$ method. Because all microRNAs express at much lower levels in *epc1* mutant comparing to W23 isogenic plants, we were not able to use $\Delta\Delta C_t$ method to quantify the miRNA level, but instead used the ΔC_t method comparing W23 and W23: *epc1* genotypes.

miRNA target mimic constructs

Figure 2.1 illustrates the design of our miRNA sponge constructs, which include three functional properties (Ebert et al., 2007). First, the miRNA target mimics share complete sequence complementarity with the targeted miRNA except for 3-4 mismatches in the middle of the sequence. This design will produce a mismatch bulge that interferes with the AGO-mediated cleavage of the artificial targets. In addition, it has been observed that sequences with perfect complementarity to miRNAs do not bind as well as sequences that harbor mismatches (Ebert et al., 2007). Secondly, three miRNA target mimics are arranged as a tandem multimer with a 14 bp spacer in between each miRNA target mimic. The spacer is designed so that it does not share sequence identity with any of the known miRNAs or other sequences in the maize genome, as assessed by BLASTN comparisons to available maize genome sequence data at the time of design. The total length of anti-miRNAs and spacers are 128-bp including *Not*I and *Spe*I restriction enzyme sites at both ends. The third feature of these anti-miRNA constructs is that they are inserted into the 3' untranslated region of the DsRed reporter protein under the control of the maize *ubiquitin1*

promoter plus first intron (Christensen and Quail, 1996). These constructs are expected to constitutively express the miRNA sponges at a high level, as well as provide a visual marker for their expression that will aid in correlating relative expression of the miRNA target mimics, its complementary miRNA, and the endogenous mRNA targets.

The 128 bp *miR172* and *miR156* target mimic constructs were synthesized by Integrated DNA Technologies, and further PCR-amplified by using primers (156/172F1: AGCGGCCGCACCTCGGACC, 156R1: ACTAGTTGAATTCGAGGTTGACAGA, 172R1: ACTAGTTGAATTCCGAGGTAGAATC). pDsRed and the PCR products were digested with *Not*I and *Spe*I, and were ligated at 25°C for 1 hour, then at 4°C overnight. For the *Ubiquitin1* promoter plus intron, these sequence were released from the plasmid pAGM100 with *Hin*dIII and the fragment inserted into pBluescript KS+. This step is necessary to add restriction sites of *Bam*HI and *Kpn*I, which are present within the pDsRed 5' multiple cloning site (MCS). Clones with the *Ubiquitin1* promoter plus intron fragment in the proper sense orientation were selected following confirmation by restriction enzyme digestion with *EcoR*I. The 2.0kb *Ubiquitin1* promoter plus intron fragment was released by digestion with *Bam*HI and *Kpn*I, gel-purified, and nserted into the MCS that is digested with *Bam*HI and *KpnI*. The entire linear fragment between the *Bam*HI and *Spe*I sites was used as DNA for biolistic bombardment.

pCAMBIA2200 contains the NPTII coding region that is driven by the CaMV35S promoter. The 35S polyA sequence was added at the end of the

NPTII coding region for efficient transcription. The 4.2 kb linear fragment between *Eco*RI and *Dra*I was cleaved, gel-purified, and used as the selectable marker.

Development of transgenic maize plants

Embyo dissection, callus initiation, micro-projectile bombardment and selection followed protocols described at http://www.agron.iastate.edu/ptf/protocol/. Callus that survive selection are first put onto regeneration media I in dark for two weeks (regeneration media I: 4.3 g/L MS salts+vitamins, 60 g/L sucrose, 5 mg/L 6-benzyl-aminopurine), and transferred to regeneration media II (MS media with 100mg/L myo-inositol, 60g/L sucrose) under 16 hour daylight for 2 weeks, and then to regeneration media III (MS media with 100mg/L myo-inositol, 30g/L sucrose) under 16 hour daylight. The above mentioned components are following D'Halluin et al., 1990; Raizada and Walbot, 2006. Under media II, plants roots will develop and under media III, green spots could be seen. Callus is then transferred to taller tissue culture jars containing regeneration media III for further development.

Calluses producing 5 cm or bigger leaves are then transferred to soil. At the same time, wildtype H99 seeds are planted to serve as pollen donor. To help the plants adjust to strong light, plants are first left in the growth chamber for two to three days and then moved to the greenhouse under shade. Pots are covered with a plastic hood to maintain moisture during the hardening-off period.

Results

glossy15 mutant alleles

Each of the *glossy15* mutant alleles accelerated the transition from juvenile to adult leaf identity (Table 2.2). The adult leaf traits glossy leaf and macrohairs appear beginning with leaf two or three in all *gl15* mutants, compared to leaf seven or eight in the wild type W64A. The *gl15* mutations also condition a shorter juvenile phase, as indicated by the production of juvenile waxes through leaves three or four compared to leaf ten in W64A. The majority of these *gl15* mutations conditioned similar phenotypes, with three subtle differences. The *gl15-911642* allele transitions to an adult identity earlier than the others, with macrohairs present at the base of leaf 2 and juvenile wax ending by leaf three compared to leaf four in other *gl15* mutants. The *gl15-C256A* mutation appears to exhibit a more abrupt loss of juvenile waxes, but the onset of macrohairs is not different compared to the other *gl15* mutations. The *gl15-ILP* allele appears to condition a weaker phenotype than the others, as the both the onset of adult and duration of juvenile traits is extended by approximately one leaf relative to the other *gl15* mutations.

The *gl15* mutant alleles are derived from different genetic backgrounds (see Materials and Methods). To determine the basis for these mutant phenotypes, the genomic region spanning the entire *gl15* transcribed region was sequenced from seven *gl15* mutant alleles, which are summarized in Figure 2.2a. Attempts to amplify *gl15* sequences from the other *gl15* alleles, each of which were obtained from a *Mutator* tagging experiment, were not successful, possibly

due to the presence of *Mutator* transposon insertions that interfered with long PCR amplification. The *gl15-H* and *gl15-L* mutant alleles are caused by *Dissociation* (*Ds)* transposon insertions in the first exon: the *Ds* element within *gl15-L* bears a target site duplication and *gl15-H* also possesses a 50bp sequence deletion that is most likely the result of imperfect repair of the target site during *Ds* transposition. The *gl15-s* and *gl15-LH82* alleles have a 1000-bp insertion within the 7th exon that shares similarity to a sequence within the bz locus. The *gl15-ILP* allele harbored a 1000-bp insertion in the last intron. As expected given their derivation from *gl15-m1*, the *gl15-911642* allele bears a 7 bp deletion and *gl15-94317* a 5bp insertion due to aberrant excisions of the dSpm element in the first exon. Notably, the *gl15-H, gl15-L, gl15-911642* and *gl15-94317* alleles all contained lesions within the first exon due to the activities of two different transposons. This may indicate that either the first exon of *gl15* is a transposon hotspot, or that mutations occurring within the first exon are more likely to produce visible *gl15* mutant phenotypes.

The effects of the *gl15* mutations on *Gl15* mRNA expression were examined by qRT-PCR of shoot apices and newly-initiated leaves sampled when the third leaf became visible. Figure 2.2 shows that each *gl15* mutant allele produces less *Gl15* transcripts, with the exception of *gl15-S* whose mRNA expressed at levels similar to the wildtype. *Gl15* transcription in *gl15-ILP, gl15-911642* and *gl15-94317* was less affected when compared to the other *gl15* mutants (Fig. 2.2b), probably because of their relatively minor sequence

modifications (*gl15-911642* and *gl15-94317*) or the insertion within the last intron (*gl15-ILP*).

miR156 declination and miR172 accumulation during transition from juvenile to adult leaf identity

The relative levels of *miR156* and *miR172* were profiled in *gl15* mutant, *Gl15-TG* and wildtype plants in both shoot apical meristems and leaves during a time period when transition from juvenile to adult leaf identity happens. Fig. 2.3 shows that relative levels *miR172* increase during vegetative phase change (Fig. 2.3 A, C), contrary to *miR156* expression patterns (Fig. 2.3 B, D). The declination of miR156 and accumulation of *miR172* during vegetative phase change are consistent with previous results (Lauter et al., 2005 and Chuck et al., 2007).

Comparing *miR172* among *gl15* mutant, *Gl15-TG* and wildtype under different genetic background gives us inconsistent results. For example, *miR172* shows higher levels in *W23: gl15* and *Nc61: gl15* samples relative to their wildtype in shoot apices (Fig. 2.3 C and E), but not in *H99: gl15* shoot apices (Fig. A and C). Levels of *miR172* are higher in *W23: Gl15-TG* background comparing with W23 (Fig. 2.3 E and C), but are lower in *H99: Gl15-TG* background comparing with H99 (Fig. 2.3 A, C). The results of *miR172* expression indicate that the effect of *Glossy15* on *miR172* is not obvious or dependent on genetic background. However, profiling *miR156* in the same set of samples indicate correlation of higher *miR156* levels and the higher abundance of *Glossy15*. Transgenic *Gl15* generally brings in more *miR156* at juvenile

tissues but not adult development tissues (Fig. 2.3 B, D and E), due to the relative low expression levels in adult tissues. Decreased *Glossy15* levels in *gl15* mutants results in lower *miR156* in Nc61 and H99 background, but not in W23 background, because W23 itself is already representing the earliest transition inbred lines.

Cg1, Tp1, Tp2 and d1 alter the expression of miR156 and miR172

Currently, only two genes for vegetative phase change have been cloned in maize, namely *Glossy15* and *Cg1*, both of which control juvenile leaf identity. *Glossy15* is regulated by *miR172* and the *Cg1* phenotype results from an overexpressed version of *miR156c/b*, which targets SPL genes (Moose and Sisco, 1996; Chuck et al., 2007). Due to the central importance of the *miR156-SPL* and *miR172-AP2* are interactions in regulating vegetative phase change it is likely that the *Tp1, Tp2, d1, vp8* and *epc1* mutations affecting vegetative phase change in maize may encode or regulate members of the *miR156*, *miR172, SPL*, or *AP2* gene families. The *Tp1* and *Tp2* mutations condition similar phenotypes as *Cg1* and also exist as single gain-of-function alleles, raising the possibility that *Tp1* and *Tp2* result from rare mutations in one of the other 11 *miR156* loci in maize, or a binding site within one of the maize *SPL* genes.

Figure 2.4 shows the results obtained when *miR156* and *miR172* expression is assayed by qRT-PCR in the vegetative phase change mutants following their introgression into the common W64A inbred background. Assays were conducted at 27 days after sowing when W64A plants have completed the

transition to the adult phase. Consistent with results obtained by *miR156* RNA gel blot analysis (Chuck et al., 2007), *miR156* expression in wild-type plants has declined to basal levels by 27 days, but it remains at high levels in the *Cg1* mutant. The expression of *miR156* is also enhanced relative to W64A in each of the *Tp1, Tp2* and *d1* mutant isogenic lines, with the relative expression increase correlating well with the degree of prolonged juvenility in each of these mutants (Moose and Sisco, 1994). As reported previously (Lauter et al., 2005), *miR172* is strongly expressed in adult shoots, as represented by the 27 DAS W64A sample. The expression of *miR172* is either similar or slightly greater than wild type in the *Tp1* and *Tp2* mutants, but remains lower in *Cg1* and *d1*. This result is consistent with the observation that the onset of the adult phase is delayed in the *Cg1* and *d1* mutants, but not in *Tp1* and *Tp2* (Moose and Sisco, 1994).

The finding that *d1* exhibits the greatest reduction of mature *miR172* expression compared to wild type, yet has relatively subtle effects on the timing of vegetative phase change suggested that *miR72* expression may be particularly sensitive to GA levels independently from phase change. This hypothesis was further investigated in another experiment conducted at earlier stages (14 DAS) when both wild type and *d1* are still in the juvenile phase. Both wild-type and *d1* mutant plants were treated with solutions containing GA_3 which was determined previously to promote vegetative phase change (Evans and Poethig, 1995). Shoot apices and newly-initiated leaves were sampled two days after GA treatment and the expression of *miR156* and *miR172* assayed by qRT-PCR.

Figure 2.5 shows that *miR156* expression was elevated in the *d1* mutant compared to wild type, and was slightly decreased in wild-type but not *d1* plants treated with GA. As observed previously in 27 DAS shoots, *miR172* expression was decreased to approximately half of wild-type levels in the *d1* mutant at 14 DAS. *MiR172* expression increased in response to exogenous GA application in both the wild-type and *d1* mutant genotypes, but GA treatment was not sufficient to restore *miR172* expression to wild-type levels in the *d1* mutant. These results indicate that GA represses *miR156* and enhances *miR172* expression, with *miR172* being more sensitive to endogenous and exogenous GA levels.

The epc1 mutation generally reduces miRNA expression

The predicted function of *epc1* as a nuclear exportin involved in microRNA biogenesis indicates that reduced *miR156* and/or *miR172* levels may condition the observed acceleration in shoot maturation. When examined at 27 days after sowing (Figure 2.6), we observed significant decreases in both *miR156* and *miR172* expression in the *epc1* mutant shoot apices relative to wild-type. However, we also found that *miR166,* whose levels are typically stable in vegetative phase change mutants and thus serves as a control reference miRNA, also were reduced in the *epc1* mutant relative to wild-type. We then compared the relative accumulation of additional miRNAs in *epc1* versus wild type from shoot apices at 12 or 27 DAS (Figure 2.6). All of the tested miRNAs (*miR156, miR172, miR166*, *miR168*, and *miRc1*) showed decreased levels for the *epc1* mutant relative to wild-type, whether examined at 12 or 27 days after sowing. It

was also observed that *epc1* had a stronger effect on reducing *miR156* and *miR172* levels at 12 compared to 27 DAS. The strong reduction in *miR156* expression in the *epc1* mutant at 12 DAS was also reflected in lower relative *Gl15* expression compared to wild-type, and is consistent with the earlier onset of adult leaf identity observed in *epc1* mutants. These results support the view that *epc1* conditions a general decrease in miRNA production by interfering with miRNA export from the nucleus during their biogenesis.

Functional redundancy among miRNA172 loci during vegetative phase change

The maize genome harbors 5 *miR172* loci, which are named *zma-miR172a-e* (Sanger miRNA database add website), each of which could potentially regulate *Glossy15*. Earlier studies showed that the *tasselseed4* phenotype is caused by a mutation in *zma-miR172e*, which alters inflorescence development but not vegetative phase change (Chuck et al., 2007b). Previous studies have established the importance of mature *miR172* (not including *miR172e*) levels in regulating vegetative phase change, but were not capable of determining the contributions of individual *miR172* loci. Although each locus produces an identical mature *miR172*, the loop regions within each precursor are different. Using a previously described method for RT-PCR assays for specific pre-miRNAs (Schmittgen et al., 2004), primer sets were designed where the forward primer binds in the loop region and the reverse primer is designed to anneal immediately after the stem-loop region.

These primers were tested in RT-PCR assays of samples from various developmental stages which demonstrated that all five maize *miR172* precursors are indeed expressed in at least one tissue or developmental stage (Fig.2.7A). *MiR172c* is expressed only in adult leaf tissues, but *miR172a, miR172b, miR172c* and *miR172e* are present in shoot apical meristems and adult tissues (Fig. 2.7A). Further analysis of the *miR172* precursors during shoot development of normal plants, in mutations affecting vegetative phase change, and following GA application found overlapping expression patterns for *miR172a, miR172b, miR172d* that were similar to those observed for mature *miR172* (Fig. 2.4) Expression levels for each of the three *miR172s* were reduced in *Cg1* and *d1* (Fig. 2.7B). The three *miR172* precursors express strongly in adult leaves (Fig. 2.7C) and show increased transcription through vegetative phase change (Fig. 2.7D). The three *miR172s* also respond to GA in a similar fashion (Fig. 2.7E) to the response of mature *miR172* to GA (Fig. 2.5D). The expression profile of the *miR172e* precursor does not correlate as closely with the above mentioned patterns, but does show stronger expression in adult leaves. The stronger expression of all five *miR172* precursors in adult leaves is complementary to the higher expression of *Glossy15* in juvenile leaves.

Transgenic plants with miRNA target mimics.

A total of five transgenic lines were generated with the *miR172* target mimic construct and another 15 transgenic lines were created with the *miR156* target mimic construct. Each of the successfully regenerated transgenic plants

was crossed to the H99 inbred line. At least 16 T_1 progeny seeds from each of these crosses were grown in the field and genotyped by PCR for the DsRed transgene. Plants testing positive for DsRed were also examined for DsRed transgene expression in leaf tissues by RT-PCR, most of the T_1 lines indeed showed DsRed expression. Under the field conditions, DsRed positive and DsRed negative plants didn't show any differences in leaf identity, flowering time or shoot architecture when compared to the control H99 inbred line. These observations indicate that although the miRNA mimic transgenes are expressed, they do not sufficiently reduce *miR172* or *miR156* levels to produce a phenotypic effect.

Leaf samples from 3 DsRed positive plants were collected from each T_1 family and tested for red fluorescence by imaging with a fluorescent microscope. The leaves of wild type plants exhibit autofluoresence (Stewart, 2006) but plants expressing DsRed will show stronger fluorescence compared to wild-type. Only one line appeared to show significant DsRed accumulation, despite our prior observation that the DsRed transgene was actively transcribed. This result suggests the DsRed protein within the miRNA target mimic transgenes may not be translated efficiently or does not assemble properly into its active form.

GAs and Glossy15 interact in an antagonistic and dosage-sensitive manner to specify leaf identity

Transgenic maize lines that overexpress *Glossy15* (*Gl15-TG)* were described previously (Lauter et al., 2005), where they increase the number of

juvenile leaves and delay shoot maturation in a dosage-dependent manner. Conversely, GAs promote vegetative phase change by increasing *miR172* and possibly decreasing *miR156* (Figure 2.5). Treatment of wild-type, *d1* mutant and *Gl15-TG* plants with different amounts of GA provides an opportunity to investigate the effects of varying the relative balance of factors that either promote (e.g. GA) or inhibit (*Gl15*) vegetative phase change. The results from such an experiment are shown in Figure 2.8, where *Gl15* activity was increased relative to wild-type when either hemizygous or homozygous for *Gl15-TG*, and GAs were reduced relative to wild-type in the *d1* mutant, or increased by treatment with either 25μg or 50μg of GA_3 during early shoot development. First Leaf Macrohairs (FLH) and Last Leaf Wax (LLW) were chosen as phenotypes to represent juvenile and adult leaf identity, whereas the width of leaf five was chosen as a GA-responsive phenotype and control for GA application. The effects of *Gl15-TG* and GA on subsequent shoot maturation were monitored by counting the total number of vegetative nodes.

In the absence of any GA treatments, both the *d1* mutation (approximately one leaf) and *Gl15-TG* (approximately two leaves) had their expected effects on delaying the transition from juvenile to adult leaf identity. In the H99 background, two doses of *Gl15-TG* produced only a slightly greater delay in the onset of leaf hairs/loss of juvenile wax compared to one dose. As expected, GA, but not *Gl15-TG*, influenced leaf width. Leaf width was increased by approximately 12 mm in the *d1* mutant, and reduced by approximately 12 mm by GA treatment in the H99 background regardless of *Gl15-TG* dosage. GA treatment of *d1* mutants restored

leaf width comparable to that of wild-type (Fig. 2.8a). The total number of nodes appeared to increase in an additive manner by approximately 1.5 leaves with dose of *Gl15-TG* or the *d1* mutation, and approximately three leaves when *d1* and *Gl15-TG* were combined together. The GA applications in wild-type plants led to the production of two fewer total nodes, but caused a reduction of at most one node in the *Gl15-TG* or *d1* backgrounds. The GA treatments produced the strongest reductions in total nodes in the *d1; Gl15-TG* combination, two leaves with 25µg GA and almost four with 50µg GA (Fig. 2.8b).

Exogenous GA application accelerated the transition to adult leaf identity in all genotypes (Fig. 2.8c and 2.8d). Typically, the 25µg GA treatment was sufficient and little difference was obtained with the higher dose of GA. In the wild-type H99 background, GA application accelerated the production of leaf hairs by about one-half leaf and adult leaf waxes by approximately two leaves. GA application completely reversed the effects of the *d1* mutation, with the FLH and LLW phenotypes appearing similar to wild-type plants treated with GA. The 25µg GA treatment completely counteracted the effect of one dose of *Gl15-TG* on FLH; however, homozygous *Gl15-TG* plants are more resistant to exogenous GA. Exogenous GA did reduce the effects of *Gl15-TG* on increasing LLW*,* but even the 50µg GA treatment was not sufficient to completely counteract the effect of hemizygous *Gl15-TG*. The production of juvenile waxes in homozygous *Gl15-TG* plants was essentially resistant to exogenous GA treatments.

Taken together, the results of the above experiment demonstrate that GA and *Gl15* act antagonistically to regulate vegetative phase change, and that this

process is sensitive to relative quantitative changes in either GA or *Gl15* levels. For leaf identity phenotypes (FLH, LLW), the non-additive effects when GA is reduced and *Gl15* is increased (*d1; Gl15-TG* genotype) indicate these two factors interact in the same pathway to specify leaf identity. However, GA and *Gl15-TG* appear to act additively for shoot maturation (leaf width and total nodes).

Discussion

The above studies further demonstrate that GAs, *miR156*, *miR172*, and *Gl15* are each important regulators in vegetative phase change and leaf identity in maize. Analysis of *gl15* mutant alleles and their expression, the expression of *miR156* and *miR172* in known mutants affecting vegetative phase change, and the effects of altered GA levels reveals additional details about how these factors interact to either promote or inhibit vegetative phase change. Many features of the regulatory network for vegetative phase change in maize are consistent with our understanding of this process in Arabidopsis; however some of the findings from our maize work were not evident in the Arabidopsis system and although many aspects of the regulatory network for vegetative phase change are conserved between maize and Arabidopsis, important differences also exist.

Prior studies of both loss-of-function *gl15* mutations and the gain-of-function *Gl15-TG* lines have established *Glossy15* as being both necessary and sufficient to program juvenile leaf identity. However, the molecular basis for the mutant phenotypes observed in *gl15* mutant alleles remained largely unknown. Data presented in this chapter determined the DNA sequence changes for seven

gl15 mutant alleles, each of which were mediated by transposon insertions or aberrant excisions within the *gl15* transcription unit. qRT-PCR analyses of the relative *gl15* mRNA expression from the entire collection of 12 independently-isolated *gl15* alleles find that all but one show reduced mRNA levels, with three alleles (*gl15-S, gl15-911642*, and *gl15-ILP*) still showing at least half the mRNA expression observed in wild-type, indicating these alleles are defective in protein function rather than transcription.

miR156 and miR172 converge to regulate Glossy15

Analysis of genotypes where either the *gl15* mutation or the *Gl15-TG* overexpression transgene are combined with other mutants affecting vegetative phase change (Moose and Sisco, 1994; Kampani, 2003) demonstrate that *Gl15* is the major gene regulating juvenile versus adult leaf identity, but acts downstream of other factors that regulate vegetative phase change. Each of the other mutant loci that delay vegetative phase change (*Cg1*, *Tp1*, *Tp2*, *d1*) express higher levels of *miR156* and reduced levels of *miR172* (Figs. 2.4, 2.5, and 2.7). Conversely, GAs promote greater *miR172* accumulation and accelerate vegetative phase and the *epc1* mutant has lower levels of *miR156* (Fig. 2.6). *Gl15* mRNA is directly cleaved by *miR172*, and *Gl15* mRNA expression during shoot development is always observed to be inversely correlated with that of *miR172*. Thus, the strong coupling between the specification of leaf identity with vegetative phase change during normal shoot development, and the phenotypic effects of all known phase change mutants on the expression of juvenile leaf

identity traits can be explained by alterations in *miR156* and *miR172* levels, which then converge to impact the relative activity of *Gl15*. Recent work with Arabidopsis indicates that *miR156* functions upstream of *miR172*. Importantly, *SPL9*, one of the targets of *miR156* in Arabidopsis, binds to the promoter region of *miR172b,* indicating direct molecular interactions among each of the *miR156, SPL, miR172,* and *AP2* genes in the phase change pathway (Wu et al., 2009). In maize, similar SPL binding sites (GTAC over-represented motifs) are present in the upstream flanking sequences of the *zma-miR172d* precursor (data not shown), raising the possibility that direct interactions between SPL proteins and *miR172* also occur in maize.

The role of GAs in regulating phase change

GAs have been shown to promote both vegetative and reproductive phase change in Arabidopsis, maize, and many other plant species. However, the mechanism by which GAs modulate the molecular pathway defined by *miR156-SPL* and *miR172-AP2* interactions has not yet been investigated. The experiments described in this thesis characterized how both reductions in GA synthesis (the *d1* mutant, Spray et al., 1996) and additional exogenously applied GA_3 affected the relative expression of mature *miR156* and *miR172*, as well as three different *miR172* precursors, during maize shoot development. GAs promote *miR172* and repress *miR156* expression, but appear to have a stronger effect on *miR172* levels, particularly during early (12 DAS) compared to late (27 DAS) shoot development. Although the regulatory interactions between *miR156*

and *miR172* are still poorly defined in maize, the results obtained suggest that GAs more directly influence *miR172* compared to *miR156* expression. This interpretation is supported by prior observations (Evans et al., 1995) and confirmed here (Fig. 2.7) that leaf identity traits are more sensitive to changes in GAs compared to the onset of flowering time. Although not tested directly, it is possible that the induction of *miR172* by GAs is in fact mediated by one or more SPL proteins, which could explain why GAs also affect *miR156* levels.

The finding that GAs increase *miR172* and decrease *miR156* levels in maize may have general functional significance to phase change. GAs affect leaf shape and size (Fig. 2.8), features that have been shown to be mediated by *miR156* activity in Arabidopsis (Wang et al., 2009), and that differ between juvenile and adult leaves independently from *Gl15* (Fig. 2.8). GAs modulate sensitivity to photoperiod and flowering time (Musa-Gottgens and Hedden, 2009) and promote flowering in maize (e.g. Fig. 2.7), which could be mediated by GA induction of either *SPL* genes or *miR172.* It has been previously shown in Arabidopsis that *miR172* functions to link photoperiod response with the induction of flowering (Jung et al., 2007). GAs are also critical to the transition from embryonic development to seed dormancy to seed germination. During seed maturation, GA_3 and GA_8, the terminal downstream products of GA_{20} decrease from 14 DAP to 27 DAP (White et al., 2000), which coincides with the onset of dormancy and could explain why *miR172* levels are initially very low in developing shoots. Conversely, the onset of *miR172* expression may reflect the

effects of an increase in bioactive GAs within seedling shoots (the plumule) immediately following seed imbibition and germination (Rood et al., 1983).

A revised model for the specification of leaf identity in maize

A number of features of vegetative phase change in maize suggest that leaf identity is regulated by factors that originate outside of the shoot apical meristem and act simultaneously on undetermined cells throughout the shoot apex (Kerstetter and Poethig, 1998). Transition leaves typically express juvenile traits in the distal portions of the leaf that differentiate first, and in a progressively smaller region at the tip of successive leaves. This is the pattern expected if the switch for vegetative phase change was relatively abrupt and those cells within the apex or pre-existing leaf primordial whose identity had not yet been determined were then programmed to express adult traits. Clonal analysis of transition leaves demonstrated that the phase-specific identity of maize leaves is determined after they are initiated (Moose and Sisco, 1994; Orkwiszewski and Poethig, 2000). Furthermore, when the shoot apex from plants that have transitioned to the adult phase is excised and cultured *in vitro*, those leaves that were already present on these apices were “rejuvenated” in proportion to their relative age at the time of culture, with the oldest leaves having the most cells expressing juvenile identity (Irish and Nelson, 1988; Irish and Karlen, 1998; Orkwiszewski and Poethig, 2000). Leaves initiated after the start of the culture period developed either as transition leaves or fully adult leaves. It has long been noted that the first five or six seedling leaves in maize are initiated in the

embryo (Abbe and Stein, 1954; Hubbard, 1951), which coincides with the typical number of juvenile leaves in maize genotypes. Thus, it appears that during normal maize shoot development, factors that promote the switch to the adult phase act soon after germination.

The apex- or meristem-patterning model described above can explain observed patterns of transitions between leaf identities in maize and other plants, and the appearance of chimeric shoots following the transition from vegetative to reproductive growth (Hempel et al., 1998). However, the question then arises as to the nature of the factor(s) that act globally on the apex and undetermined organ primordia? The root system does not appear to be the source for factors promoting vegetative phase change in maize, because rejuvenated adult maize shoots do not produce roots until after new adult leaves have initiated (Orkwiszewski and Poethig, 2000) and maize mutants with greatly impaired root systems still have normal vegetative phase change (Hochholdinger et al., 1996). Floral induction is often mediated by factors produced by leaves, and it has previously been proposed that shoot maturation depends on factors produced by existing leaf primordia (Irish and Karlen, 1998). It is known that GAs are synthesized in leaves (Eisenreich et al., 2001, Kasahara et al., 2002), rapidly increase in the maize shoot following germination (Rood et al. 1983), and act globally on shoot development. The properties of GAs, when coupled with our finding that GAs induce *miR172* levels, suggest that GAs may be the factor that programs the transition from juvenile to adult leaf identity in maize.

In our “GA-patterning” model (Fig. 2.9), we propose that the amounts of active GAs, derived from both the germinating seed and new synthesis in young leaves, rise in the maize shoot following germination. Initially in normal shoots, the levels of *miR156* are sufficient to attenuate the induction of *miR172* by GA. As *miR156* expression declines beginning approximately six days after sowing, GAs would increase *miR172* levels but *Gl15* activity remains high enough to counteract *miR172* and maintain juvenile leaf identity. Orkwiszewski and Poethig (2000) showed that an eight-day-old maize seedling has initiated eight leaves, where the eighth leaf is often a transition leaf expressing juvenile identity at the tip and adult identity at its base. By approximately 12 days after sowing, *miR172* expression becomes sufficient to downregulate *Gl15* below the threshold required to repress adult and promote juvenile leaf identity traits, leading to adult leaf identity in the later maturing portions of transition leaves, and all subsequently initiated leaves.

The “GA-patterning” model can explain a number of features associated with altered vegetative phase change in maize. The fact that neither the *epc1* mutant nor null alleles of *gl15* completely eliminate the juvenile phase is consistent with the juvenile identity of the first two leaves being the “default” state that is determined independently from *Gl15* during late embryogenesis when active GA levels are very low. The onset of adult leaf identity occurs approximately one leaf earlier in *epc1* compared to *gl15* null mutant alleles, which may indicate the impact of reductions in *miR156* (Fig. 2.6). Our GA treatments of H99 or *d1* mutant shoots at 10 days after sowing (Fig. 2.8) were

sufficient to accelerate the onset of adult leaf identity by at least one leaf, indicating that GA levels within 10 DAS shoots were indeed limiting; conversely, increasing *Gl15* activity suppressed the effects of GA on promoting adult leaf identity. The rejuvenation of leaves produced from cultured adult shoot apices may reflect the loss of bioactive GA from more mature leaves, which could lead to decreases in *miR172* expression and a corresponding reactivation of *Gl15* until enough newly synthesized GA accumulates to again promote the transition to an adult leaf identity.

The pattern of juvenile wax production in the latest leaves from *Glossy15-TG* plants to express juvenile traits, which appears as stripes along the midrib and veins (Fig. 2.10), could also be explained by our model. The study of *narrow sheath* (*ns*) mutant in maize (Scanlon, 2000) pointed to the fact that founder cells in the leaf primordia dome will form midrib first and then progress toward formation of veins and leaf margins through recruitment of lateral meristem cells. The identity of these leaves would be determined relatively early in leaf development, and apparently is specified when *Gl15* activity remains in these leaf founder cells, and possibly throughout the entire L1 cell layer within the shoot apex. As additional cell divisions continue to expand the leaf in a lateral dimension, *Gl15* levels apparently have declined enough that they acquire and adult identity.

References

Abbe, E.C. and O.L. Stein. 1954. The Growth of the Shoot Apex in Maize: Embryogeny. *American Journal of Botany*, 41(4): 285-293.

Aukerman, M.J., and H. Sakai. 2003. Regulation of flowering time and floral organ identity by a microRNA and its APETALA2-like target genes. Plant Cell 15:2730-2741..

Bollman, K.M., M.J. Aukerman, M.Y. Park, C. Hunter, T.Z. Berardini, R.S. Poethig. 2003. HASTY, the Arabidopsis ortholog of exportin 5/MSN5, regulates phase change and morphogenesis. *Development* 130(8):1493-1504.

Chuck, G., A.M. Cigan, K. Saeteurn, S. Hake. 2007. The heterochronic maize mutant Corngrass1 results from overexpression of a tandem microRNA. *Nat Genet*, 39(4):544-549.

Chuck, G., R. Meeley, E. Irish, H. Sakai, and S. Hake. 2007b. The maize tasselseed4 microRNA controls sex determination and meristem cell fate by targeting Tasselseed6/indeterminate spikelet1. Nature Genetics 39:1517-1521.

Chuck, G., C. Whipple, D. Jackson and S. Hake. 2010. The maize SBP-Box transcription factor encoded by tasselsheath4 regulates bract development and the establishment of meristem boundaries. Development 137: 1243-1250.

Christensen, A.H., and P.H. Quail. 1996. Ubiquitin promoter-based vectors for high-level expression of selectable and/or screenable marker genes in monocotyledonous plants. Transgenic Research 5:213-218.

D'Halluin, K., E. Bonne, M. Bossut, M.D. Beuckeleer, J. Leemans. 1992. Transgenic Maize Plants by Tissue Electroporation. The Plant Cell 4:1495-1505.

Dudley, M., R.S. Poethig. 1993. The Heterochronic Teopod1 and Teopod2 Mutations of Maize Are Expressed Noncell-Autonomously. *Genetics* 133(2):389-399.

Ebert, M.S., J.R. Neilson, and P.A. Sharp. 2007. MicroRNA sponges: competitive inhibitors of small RNAs in mammalian cells. Nature Methods 4:721-726.

Eisenreich, W., Rohdich, F., and Bacher, A. 2001. Deoxyxylulose phosphate pathway to terpenoids. *Trends Plant Sci.* 6: 78–84.

Evans, M.M.S., H.J. Passas, R.S. Poethig. 1994. Heterochronic Effects of Glossy15 Mutations on Epidermal-Cell Identity in Maize. *Development* 120(7):1971-1981.

Evans, M.M.S., R.S. Poethig. 1995. Gibberellins Promote Vegetative Phase-Change and Reproductive Maturity in Maize. *Plant Physiology* 108(2):475-487.

Evans, M.M.S., R.S. Poethig. 1997. The viviparous8 mutation delays vegetative phase change and accelerates the rate of seedling growth in maize. *Plant Journal* 12(4):769-779.

Galinat, W.C. 1966. The corngrass and teopod loci involve phase change. *Maize Genet Coop. News Lett.* 40, 102-103.

Gallavotti, A., J.A. Long, S. Stanfield, X.A. Yang, D. Jackson, E. Vollbrecht, and R.J. Schmidt. 2010. The control of axillary meristem fate in the maize ramosa pathway. Development 137:2849-2856.

Hempel, F.D., P.C. Zambryski, and L.J. Feldman. 1998. Photoinduction of flower identity in vegetatively biased primordia. Plant Cell 10:1663-1675.

Hochholdinger, F., Wetz, W and Feix, G. 1996. Juvenile-adult phase transition of vegetative traits is not affected in the root deficient mutant *rtcs. Maize Genetic Cooperation Newsletter* 70: 23.

Hubbard, J.E. 1951. Leaf patterns in mature embryos of inbred lines of corn. M.S. thesis, University of Illinois.

Irish, E.E., and T.M. Nelson. 1988. Development of Maize Plants from Cultured Shoot Apices. Planta 175:9-12.

Irish, E.E., and S. Karlen. 1998. Restoration of juvenility in maize shoots by meristem culture. International Journal of Plant Sciences 159:695-701.

Kampani, A.V. 2003. The generation and characterization of the maize Glossy15 transgenic line. Master Thesis, University of Illinois at Urbana-Champaign.

Kasahara, H., Hanada. A., Kuzuyama, T., Takagi, M., Kamiya, Y., and Yamaguchi, S. 2002. Contribution of the mevalonate and methylerythritol phosphate pathways to the biosynthesis of gibberellins in Arabidopsis. *J. Biol. Chem. 277*: 45188–45194.

Kerstetter, R.A., and R.S. Poethig. 1998. The specification of leaf identity during shoot development. Annual Review of Cell and Developmental Biology 14:373-398.

Jung, J.H., Y.H. Seo, P.J, Seo, J.L., Reyes, J. Yun, N.H. Chua and C.M. Park. 2007. The GIGANTEA-regulated microRNA172 mediates photoperiodic flowering independent of CONSTANS in Arabidopsis. *Plant Cell* 19: 2736-2748.

Lauter, N., A. Kampani, S. Carlson, M. Goebel, S.P. Moose. 2005. microRNA172 down-regulates glossy15 to promote vegetative phase change in maize. *P Natl Acad Sci USA* 102(26):9412-9417.

Livak, K.J., T.D. Schmittgen. 2001. Analysis of relative gene expression data using real-time quantitative PCR and the 2(T)(-Delta Delta C) method. *Methods* 25(4):402-408.

Moose, S.P., Sisco, P.H. 1994. Glossy15 Controls the Epidermal Juvenile-to-Adult Phase-Transition in Maize. *Plant Cell* 6(10):1343-1355.

Moose, S.P., Sisco, P.H. 1996. Glossy15, an APETALA2-like gene from maize that regulates leaf epidermal cell identity. *Gene Dev* 10(23):3018-3027.

Moose, S.P., N. Lauter, and S.R. Carlson. 2004. The maize macrohairless1 locus specifically promotes leaf blade macrohair initiation and responds to factors regulating leaf identity. Genetics 166:1451-1461.

Moose, S.P., J.W. Dudley, and T.R. Rocheford. 2004b. Maize selection passes the century mark: a unique resource for 21st century genomics. Trends in Plant Science 9:358-364.

Musa-Gottgens, E. and Hedden, P. 2009. Gibberellin as a factor in floral regulatory networks. *J. Exp. Bot*. 60: 1979-1989.

Orkwiszewski, J.A., R.S. Poethig. 2000. Phase identity of the maize leaf is determined after leaf initiation. *P Natl Acad Sci USA* 97(19):10631-10636.
Poethig, R.S. 1988. Heterochronic Mutations Affecting Shoot Development in Maize. Genetics 119:959-973.
Raizada, M.N. and V. Walbot. A protocol for stable maize transformation. Protocol for department of biological sciences, Stanford university.
Rogler, C.E., W.P. Hackett. 1975. Phase-Change in Hedera-Helix - Induction of Mature to Juvenile Phase-Change by Gibberellin-a3. *Physiol Plantarum* 34(2):141-147.
Rood, S.B., R.P. Pharis, and M. Koshioka. 1983. Reversible conjugation of gibberellins *in situ* in maize. *Plant Physiol.* 73: 340-346.
Scanlon, M.J. 2000. NARROW SHEATH1 functions from two meristematic foci during founder-cell recruitment in maize leaf development. *Development* 127:4573-4585.
Schmittgen, T.D., J.M. Jiang, Q. Liu, L.Q. Yang. 2004. A high-throughput method to monitor the expression of microRNA precursors. *Nucleic Acids Res* 32(4):
Spray, C.R., M. Kobayashi, Y. Suzuki, B.O. Phinney, P. Gaskin and J. Macmillan. 1996. The dwarf-1 (dt) Mutant of Zea mays blocks three steps in the gibberellin-biosynthetic pathway. PNAS 93 (19): 10515-10518.
Stewart, C.N. 2006. Go with the glow: fluorescent proteins to light transgenic organisms. Trends in Biotechnology 24:155-162.
Telfer, A., K.M. Bollman, R.S. Poethig. 1997. Phase change and the regulation of trichome distribution in Arabidopsis thaliana. *Developmen* 124 (3): 645-654.
Telfer, A, R.S. Poethig. 1998. HASTY: a gene that regulates the timing of shoot maturation in Arabidopsis thaliana. *Development* 1998, 125(10):1889-1898.
Vega, S.H., M. Sauer, J.A.J. Orkwiszewski, R.S. Poethig. 2002. The early phase change gene in Maize. *Plant Cell* 14(1):133-147.
Wang, J.W., B. Czech, and D. Weigel. 2009. miR156-Regulated SPL Transcription Factors Define an Endogenous Flowering Pathway in Arabidopsis thaliana. Cell 138:738-749.
White, C.N., Proebsting, W.M., Hedden, P. and Rivin, C.J. 2000. Gibberellins and seed development in Maize. I. Evidence that Gibberellin/Abscisic Acid balance governs germination versus maturation pathways. *Plant Physiology* 122:1081-1088.
Wu, G., R.S. Poethig. 2006. Temporal regulation of shoot development in Arabidopsis thaliana by miR156 and its target SPL3. *Development* 133(18):3539-3547.
Wu, G., M.Y. Park, S.R. Conway, J.W. Wang, D. Weigel, R.S. Poethig. 2009. The sequential action of miR156 and miR172 regulates developmental timing in Arabidopsis. *Cell* 138: 750-759.

Zhang, L.F., J.M. Chia, S. Kumari, J.C. Stein, Z. Liu, A. Narechania, C. A. Maher, K. Guill, M.D. McMullen and D. Ware. 2009. A genome wide characterization of microRNAs genes in maize. Plos genetics 5 (11): e1000716

Table 2.1: Primers used in this chapter.

Expanding long template PCR primers	
Gl15_1245+	ACGAGATGGGCGCTGTGTATTC
Gl15_4504-	CACGGCGCAGGGACGATGGATG
***Glossy15* sequencing primers**	
Gl15_1440+	CCTGCTCAGAGATCTTTCGCTTTCCTTAC
Gl15_1900-	TGGCATTGCTCCTCCATCGT
Gl15_2014+	CCGCCACCCAGCAGTTCTTT
Gl15_2880+	CTGCCGCGTCAAATGCTTCAGATGA
Gl15_2933-	CAACACGAACTCCTCCTTGCTCAAG
Gl15_3373+	GACAAGGAGCTCCAGTCGCA
Gl15_4000R2-	ACGACAGGAAAGGCTCAGCAGC
***miR172* primary transcript (precursors) primers**	
Q195045(miR172d)F	CTCGATTGCTCAGTCCGGTTTC
Q195045(miR172d)R	TCGATCTGTGCATGATGAGATGAGAAT
Q35698(miR172b)F	GCTGCATGGTCGTTAATTCAATTCAT
Q35698(miR172b)R	ATCAGCAGACACTCACTAGCTCA
Q2147(miR172c)F	TTGTTGGGGTACGTTGGTGTGA
Q2147(miR172c)R	GTGATGTCTCGCAGCAGCTAT
Q40169(miR172a)F	CACAAACGTTCGTAGGCGCTT
Q40169(miR172a)R	CACAACCCATCAATCCGAACC
Q526464(miR172e)F	TGCATGAACACGCGCATTATGT
Q526464(miR172e)R	CAGCCGGTGATTTCTGGAGTG
Transgenic plants screening primers	
NPTIIF1	ATCTCCTGTCATCTCACCTTGC
NPTIIR1	CAAGCTCTTCAGCAATATCACG
DsRED(DNA)F	GCGAGATCCACAAGGCCCTGAA
DsRED(DNA)R	TGCTCCCGGCATCCGCTTA
DsRedF1(cDNA)	GCCCATAGTCTTCTTCTGCATTACG
DsRedR1(cDNA)	GTGGTGACCGTGACCCAGGA

Table 2.2: Leaf identity phenotypes of *glossy15* mutant alleles in common W64A inbred background.

	FLGL	FLH	LLW
W64A	7.75	6.75	10
W64A: *gl15-m1*	2.5	2.5	4
W64A: *gl15-H*	2.5	2.75	4
W64A: *gl15-L*	2.5	2.5	4
W64A: *gl15-S*	2.5	2.5	4
W64A: *gl15-956*	2.5	2.5	4
W64A: *gl15-911642*	2.25	1.75	3
W64A: *gl15-94317*	2.5	2.5	4
W64A: *gl15-63*	2.5	2.5	4
W64A: *gl15-C256A*	2.25	2.75	3
W64A: *gl15-46*	2.5	2.5	4
W64A: *gl15-98*	2.75	2.75	4
W64A: *gl15-ILP*	3.5	3.5	4
LH82: *gl15*	2	2.5	2

Figure 2.1: miRNA target mimic constructs. A. Anti-miRNA sequence for *miR172*. B. Tandem array of three anti-miRNA sequences. C. Insertion of miRNA target mimics at the 3'UTR of DsRED, expression of which is driven by the maize Ubiquitin promoter. D. Structure of selectable marker NPTII driven by CaMV35S promoter.

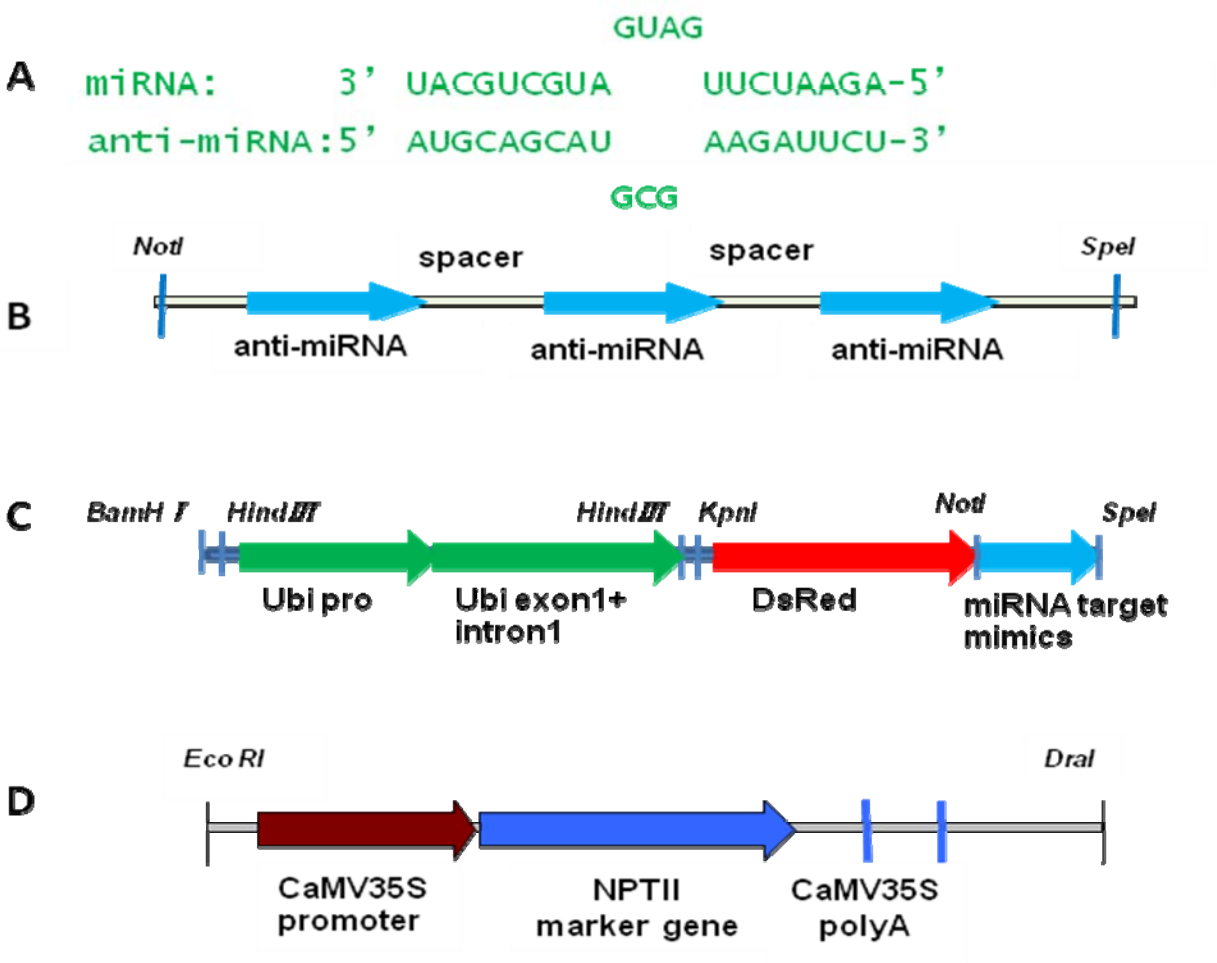


Figure 2.2a: Sequences of selected *glossy15* mutant alleles. Blue solid bars represent exons; green triangles represent insertions; large parenthesis indicate deletions and asterisks mark other small insertions/deletions compared to the reference *Gl15* genomic sequence from the W64A inbred line; red bar marks the region where *Gl15* qRT-PCR amplifies

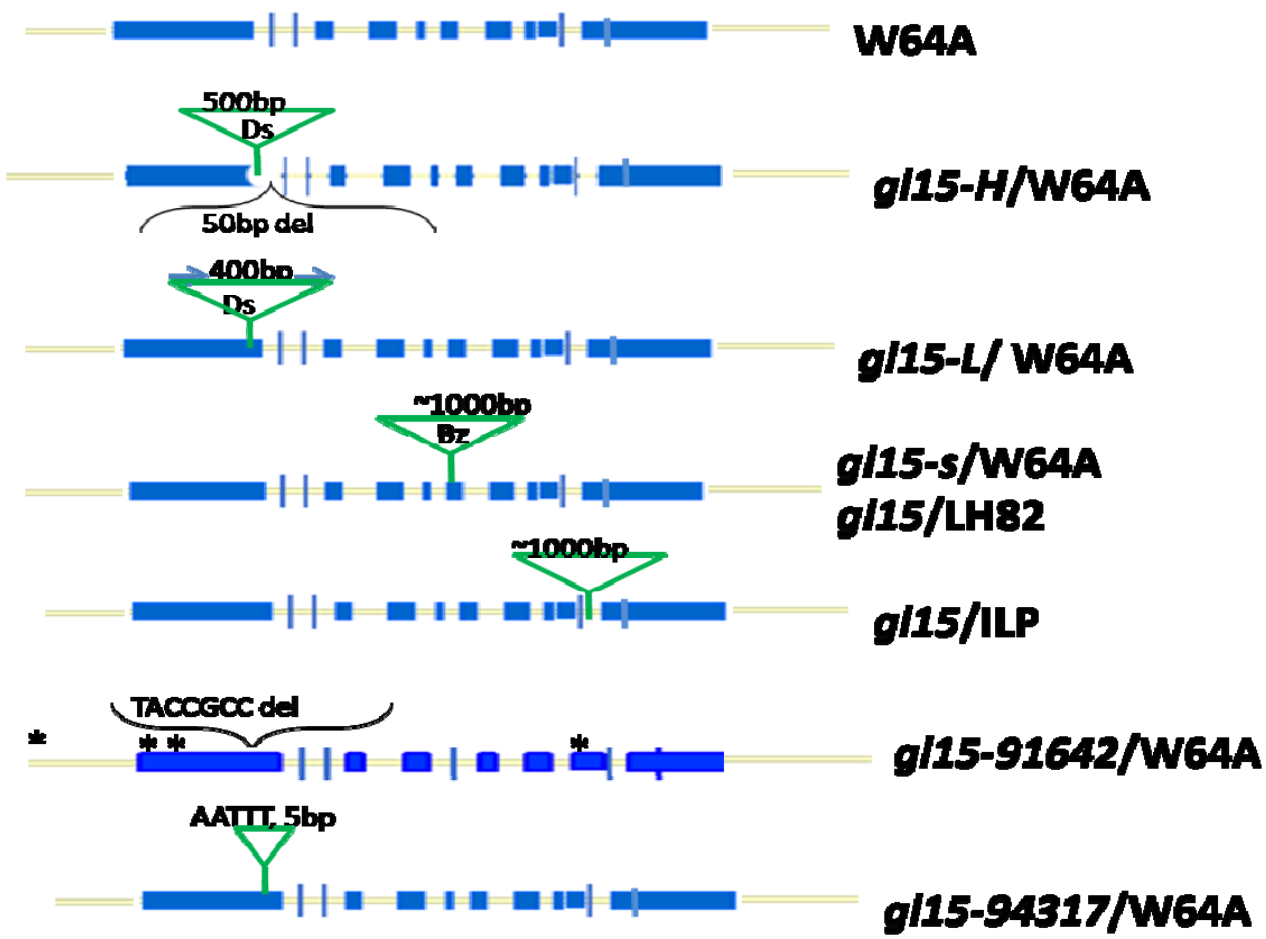


Figure 2.2b: *Glossy15* mRNA expression in shoot apical meristems of various *gl15* mutants when plants have three visible leaves. Expression values obtained via RT-PCR and reported relative to the W64A inbred line.

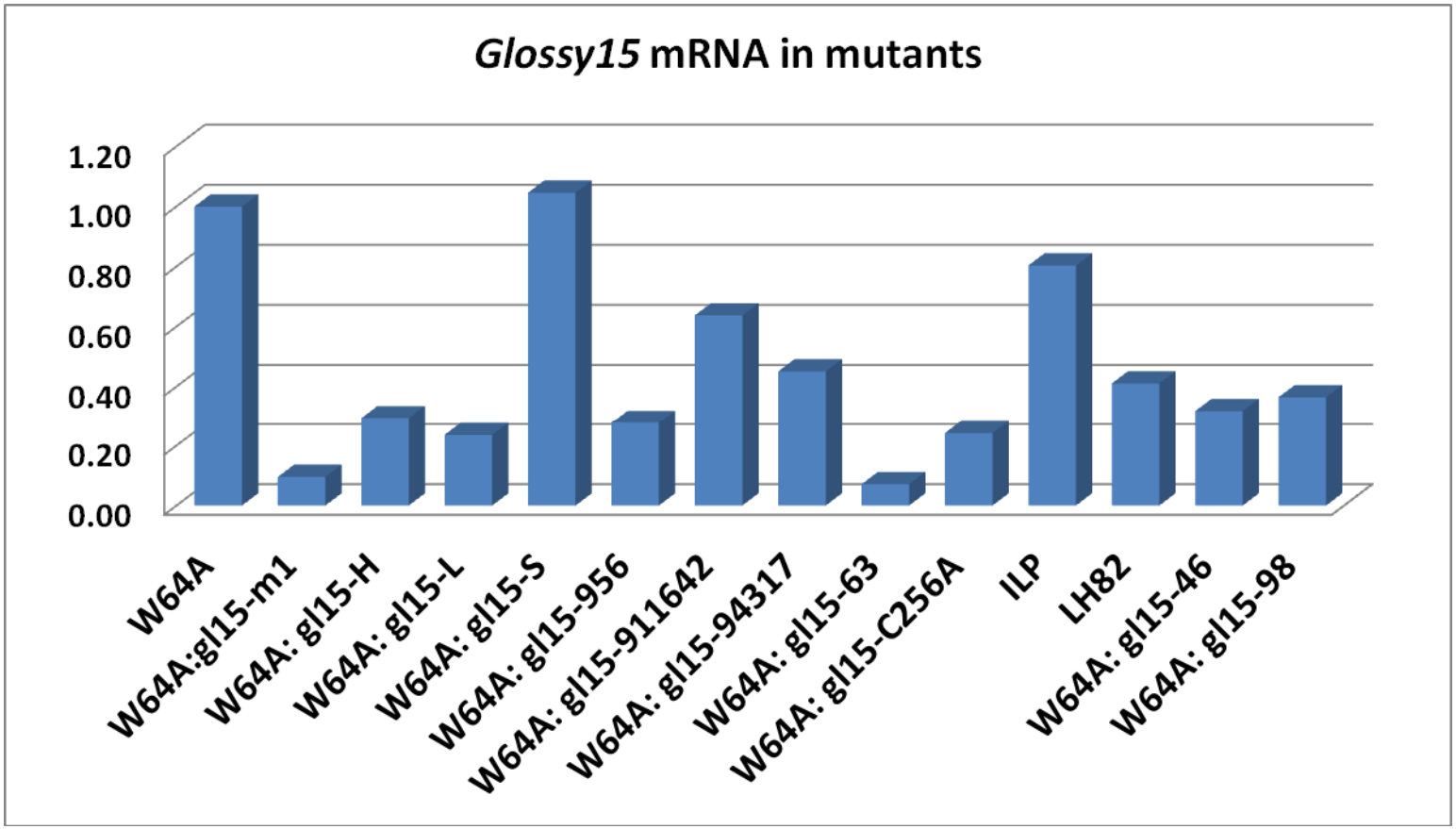


Figure 2.3: *miR156* declination and *miR172* accumulation during transition from juvenile to adult leaf identities. A, C and E: *miR172* relative expression. B, D and F: *miR156* relative expression. Abbreviation: L-Leaf; D: days after sowing (DAS).

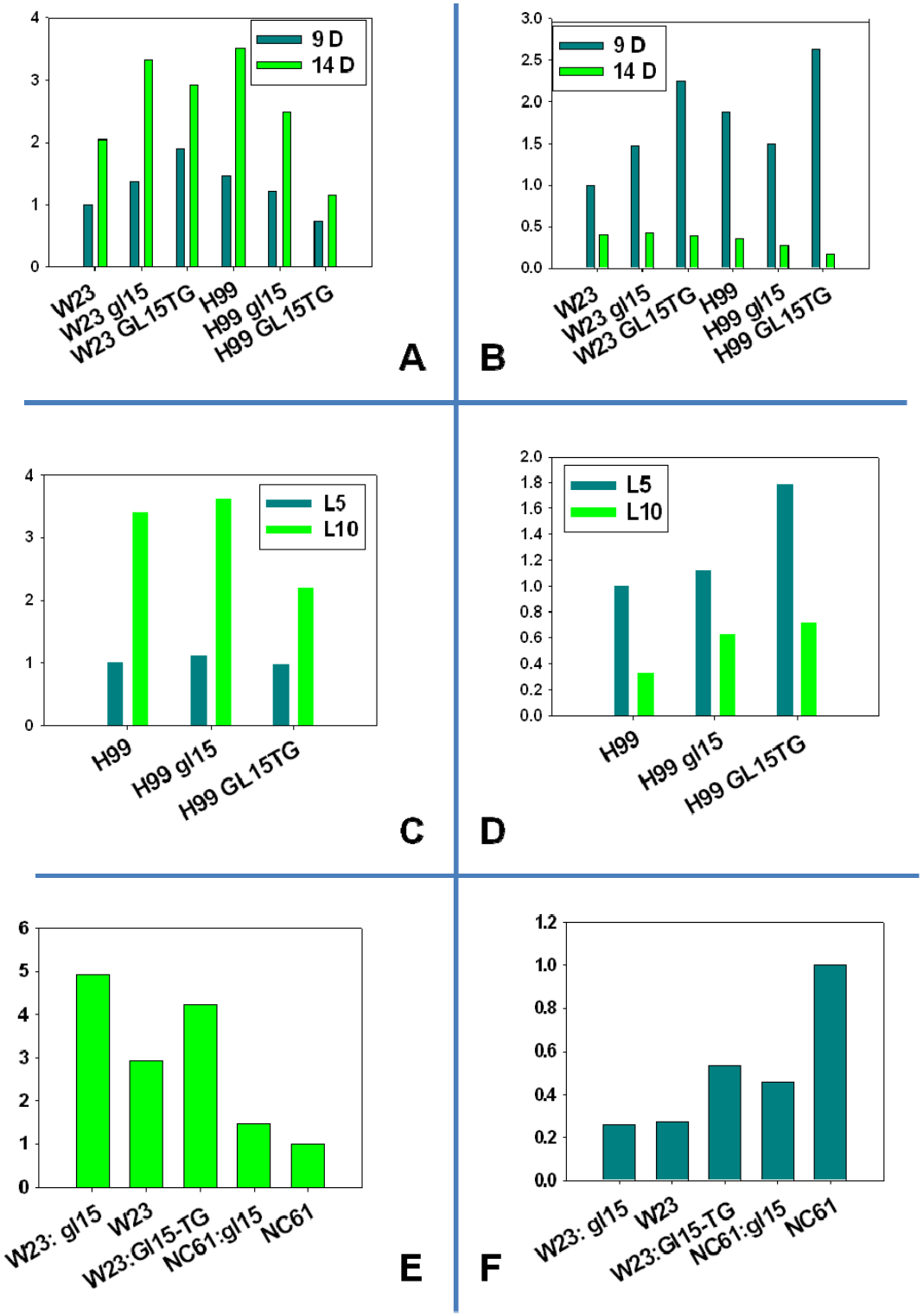


Figure 2.4: Relative *miR156* and *miR172* expression in mutants with delayed vegetative phase change. (a) Delayed phase change mutants could maintain a high level of *miR156* in later developmental stages (27 D), a time when wild-type plants have enter adult stage and marked by minimum *miR156* level. (b) At 27 days, *miR172* has increased to a level that represents the adult leaf stage, except in *Cg1* and *d1* mutants. *d1* mutants have half *miR172* as isogenic W64A at 27 DAS.

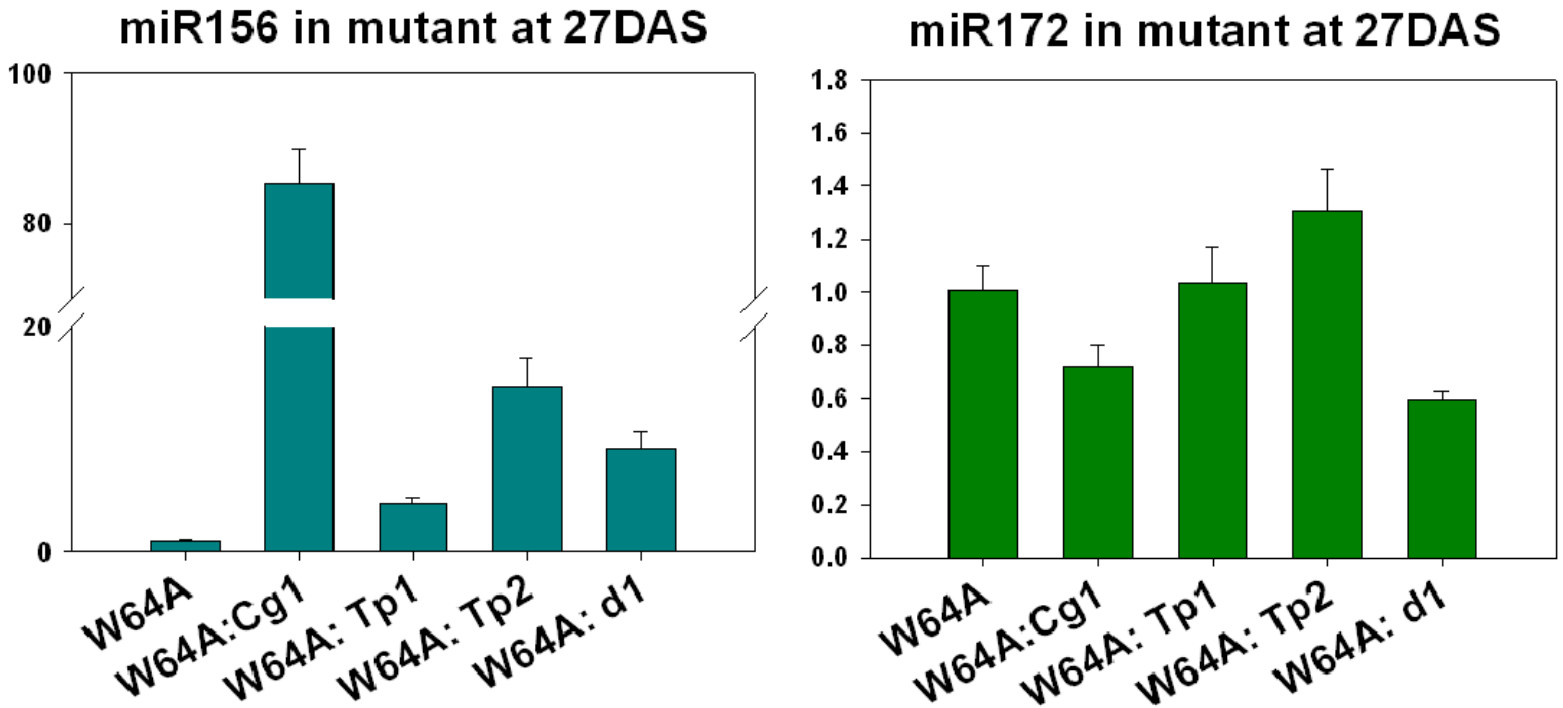


Figure 2.5: Relative expression of *miR156* (A) and *miR172* (B) in response to GA treatment.

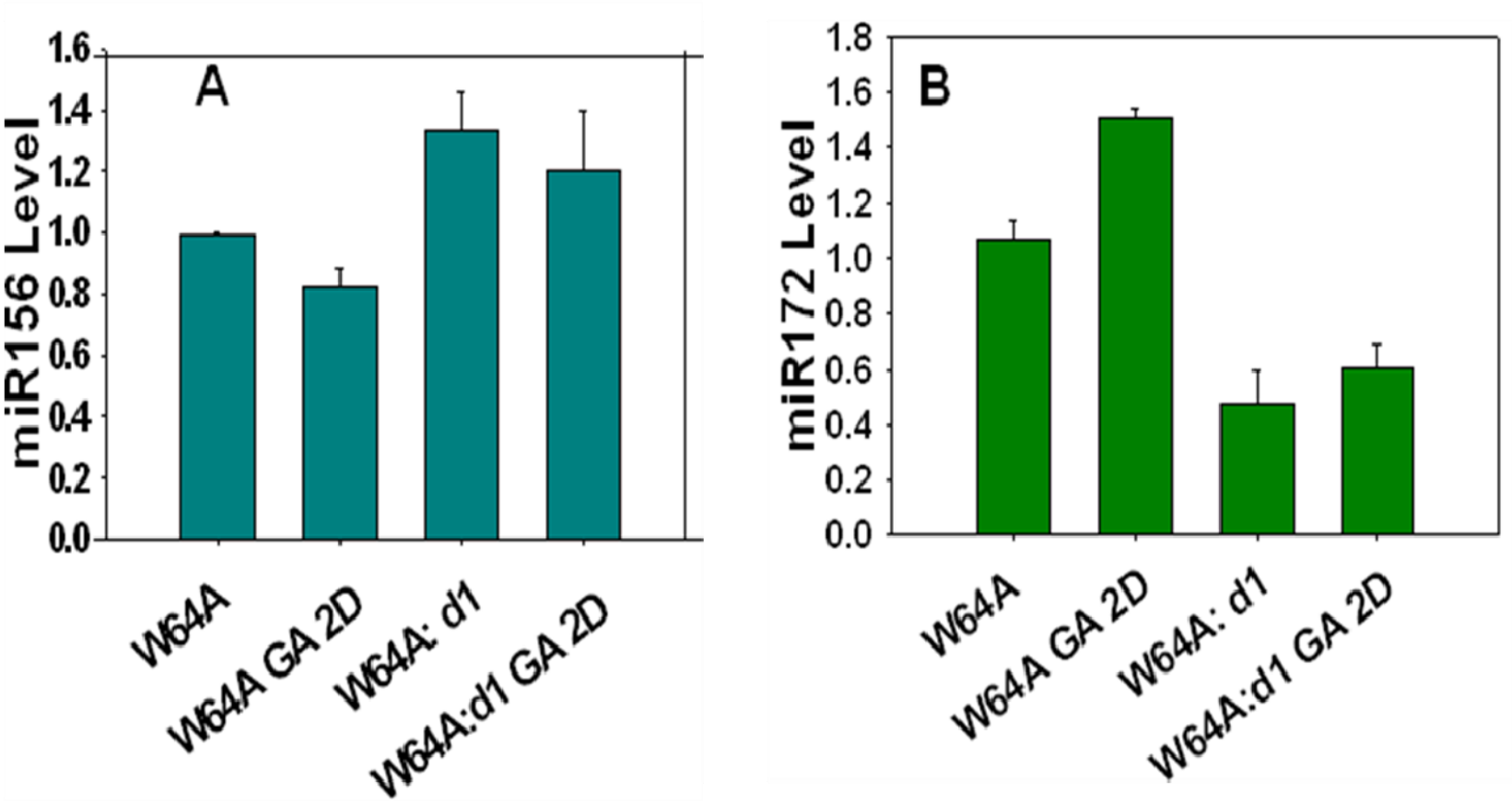


Figure 2.6: Reduced expression of miRNAs and *Glossy15* in the *Early vegetative phase change1* mutant. (a) Lower level of *miR156, sRc1* and *miR172* at 12 days in *epc1* comparing to those in W23. (b) Lower levels of miRNAs in *epc1* at 27 days.

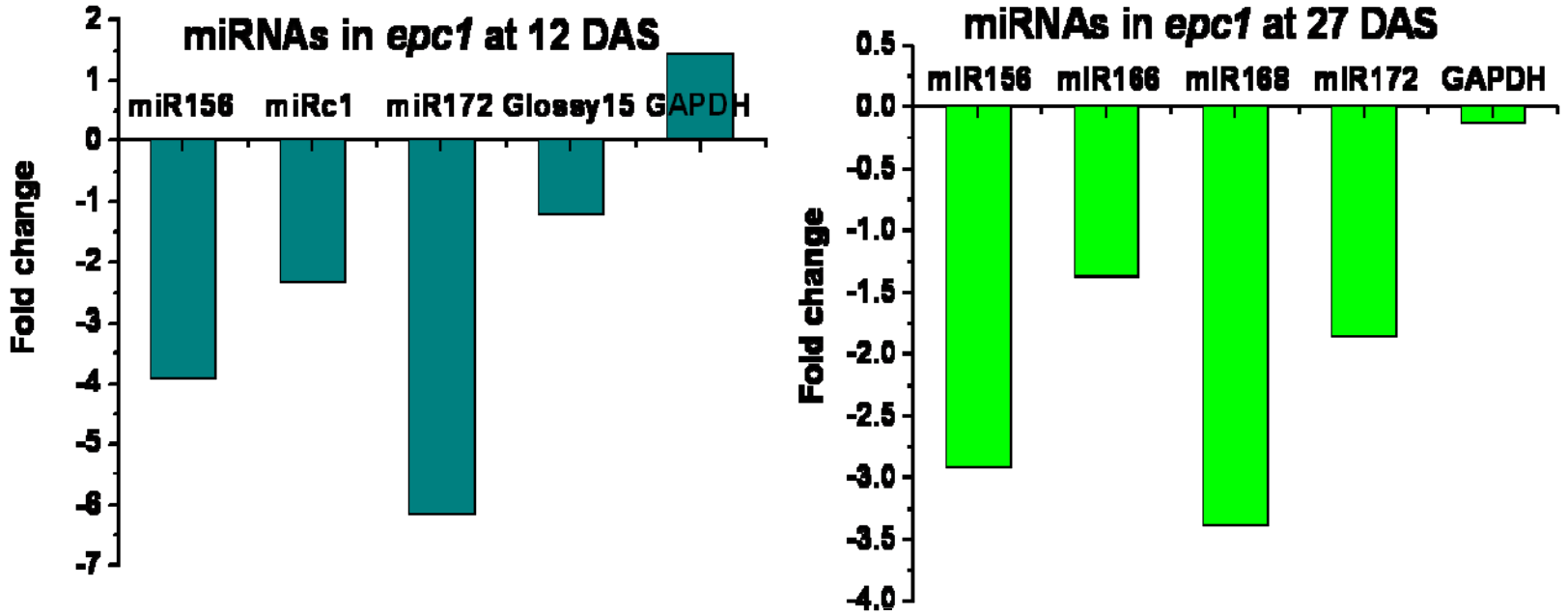


Figure 2.7: Expression profiles of individual pre-*miR172* transcripts. A. Profiling of *miR172* precursors in various developmental tissues. Lane 1-6 were samples from shoot apical meristems; lane 8 is from ear primordial at 48 days. Other abbreviations: DAS-days after sowing; J.L.-juvenile leaves; A.L.-Adult leaves; J.V.-veins from juvenile leaves; A.V.-veins from adult leaves.

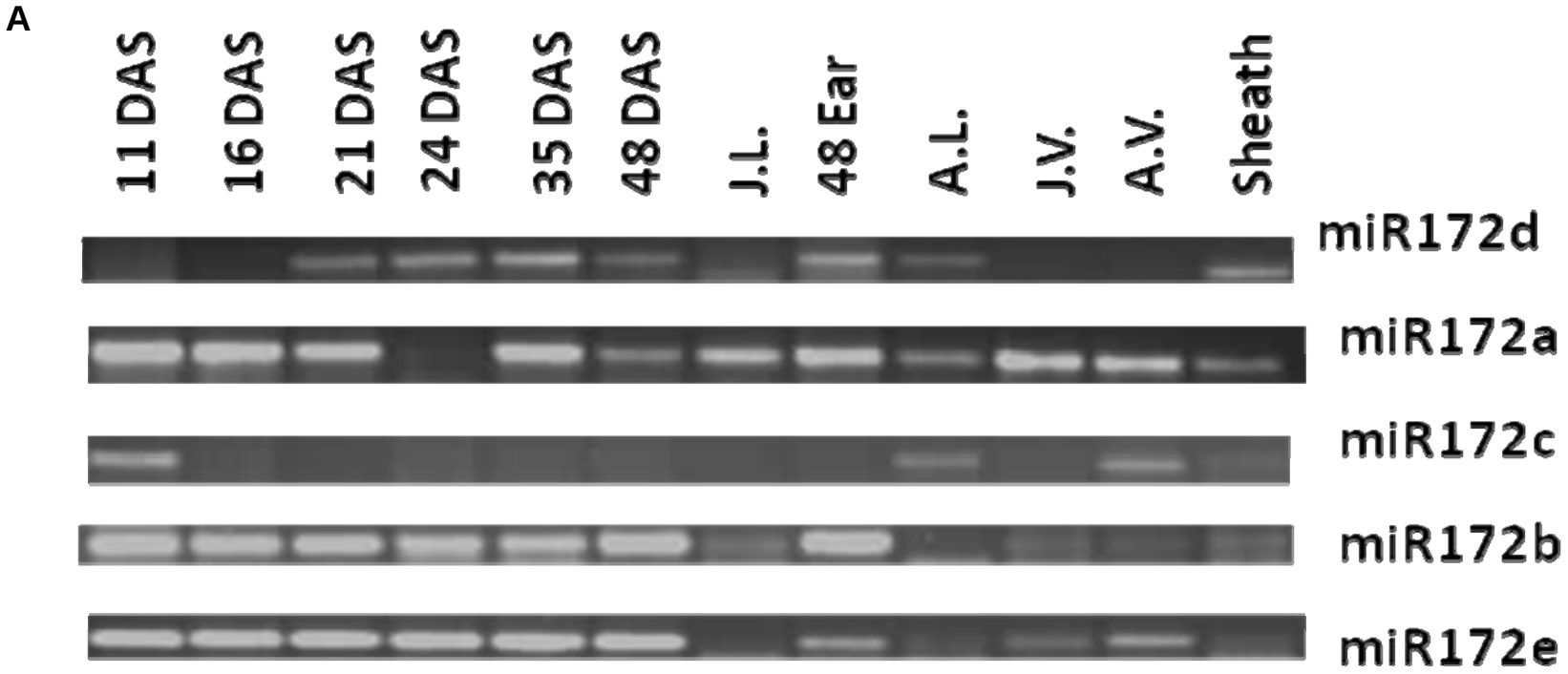


Figure 2.7 (continued): B: Relative expression in 27 DAS shoot apices of *miR172a*, *miR172b* and *miR172d* precursors in mutants that delay phase change compared to wild-type (W64A, set to relative expression of 1.0 for each *miR172* precursor). C: Increased transcription of *miR172* precursors in adult compared to juvenile leaves in B73. D: Increased transcription of *miR172* precursors during B73 shoot development (B73 at 7 days set to one for each precursor). E: Responsiveness of *miR172a*, *miR172b* and *miR172d* precursors to endogenous and exogenous GA.

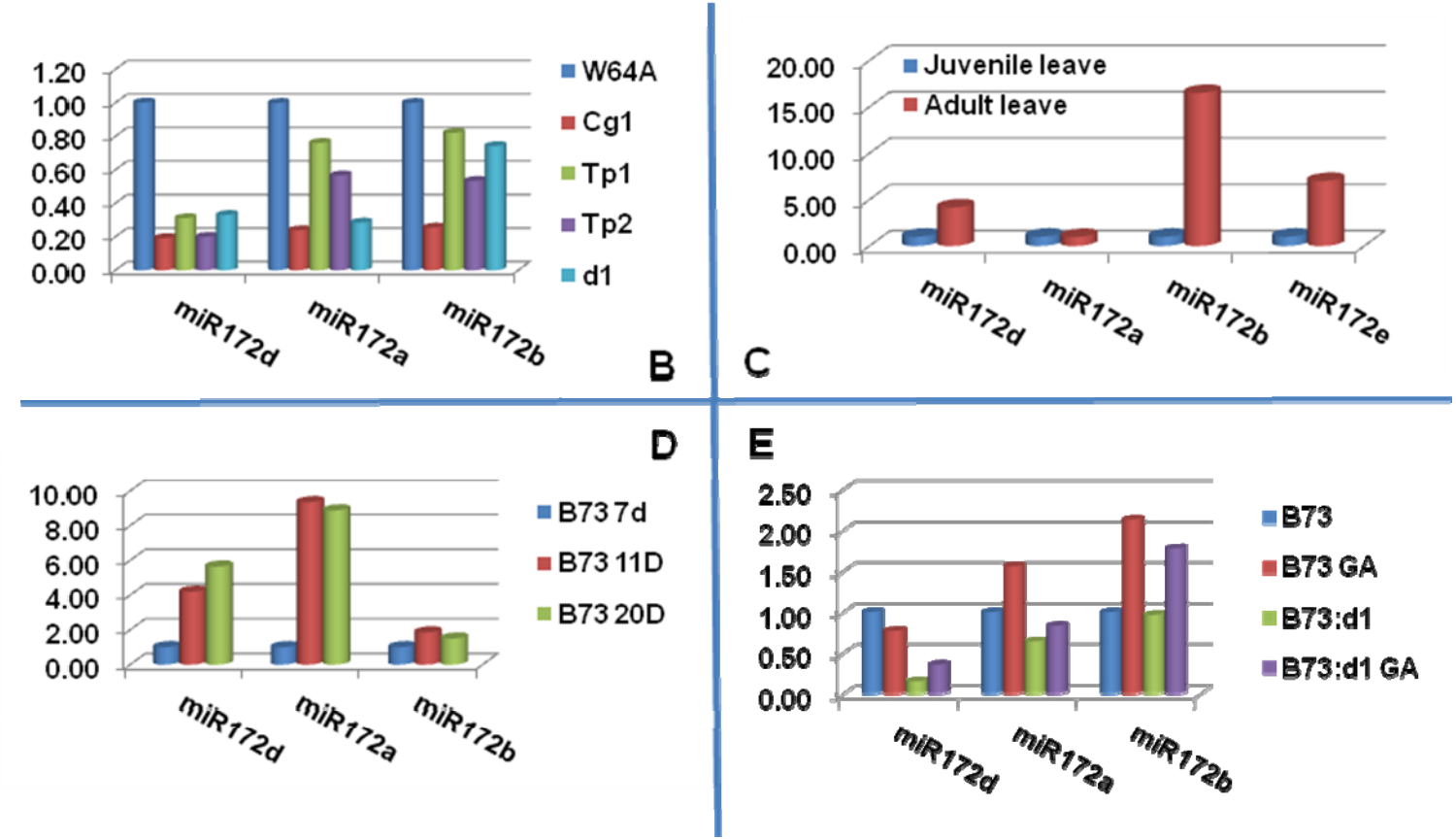


Figure 2.8: *Glossy15* and GA have opposite effects on vegetative phase change. (a) Leaf 5 Width, (b) Total Nodes, (c) First Leaf macroHair and (d) Disappearance of juvenile leaf identity- Last Leaf Waxy. Error bars were drawn from at least 10 replicate plants.

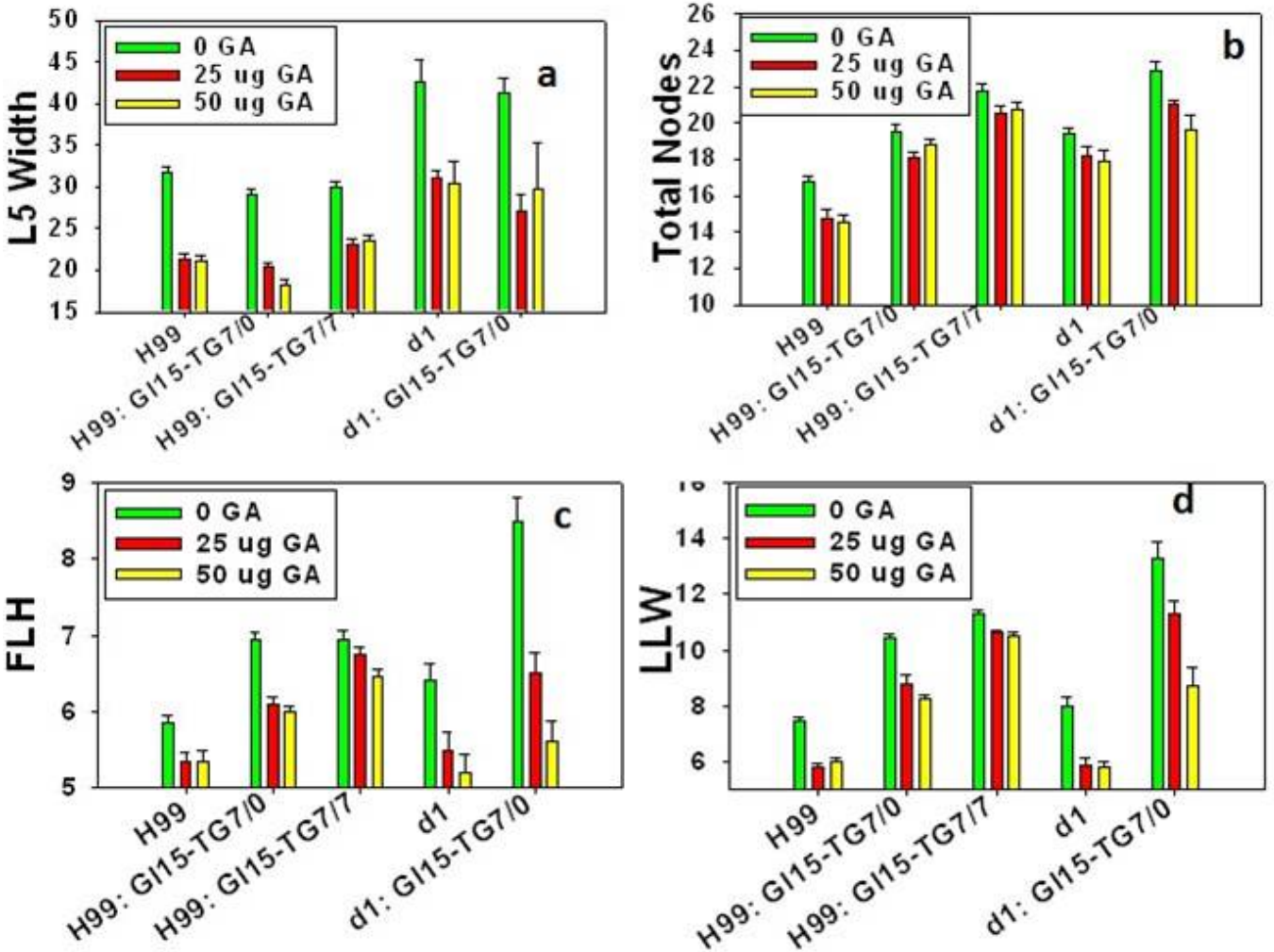


Figure 2.9: Proposed model of leaf identity regulation in maize. A. GA, *Cg1, Tp1, Tp2* and e*pc1* regulate leaf identity through modulating *miR156* and *miR172*, which converge to regulate *Glossy15*. B. Seed embryos initiate 5-6 leaf primordial. C. During germination, adult factor is not strong enough to antagonize juvenile factors, leaf primordia are determined as juvenile leaves. D. After GA burst associated with seed germination, adult leaf factors are stronger than juvenile factors, undetermined leaf primordia acquire adult leaf identity (leaf 8, 9, 10). E. In the absence of *Glossy15*, the GAs promote adult leaf identity in all leaves whose identity was not determined prior to embryo dormancy.

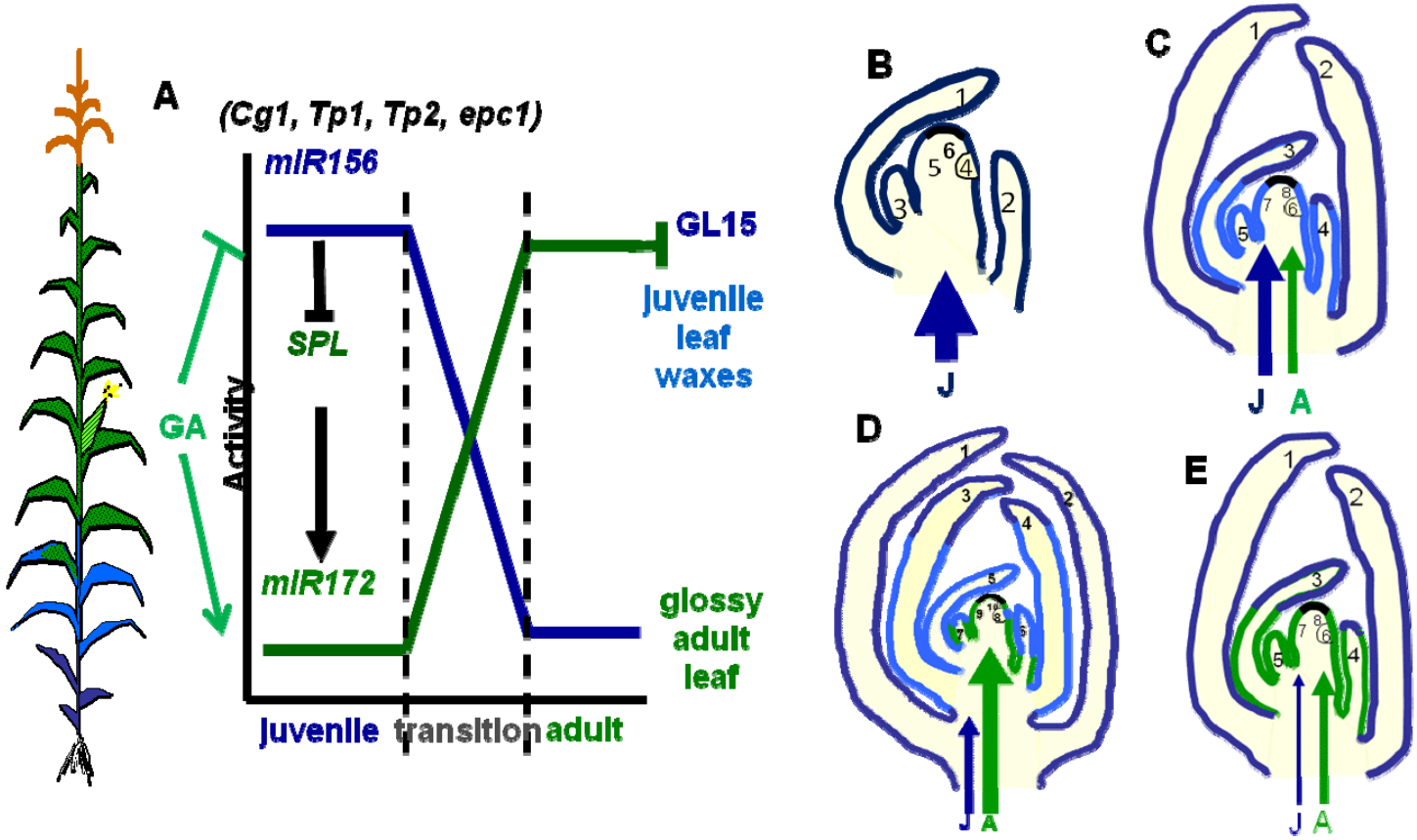
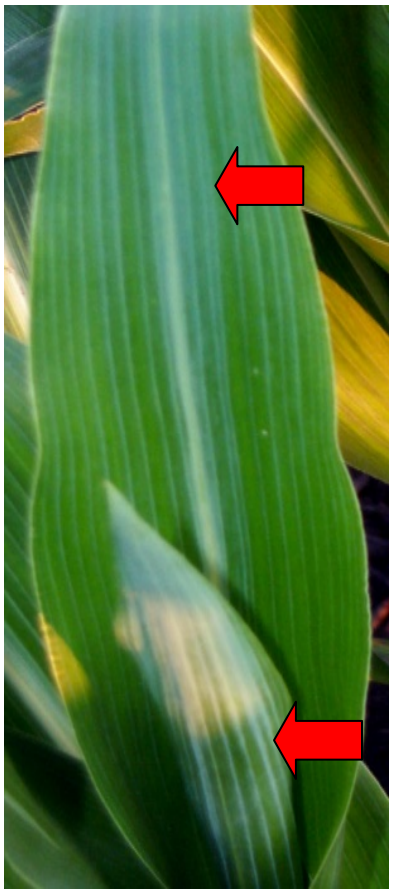


Figure 2.10: Juvenile wax stripes in *Glossy15*-TG plants.



Chapter 3:

Expression variation for genes regulating vegetative phase change mediates quantitative inheritance of the transition from juvenile to adult leaf identity in maize

Abstract

Higher plants progress through distinct phases of vegetative growth marked by the production of leaves that differ for suites of morphological and physiological traits, many of which contribute to fitness in natural populations and crop productivity. Maize populations exhibit significant phenotypic diversity for the duration of the juvenile vegetative phase and for the onset of adult vegetative phase, which is typically inherited as a quantitative trait. Genetic mapping experiments in two distinct recombinant inbred populations identified *Glossy15*, which is known to be both necessary and sufficient for maintaining juvenile leaf identity, as the strongest QTL for vegetative phase change. Two other major-effect QTLs coincide with the genomic intervals containing *zma-miR156g* and maize SQUAMOSA PROMOTER BINDING LIKE PROTEIN *SBP5*. Expression variation for each of *Glossy15, SBP5, miR156* and *miR172* was correlated with the differences in the timing of vegetative phase change among parental lines. Recombinant inbred lines selected for both early and late vegetative phase change also showed significant changes (1.5 – 4-fold) in the relative activities of *miR156*, *miR172*, and *Gl15,* demonstrating that each of these factors are associated with quantitative variation in the timing of vegetative phase change.

Introduction

Vegetative phase change in maize is primarily defined by the transition from juvenile to adult leaf identity during vegetative growth. Juvenile leaves and adult leaves differ in a set of epidermal leaf traits, which includes wax composition, macrohairs and cell wall biochemistry (Moose and Sisco, 1994). Some of the leaf epidermal traits contribute to tolerance of environmental stresses and resistance to disease, insect pests, and herbivory (Riederman and tracy, 2008, 2010). Molecular and genetic studies in Arabidopsis and maize have identified the main factors that control the timing of this transition. The maize transcription factor *Glossy15 (Gl15)* was the first cloned gene for vegetative phase change. *Glossy15* encodes an AP2 domain protein, which promotes juvenile and suppresses adult leaf identity traits (Moose and Sisco, 1994, Moose and Sisco, 1996). *microRNA172* (*miR172*) binds by complementary base pairing to the *Glossy15* mRNA and triggers mRNA cleavage, thus promote the onset of adult leaf identities (Lauter et al., 2005). In Arabidopsis, SQUAMOSA PROMOTER BINDING LIKE PROTEIN transcription factors (SPL3, SPL9/15, SPL2/10/11) condition expression of adult identity traits, which are repressed by *microRNA156* (*miR156*, Wu and Poethig, 2006, Schwarz et al., 2008; Wang et al., 2008 and Wu et al., 2009). Overexpression of *miR156* in Arabidopsis delays vegetative phase change (Wu and Poethig, 2006), and is also associated with the prolonged juvenile phase of the maize mutants *Cg1, Tp1, Tp2* and *d1* (Chuck et al., 2007, Zhang et al., Chapter 2). On the contrary, titration of *miR156* could promote the onset of adult traits (Wang et al., 2008 and

Wu et al., 2009). Recent studies in Arabidopsis show that the *miR172* and *miR156-SPLs* pathways are connected by the *miR156*-targeted proteins SPL9 and SPL10. These two proteins appear to bind the promoter region of *miR172b* in Arabidopsis, promoting the expression of *miR172b* precursor and increased levels of mature *miR172* (Wu et al., 2009). The complementary expression nature of *miR156* and *miR172* in both maize (Chuck et al., 2007) and Arabidopsis (Aukerman and Sakai, 2003, Wu and Poethig, 2006), suggests that similar regulation of *miR172* by SPLs may also occur in maize.

Studies of vegetative phase change in maize are mostly based on observed phenotypic effects of single gene mutations or transgenic overexpression, which introduce large phenotypic effects (Moose and Sisco, 1994; Lauter et al., 2005; Chuck et al., 2007). The validity of the above factors in larger populations that exhibit quantitative phenotypic variation has not been assessed. Because of the position of *miR156* and *miR172* within regulatory networks affecting key developmental processes in plants, they are expected to contribute to variation within species, as evidenced by the extreme phenotype of *Cg1* resulting from greatly enhanced *miR156* expression (Chuck et al., 2007). However, the role of miRNAs in mediating intraspecific variation within natural or selected breeding populations has yet to be documented. The timing of vegetative phase change is easily marked by the first leaf with adult macrohair (FLH), first leaf with adult glossy (FLGL) and the last leaf with juvenile wax (LLW), each of which can be measured quantitatively (Revilla et al., 2000 and Revilla et al., 2002). Moreover, traits associated with vegetative phase change

show significant additive inheritance, high heritability (>65%) and limited interaction with environment (Revilla et al., 2004). The quantitative nature and the high heritability of phase transition traits suggest that quantitative trait loci (QTL) mapping approaches may offer insights into the regulation of leaf identity phenotypes. Chandler and Tracy (2007) recently used a sweet corn population of 130 S_3 lines to successfully identify a single significant QTL controlling vegetative phase change that mapped to the genomic region containing *Glossy15*.

A high resolution genetic map for maize was developed from the intermated B73 X Mo17 recombinant inbred lines (IBM) population (Lee et al., 2002; Sharopava et al., 2002), which has made QTL mapping a viable tool for gene discovery. The IBMs population is developed by crossing B73 and Mo17, followed by 4 cycles of random mating to increase the potential for recombination before developing inbred lines (Lee et al., 2002). The IBM-derived genetic map contains over 3000 markers including 1051 novel simple sequence repeat (SSR) markers (Sharapova et al., 2002) and 1329 novel indel polymorphism (IDP) markers (Fu et al., 2006). Balint-Kurti et al. (2007) mapped QTL for resistance to southern leaf blight in both the IBM population and a conventional F_2-derived recombinant inbred line population derived from the same parents, B73 and Mo17. They found that for the QTL detected in both populations, the IBM population provided between 5 and 50 times greater resolution in the position of the QTL than the conventional population. We have used the IBM population to quantitatively map genes for nitrogen use efficiency (Nichols, 2008) and shoot

maturation traits (Lauter et al., 2008). Four major QTLs controlling shoot maturation in the IBM population have recently been identified using composite interval mapping through three years of replicated phenotypic data (Lauter et al., 2008).

In our study, we used the IBM population as well as a conventional recombinant inbred (RI) population derived from NC61 crossed with W23 (NWRILs) to map leaf identity QTLs. While the IBM population could provide the highest possible resolution in maize, NC61 and W23 represent the phenotypic extremes for the duration of the juvenile phase among a large collection of maize inbred lines (Moose, 1995), which may offer a broader range of phenotypic distribution and stronger allelic effects in the mapping population. From the two populations, we identified several regions as major QTLs for leaf identity traits. Our results confirmed *Glossy15* as the major QTL in both the IBM and NWRIL populations, and that the *miR156*, *SPL*, and miR172 genes each contribute to the phenotypic differences between parents and within the in recombinant inbred lines.

Materials and Methods

NC61 X W23 mapping population construction

A single F_1 plant from the cross of NC61 X W23 was selfed to generate a F_2 population of 200 plants, which were selfed 7 generations to obtain 166 recombinant inbred lines.

Leaf identity measurements

384 IBM lines and 166 NWRILs were grown in field plots at the Crop Sciences Research and Education in Urbana, IL. Leaf identity phenotypes were measured from five plants for each genotype in each of two replicate years: First Leaf Glossy (FLGL), First Leaf macroHair (FLH) and Last Leaf Waxy (LLW). Measurements for FLGL and FLH were approximated to the nearest quarter of the entire length of leaf blade which expressed the trait and averaged, whereas LLW was recorded as the last whole leaf that showed any visible juvenile epicuticular waxes at the tip of the leaf blade. In the 2005 replicate of the NWRILs, LLW was measured as the mean of three plants for each genotype, whereas the 2006 replicate used the median LLW for five plants from each genotype.

DNA sampling and extraction

For each inbred line, 2 leaf punches were pooled from 10 individual plants and were frozen at -80°C prior to DNA extraction. Samples were ground to powder in a Genogrinder at 4000 strokes/minute for one minute. DNA extraction was performed by DNA extraction solutions from 5 PRIME (cell lysis solution and protein precipitation solution) following manufacturer's instructions except for a few minor modifications: ground samples were placed in water bath at 65° for >1 hour in cell lysis buffer and protein precipitation on ice for > 1 hour.

Sequencing Glossy15

Gl15 primers were designed based on cloned *Glossy15* sequences from the inbred line W64A (Moose et al., 1996) and the B73 genome sequences. *Gl15* sequences were amplified by primers Gl15_1440+ and Gl15_4504- and by primers Gl15_150+ and Gl15_1660- using EXPAND LONG TEMPLATE PCR SYSTEM from Roche. 500ng DNA, 17.5 um dNTP, 15 nm of each primer, 1 μl DMSO and 0.75 μl Taq polymerase were used in a 50 μl PCR reaction under the following thermo cycles: initial denaturation at 94°C for 2 minutes; 11 cycles of 94°C for 15 sec, 60°C for 30 sec, 68°C for 6 minutes and 20 sec; 16 cycles of 94°C for 15 sec, 60°C for 30 sec, 68°C for 6 minutes and 30 sec; followed by 4 additional cycles where elongation time increase from 6 minutes and 30 sec by 20 sec in each cycle, and a final extension at 68 °C for 7min. The PCR products from W23 and NC61 were then sliced from agarose gel, purified and cloned into pGEM-Teasy vector (Promega). Three clones for W23 and NC61 were each picked and sequenced with several *Glossy15* sequencing primers.*Glossy15* from Mo17 and from IBM lines that harbor recombinants between *umc1688* and *umc1691* were sequenced directly from PCR products.

QTL analysis

The IBM genetic linkage map was downloaded from http://www.maizegdb.org/ibm302scores.html. Markers were added or deleted as described in Lauter et al. (2008). The QTL analysis was performed using Windows QTL Cartographer Version 2.5. Composite interval mapping (CIM) was

performed at a “walking speed” of 0.5 cM and a “window size” of 5.0 cM instead of the default values of 2.0 and 10.0, due to the high resolution of the genetic map used (Lauter et al., 2008). Permutation tests (Zmapqtl in linux) were used to determine the experimental-wise LOD significance threshold for each trait (Churchill and Doerge, 1994). Mapchart was used to obtained high-resolution views of the QTLs. All statistics and marker-phenotype associations were conducted by fit model analysis through JMP4.04 software; interactions between markers were estimated by crossing of two markers in the model.

Phylogenetic tree construction

Arabidopsis SPL proteins were downloaded from NCBI (http://www.ncbi.nlm.nih.gov/); rice SPL proteins were downloaded from GRAMENE (www.gramene.com) as indicated by Miura et al., 2010; maize SPL proteins were downloaded from NCBI (ZmSPLs) and by blasting SPL genes in Chuck et al., 2007 to the NCBI database, some of the SPL proteins were downloaded from maizesequence.org as indicated by Miura et al., 2010. Maize SPL proteins were combined if sequences from the two databases completely matched. Phylogenetic and molecular evolutionary analyses were conducted using *MEGA* version 4 (Tamura et al., 2007). BT084089, BT068292, BT054654 and LOC001175514 were manually added to the phylogenetic tree based on online phylogenetic server analysis results (http://www.phylogeny.fr/version2_cgi/simple_phylogeny.cgi).

Polyacrylamide gel electrophoresis of Gl15 alleles in NC61 X W23 RI lines

Markers that defined QTL peaks in the IBM population were tested for polymorphisms between NC61 and W23. Polymorphic markers were then assayed and scored in a 3% Metaphor gel for the entire population of 166 NWRILs. *Gl15* marker primers (Gl15_3373+ and Gl15_3500-) were designed to differentiate the 7bp difference between W23 and NC61 alleles, and run for 120 selected NWRI lines representing early or late onset of adult traits. This marker was assayed following the protocols of Wang et al., 2003, using gels that contain 6% (w/v) acrylamide/bis-acrylamide (19:1), 0.5x TBE buffer, 0.07% (w/v) ammonium persulfate, and 0.08% (w/v) TEMED.

RNA sampling and RNA isolation

Two biological replicates of W23 and NC61 plants were grown in a greenhouse under 16 hour day light. Five shoot apices from each line were dissected at 6, 9, 12, 15, 18 and 21 days, and the basal 1.5 centimeters was used for RNA isolation. Selected NWRILs phenotypic tails were grown in summer nurseries in two years and three shoot apices were sampled at nine DAS or 12 DAS. B73 and Mo17 are grown in several replicate experiments and three shoot apices were sampled each time. The shoot apices samples were dipped into liquid nitrogen for two minutes and stored in at –80°C. For RNA isolation, samples were ground in the Genogrinder for 15 secs, followed by Trizol and chloroform extraction, isopropyl precipitation and 75% ethanol wash. RNA

integrity after extraction was tested by electrophoresis in RNA formaldehyde gels.

Profiling Glossy15 mRNA and miRNA

Reverse transcription reactions were performed on 1µg total RNA at 42°C in 20µl reaction volume by oligo(dT) and NEB reverse transcription kit. The $\Delta\Delta C_t$ method was used as described in Livak and Schmittgen (2001) to quantify target mRNA or microRNA levels. Realtime PCR primers were tested for primer dimers in the Opticon2 (MJ Research) real-time PCR machine prior to mRNA quantitation. Relative *Gl15* and *SBP5* mRNA abundance was estimated by performing real-time PCR by using SYBR-green at 63ºC, and by using maize *Actin* as a control gene. Error bars represent 3 technical replicates. 10ng RNA was used for ABI Taqman *miR156a*, *miR166a* and *miR172a* reverse transcription following manufacturer's suggestion; *miR156*a and *miR172a* were quantified by using *miR166a* as internal standard.

Results and Discussion

Parental and progeny phenotypes

The parental lines from which the NWRILs were derived have marked phenotypic differences for the leaf identity traits, as shown in Table 3.1. NC61 has juvenile wax as far as leaf 11 and delays the onset of macrohairs as far as leaf 8; while W23 ends juvenile identity at leaf 5 and begins the onset of adult leaf macrohairs as early as leaf 3. Leaf identities of B73 and Mo17 are

intermediate between W23 and NC61: adult macrohairs start at leaf 6 and juvenile wax lasts until leaf 7. B73 and Mo17 differ by less than one-half leaf for the onset of adult macrohairs and show no difference for the duration of juvenile wax. The phenotypic ranges in the progeny recombinant inbred populations are consistent with the differences observed between the parental lines. The NWRILs population has a range of 3.75 – 9.67 for the onset of macrohairs and 5.0 – 13.0 for the duration of juvenile wax, compared with a range of 3.44 - 8.33 for the onset of macrohairs, and 4.33 – 8.56 for the duration of juvenile wax in the IBMs population. Transgressive segregation is more obvious in the IBM compared to the NWRILs population.

Characterized vegetative phase change genes are present within identified QTLs for leaf identity in the IBM population

Two leaf identity traits were used for QTL analysis: FLH, which monitors the onset of adult leaf identity and LLW, which measures the duration of the juvenile phase. Using CIM and controlling experimental-wise type I error at $p < 0.05$, we could identify a few regions with significant LOD scores for both measured traits in the IBM population (Fig. 3.1). One of the major QTL, which has a LOD score over 15 for both traits in two replicate years (compared with an experiment-wise LOD of 3.6), is located between markers *umc1271* and *umc114* on chr. 9.07. This region covers a physical distance of 9.7Mb and genetic distance of 11.3cM. The two markers (*umc1688* and *umc1691*) that flank the peak QTL position are located within the *Glossy15* gene (AY714877.1), with

umc1691 located before the *Gl15* start codon and *umc1688* 400bp before the stop codon. Another QTL for both traits is located between markers *umc2041* and *umc1393* on chromosome 7.02. This region spans 12.1cM and 11.8Mb, and harbors *zma-miR156g*. The third common region for both leaf identity traits is near marker *umc1396* on chromosome 1.06, and covers a distance of 9.7Mb and 36.3cM. One of the SPL genes in maize that was previously shown to be down-regulated by *miR156* (*SBP5*, AJ0116181 in NCBI or TC305612 in Chuck et al., 2007) is present within this chromosomal interval. The last identified QTL was only significant for the LLW, and is between *umc36a* and *bnl17.14* on chromosome 2.09. Although the genetic distance between the two markers covers 21.8cM, the physical distance is only 4.4Mb. No previously identified leaf identity factors are found in this region through gene scan and gene prediction analysis.

QTLs found in the IBM population also control leaf identity variation in NC61 X W23 RI population

Based on the four major QTLs identified in the IBM population, we genotyped the QTL markers in the 166 NWRIL population. Markers *nc134* (on *Glossy15*), *umc2092*, *umc1396* and *umc1704* (pointed by arrows in Fig. 3.1), which represent QTLs in chromosome bins 9.03, 7.02, 1.06 and 2.09, respectively, were able to differentiate W23 and NC61 alleles. To monitor the contribution of each of these markers to phenotypic variation in the NWRIL population, a least squares linear model was used to construct models for FLH

and LLW by the four markers and their interactions (JMP4.04, SAS Institute). Table 3.2 summarizes the results from this analysis. The four markers combined are estimated to contribute 31% to 57% ($p<0.0001$) of the total phenotypic variation for leaf identity traits in the two replicate years. Marker *nc134* is important for all tested traits ($p<0.0001$), contributing the largest additive effects (approximately 0.8 leaves for the FLH and 0.6 leaves for the LLW for both years). *Umc2092* is important for all tested traits except for LLW measured in 2006, contributing about 0.3 leaves. For markers *umc1396* and *umc1704*, we are not able to consistently identify their importance in the NWRILs population, although the interaction of *umc1396* with *nc134* was detected as significant for all measured traits except LLW in 2006. Therefore, our molecular analyses focused on the effect of *nc134* (*Glossy15*) and *umc2092* (*zma-miR156g*).

Heritability and QTL effects

To assess the relative contribution of genotype and environment, genotype and year effects were estimated by linear mixed model analysis (JMP4.04). Broad sense heritability H_B is estimated for FLH and LLW in both populations (Table 3.5). The heritability in the IBM population is high, 0.74 for the FLH and 0.76 for the LLW. It is also high in the NWRIL population for the FLH, which reaches 0.86, but drops to 0.28 for LLW. The effect of year was significant for traits in both populations ($p<0.01$), but contributes less than 10% to the total variation, except for LLW in the NWRILs, where the effect of year accounted for 42% of total variation (Table 3.5). The LLW data from the two

years were highly correlated ($p<0.0001$), and we attribute the large effect of year to the fact that this trait was scored as the mean of five plants in 2005 by Nick Lauter, but as the median of five plants by Dr. Moose in 2006.The large year effect for LLW could explain the lower heritability for this trait and inconsistent detection of significant associations between the *umc2092* marker and the interaction between the *umc1396* and *nc134* markers..

The marker' effects were also estimated in the IBM population through fit model analysis. The allelic variations in the four markers contribute to 33% variation for FLH and 46% variation for LLW, which translates to 44% and 60% of total genetic variation in the IBM population. In the NWRILs, the four markers contribute over 60% of genetic variation for FLH. Notably, *nc134* is most strongly-associated with leaf identity phenotypic variation. For example, the R^2 for *nc134* alone is 0.43 for FLH in 2005, with the other four markers and their interactions having a total R^2 of 0.57.

SBP5 on chr. 1.06 is an ortholog of Arabidopsis SPL9/15

Arabidopsis SPL9 and SPL15 are close paralogs. Loss-of-function mutations in either SPL9 or SPL15 have minor effects on development. However, plants doubly mutant for these two genes delayed the production of abaxial trichomes that define adult leaf identity (Schwarz et al., 2008 and Wu et al., 2009). Transgenic Arabidopsis plants that express a *miR156*-insensitive version of SPL9 accelerate all adult-specific leaf traits (Wu et al., 2009).

The rice and maize genomes also contain large SPL gene families. The 15 rice SPL genes and the predicted maize SPL genes are aligned together with Arabidopsis SPLs and built into phylogenetic tree (Fig. 3.2). From our genomic search for maize SPL genes, it appears that the maize genome harbors 34 SPL homologs, which include the characterized genes *Liguless1, Teosinte glume architecture1* and *Tasselsheath4*. The SPLs that could be targeted by *miR156* from the three species are grouped together, which are visualized by color underlined in Fig. 3.2. From the grouping, maize SPL5, together with several other maize SPLs, groups together with AtSPL9/15. Based on their close relationships, we consider that maize SPL5 is likely to share with AtSPL9/15, a functional role in promoting adult leaf identity.

Allelic variation for Glossy15 is strongly associated with the timing of vegetative phase change in both the IBM and NWRIL populations.

From the above result, *Glossy15* contributes to over 75% of observed QTL effects. Therefore, we assessed the *Gl15* allelic differences in NC61 and W23, and in B73 and Mo17, which might be the cause of the *Gl15* QTL. The B73 sequence was available from the maize genome sequence, we cloned and sequenced the *Glossy15* genomic region from W23, NC61 and Mo17. Figure 2 shows the positions where *Gl15* in NC61 differs from W23, and where it in B73 differs from Mo17. In the IBM population, *umc1691* captures the SSR differences before the start codon and *umc1688* captures a 27-bp deletion in Mo17 which was also identified in Gl15 cDNAs and removes 9 amino acids from the

GLOSSY15 protein. In addition, some insertions are observed in the promoter regions of Mo17 and NC61, among them, a 300bp insertion was observed 1300-bp upstream of the start codon.

A set of 120 NWRILs were chosen from the NWRILs that included the 60 lines representing early juvenile to adult leaf identity transition and the 60 RI lines representing late transition. These RI lines were scored with the *GI15* marker defined by PCR primers GI15_3373+ and GI15_3500- , which was able to identify a 7bp difference between NC61 and W23 (Fig. 3.3). The results found that all RIs were homozygous for either the W23 or NC61 alleles, but their frequencies were strongly associated with the divergent leaf identity phenotypes of the two selected subpopulations. The frequency of the W23 allele in the early transition RIs was 0.91 ($p<0.0001$ for X^2 test of deviation from expectation of 0.5); conversely, the frequency of the allele in the late transition RIs was only 0.14 ($p<0.0001$ for X^2 test of deviation from expectation of 0.5) (Table 3.3).

The genetic distance between *umc1688* and *umc1691* is 3.5 cM in the IBM genetic map, indicating intragenic recombination events were present within GI15 in the IBM population. We rescored the two markers and found 7 recombinant IBM RI lines. We also scored the 300-bp difference but only found 1 recombinant IBM RI line. After sequencing *Glossy15* from the 7 RI lines, the recombination event(s) in all seven lines was located between positions 2640 and 3210 (based on AY714877.1), a region where no allelic differences exist between B73 and Mo17. All seven lines have the Mo17 haplotype before position 2640 and the B73 haplotype after position 3210. Ideally, if we suppose there are

n genetic factors that are responsible for a certain quantitative traits, and by stabilizing n-1 factor alleles, the lines for the last factors are near isogenic lines. In our study, the four QTLs contribute nearly 50% of the observed genetic variance. If we only consider the four detected QTLs, IBM can be deemed as "near-isogenic" lines for *Glossy15* when we select for the same alleles at flanking markers for the other major QTL intervals on chromosomes1.06, 2.09 and 7.02. Comparisons of leaf identity phenotypes in IBMs with contrasting *Gl15* alleles but fixed for the other QTL positions found that recombination within the *Gl15* coding consistently had a moderate phenotypic effect where the B73 allele accelerated phase change one-half to one full leaf relative to Mo17 (Table 3.4). Given that null *gl15* mutations accelerate phase change by approximately three leaves in both the B73 and Mo17 backgrounds Table 3.1, the differential activity of the B73 and Mo17 haplotypes can be estimated to be 15-30% as strong as a complete loss of *gl15* function.

***Relative levels of Glossy15, miR156 and miR172 expression correlate with differences in the timing of vegetative phase change among parental lines of mapping populations*.**

The finding of QTL intervals that contain *Gl15, miR156*, and *SPL* genes in two different mapping populations suggests that expression variation in these key regulatory genes may account for the QTL effects. We tested this hypothesis by comparing RNA levels for *Gl15*, *SBP5*, *miR156* and *miR172* in the parental inbred lines for the two mapping populations. Prior research with the H99

genotype (which produces six juvenile leaves typical for most maize lines) showed that *Glossy15* mRNA is limited to the first 20 days after sowing (DAS) and *miR172* is not detected prior to nine DAS (Lauter et al., 2005); therefore, we collected samples between six and 21 (DAS). A Three day interval was chosen as this represents the typical length of time for individual leaves to progress from a newly-initiated primordia to the stage where leaf identity is specified. Inspection of dissected shoot apices showed that leaf initiation rates do not differ greatly among these genotypes, except that NC61 initiates one additional leaf compared to W23 by 9 DAS.

Figure 3.4 shows the results for four separate experiments that examined the relative expression of *Gl15* mRNA in B73 and Mo17 from 8 – 21 DAS. Although the magnitude of the differential expression varied among experiments, which we attribute to environmental effects on the rate of early seedling growth, there is a consistent trend in all samples for stronger *Gl15* expression in B73 compared to Mo17. The degree of differential expression seems greatest between 10 and 12 DAS. The samples collected in experiment three were used to assay the expression of SBP_5 mRNA, *miR156*, and *miR172*. SBP_5 showed higher expression in Mo17 compared to B73 at 15 DAS but not earlier stages. *MiR156* was expressed 1.5 to 2-fold higher in B73 compared to Mo17 at each developmental stage. The levels of *miR172* were similar between B73 and Mo17 at 8 and 15 DAS, but were approximately 2.5-fold higher in B73 compared to Mo17 at 11 DAS. For *miR156* or *miR172*, both B73 and Mo17 showed similar relative expression and rates of decline (*miR156*) or increase (*miR172*) with

development, except for a slightly higher initial expression of *miR156* in B73 at 8 DAS.

The higher expression of *miR156* in B73 compared to Mo17 is reflected in the lower expression of its target SBP_5, and is consistent with the observation that B73 exhibits a delay in the onset of adult leaf identity by approximately one leaf relative to Mo17, which occurs independently from *GI15* activity (Table 3.1). These expression patterns are also consistent with the finding that the B73 alleles for the QTLs containing both SBP_5 and *miR156* delay vegetative phase change in the IBM population (Fig. 3.1). The observed difference in *miR172* expression between B73 and Mo17 at 11 DAS does not appear to lead to a corresponding decrease in its target, *GI15*, suggesting it may not be functionally significant. We also note that although SPL 9/10 appear to promote *miR172* expression in Arabidopsis, we did not observe higher levels of *miR172* in Mo17 compared to B73 at 15 DAS despite Mo17 showing stronger SBP_5 expression.

We found *GI15* expression to be higher in B73 compared to Mo17, which is consistent with the later onset of adult traits in B73. However, in the IBM population the B73 allele for *GI15* appears to have the opposite effect of accelerating vegetative phase change. One possible explanation for this apparent discrepancy is that *GI15* mRNA expression is more likely to depend on variation in regulatory sequences, whereas the QTL effect in the IBM population is estimated from allelic substitution of the *GI15* protein coding region, which may have stronger and opposing functional consequences on overall *GI15* activity. This hypothesis is supported by the phenotypic effects of recombinants within

Gl15 when variation at the other significant vegetative phase change QTL were fixed in IBM lines (Table 3.4). The amino acid deletion in Mo17 detected by the *umc1688* marker has a strong effect on delaying leaf identity traits, but the polymorphism in the 5'UTR revealed by the *umc1691* marker has weaker effects on leaf identity where the Mo17 variant is associated with accelerated vegetative phase change.

Since NC61 and W23 represent phenotypic extremes for the timing of vegetative phase change among maize inbred lines, expression variation for genes in the leaf identity pathway may be greater than that observed between B73 and Mo17.

Figure 3.5 shows the *Glossy15* mRNA, *miR156* and *miR172* expression patterns in NC61 and W23. *Glossy15* mRNA is higher in NC61 compared to W23 starting from 6 DAS, and at 15 DAS, *Glossy15* remains at a high level in NC61 but drops significantly in W23 (Fig. 3.5, upper left). It is obvious that *Glossy15* in NC61 expresses stronger and persists longer. This result is consistent with the QTL mapping results where the NC61 allele of *Glossy15* prolongs juvenility. In both genotypes, *Glossy15* mRNA falls to a minimum level by 21 DAS, when leaf 9 in NC61 (the first fully adult leaf) has reached 3 cm in length and hence at the stage where leaf identity is specified (Orwiszewski and Poethig, 2000). The decline of *Gl15* mRNA thus correlates with the production of fully adult leaves.

Figure 3.5 also presents the expression profiles for *miR172* (lower left) and *miR156* (lower right) in the W23 and NC61 genotypes. W23 begins with a higher *miR172* level, which correlates with the lower *Gl15* mRNA expression

compared to NC61. In NC61, *miR172* expression does not reach the level observed for W23 at 6 DAS until 12 DAS. At 15 DAS, *miR172* in both genotypes has risen to the same maximum level, which is followed by a sharp dip of *Glossy15* mRNA by 18 DAS (Fig. 3.5, upper left). Leaf 9 is the first NC61 leaf to express adult traits, and is initiated at 15 DAS which coincides with the onset of strong expression of *miR172*. These results demonstrate that differences in the temporal profile of *miR172* expression and its relative abundance during early shoot development are indeed correlated with observed variation in the transition from juvenile to adult leaf identity.

The expression profile for *miR156* is generally the opposite of that observed for *miR172*, initially high and then decreasing more than ten-fold to a minimum by 18 DAS in both NC61 and W23 (Fig. 3.5, lower right). The rate of decrease is faster in W23 compared to NC61, particularly between 9 and 12 DAS. The longer expression of *miR156* correlates with the lower expression of SBP_5 (upper right) in NC61 from 6 DAS to 15 DAS. Taken together, the expression profiles for each of *Gl15*, SBP_5, *miR156* and *miR172* during early shoot development correlate with the early vegetative phase change observed in W23 and the late phase change in NC61.

Glossy15 mRNA, miR156 and miR172 expression patterns in leaf identity tails of NWRILs population

Earlier studies have shown that vegetative phase change phenotypes are characterized by heritabilities of greater than 65% (Revilla et al., 2004). This high

heritiability for leaf identity phenotypes in the NC61 x W23 RI mapping population (86% for FLH) could be reflected in RNA expression levels of the key regulatory genes *miR156, miR172*, and *Gl15*. Based on a histogram of the values for first leaf hairs among the 166 NC61 x W23 recombinant inbred lines, we chose the ten lines with either the highest or lowest mean values for the first leaf with hairs to reduce the number of samples to be assayed.

We initially examined the accumulation of *Gl15, miR156* and *miR172* in these 20 divergent lines at 12 DAS. *Glossy15* (Fig. 3.6, upper panel) showed a clear trend of lower expression in the lines with earlier vegetative phase change compared to those with later onset of the adult phase. Although not shown here, *miR156* showed lower expression in the lower tail, but *miR172* expression did not show significant differences between the two selected groups. However, at 9 DAS (Fig. 3.6, lower panel), significantly higher *miR172* (lower right) and lower *miR156* (lower left) expression is observed in the ten lines selected on the basis of early macrohairs. Collectively, the data indicates a strong correlation between the relative expression levels of each of *miR156, miR172* and *Gl15* and the duration of the juvenile phase in the NWRIL mapping population. The results also support the hypothesis that RNA expression variation for *Gl15* and *zma-miR156g* could be the basis for the QTL controlling vegetative phase change that were found on chromosomes 9 and 7, respectively, in the NWRILs.

Interactions among QTLs

From previous studies (Lauter et al., 2005, Wu and Poethig, 2006, Chuck et al., 2007, Wu and Poethig, 2009) and our results, interactions between *miR172* and *Glossy15*, as well as between *miR156* and *SPLs* are well established. As the only two cloned genes for vegetative phase change in maize, *miR156* and *Gl15* interact in the way that *Glossy15* transgenic overexpression or mutation could affect *Cg1* (*miR156* overexpression) the same way as they affect the wildtype plants (Moose and Sisco, 1994; Moose lab unpublished), and that *miR172* is regulated by SPL9/10 in Arabidopsis (Wu et al., 2009). These evidences suggest *miR156* is acting upstream of *Gl15*. Although plant miRNAs play important roles in defining plant development (Chen, 2009), no previous results ever identified miRNA genes as QTLs. In our study, we found one QTL near *miR156g*. Our results showed that the allelic variation of both upstream gene (*miR156g*) and downstream gene (*Glossy15*) in the vegetative phase change pathway contribute to phenotypic variations in NWRILs population.

If *miR156g* and SBP_5 are the underlying QTLs on Chr. 7.02 and Chr. 1.06, we could test the interactions between *miR156g* and SBP_5, and between *miR156g* and *Gl15* in linear model analysis by using markers near or on these genes (Table 3.2). The crossing between *umc2092* (near *miR156g*) and *umc1396* (near SBP_5) in controlling leaf identity traits is not significant for all traits in both populations. We could, however, detect interaction between marker on *Glossy15* (*nc134*) and marker near SBP_5 (*umc1396*) in NWRILs population (table 3.3, $p<0.01$) and interaction between QTL on chr. 2.09 and *umc2092* for FLH and

LLW in IBMs. Notably, the interactions of the above markers were not consistent in the two populations. While QTL analysis method is good to detect correlation between allelic variations and phenotypic variation, the capability of detecting interactions between QTLs is not consistent with our molecular data and across populations. It is possible that some unidentified gene but not *miR156g* is the underlying QTL on Chr. 7.02, and this gene is working independently of the known genetic work of leaf identity regulation or working distantly from *Glossy15*. In our last chapter, we show that GAs is adult factor that works antagonistically with *Glossy15* through regulating *miR172*. However, no direct target of GAs in regulating the known genetic network genes is found yet If the underlying QTL on Chr. 7.02 is a GA responsive gene, detection of interaction between *nc134* and *umc1396* but not between *nc134* and *umc2092* (Table 3.2) is logical.

Conclusion

In this paper, we explored the factors that underlie the vegetative phase transitions. In two mapping populations- IBM and NWRILs, we consistently found QTLs that in combination explains over 40% phenotypic variation. Those QTLs are near previously established phase change related genes: *Glossy15, SBP_5* and *miR156* gene. *Glossy15* alone contributes to over 75% of all tested markers' effect. We correlated the expression patterns of *Glossy15 mRNA, miR156* and *miR172* with the time course of the transition through juvenile leaves to adult leaves in vegetative phase change extremes W23 and NC61. We were able to show that the correlation of stronger *Glossy15* with the late transition phenotype

in NC61could be passed to recombinant inbred lines through inheritance of *Glossy15* DNA. We are confident that *Glossy15* DNA and mRNA variation underlines Chr. 9.07 QTL.

References

Aukerman, M.J., and H. Sakai. 2003. Regulation of flowering time and floral organ identity by a microRNA and its APETALA2-like target genes. Plant Cell 15:2730-2741.

Balint-Kurti, P.J., J.C. Zwonitzer, R.J. Wisser, M.L. Carson, M.A. Oropeza-Rosas, J.B. Holland, and S.J. Szalma. 2007. Precise mapping of quantitative trait loci for resistance to southern leaf blight, caused by Cochliobolus heterostrophus race O, and flowering time using advanced intercross maize lines. Genetics 176:645-657.

Chandler, M.A., and W.F. Tracy. 2007. Identification of genomic regions affecting vegetative phase change in a sweet corn (Zea mays L.) population. Maydica 52:407-414.

Chen, X., 2009. Small RNAs and their roles in plant development. Annu. Rev. Cell Dev. Biol. 35:21–44.

Chuck, G., A.M. Cigan, K. Saeteurn, and S. Hake. 2007. The heterochronic maize mutant Corngrass1 results from overexpression of a tandem microRNA. Nature Genetics 39:544-549.

Churchill, G.A., and R.W. Doerge. 1994. Empirical Threshold Values for Quantitative Trait Mapping. Genetics 138:963-971.

Fu, Y., T.J. Wen, Y.I. Ronin, H.D. Chen, L. Guo, D.I. Mester, Y.J. Yang, M. Lee, A.B. Korol, D.A. Ashlock, and P.S. Schnable. 2006. Genetic dissection of intermated recombinant inbred lines using a new genetic map of maize. Genetics 174:1671-1683.

Jiao, Y.Q., Y.H. Wang, D.W. Xue, J. Wang, M.X. Yan, G.F. Liu, G.J. Dong, D.L. Zeng, Z.F. Lu, X.D. Zhu, Q. Qian, and J.Y. Li. 2010. Regulation of OsSPL14 by OsmiR156 defines ideal plant architecture in rice. Nature Genetics 42:541-U36.

Lauter, N., A. Kampani, S. Carlson, M. Goebel, and S.P. Moose. 2005. microRNA172 down-regulates glossy15 to promote vegetative phase change in maize. Proceedings of the National Academy of Sciences of the United States of America 102:9412-9417.

Lauter, N., M. J. Moscou, J. Habiger, and S. P. Moose. 2008**.** Quantitative Genetic Dissection of Shoot Architecture Traits in Maize: Towards a Functional Genomics Approach. The Plant Genome, 1(2): 99 – 110

Lee, M., N. Sharopova, W.D. Beavis, D. Grant, M. Katt, D. Blair, and A. Hallauer. 2002. Expanding the genetic map of maize with the intermated B73 x Mo17 (IBM) population. Plant Molecular Biology 48:453-461.

Livak, K.J., and T.D. Schmittgen. 2001. Analysis of relative gene expression data using real-time quantitative PCR and the 2(T)(-Delta Delta C) method. Methods 25:402-408.

Miura, K., M. Ikeda, A. Matsubara, X. Song, M. Ito, K. Asano, M. Matsuoka, H. Kitano and M. Ashikari. 2010. OsSPL14 promotes panicle branching and higher grain productivity in rice. Nature Genetics 42: 545-549.

Moose, S.P., and P.H. Sisco. 1994. Glossy15 Controls the Epidermal Juvenile-to-Adult Phase-Transition in Maize. Plant Cell 6:1343-1355.

Moose, S. P., 1995. Molecular genetic analysis of the maize *Glossy15* gene and the control of juvenile versus adult leaf identity. Ph.D. Dissertation, North Carolina State University.

Moose, S.P., and P.H. Sisco. 1996. Glossy15, an APETALA2-like gene from maize that regulates leaf epidermal cell identity. Genes & Development 10:3018-3027.

Orkwiszewski, J.A.J., and R.S. Poethig. 2000. Phase identity of the maize leaf is determined after leaf initiation. Proceedings of the National Academy of Sciences of the United States of America 97:10631-10636.

Riedeman, E.S., M.A. Chandler, and W.F. Tracy. 2008. Divergent recurrent selection for vegetative phase change and effects on agronomic traits and corn borer resistance. Crop Science 48:1723-1731.

Riedeman, E.S., and W.F. Tracy. 2010. Vegetative Phase Change Characteristics and Resistance to Common Rust of Corn Cultivars Developed in Different Eras. Crop Science 50:87-92.

Revilla, P., P. Velasco, R.A. Malvar, P. Soengas, and A. Ordas. 2000. Variability for phase transition among races of maize and related wild forms. Maydica 45:35-44.

Revilla, P., R.A. Malvar, A. Butron, W.F. Tracy, B.G. Abedon, and A. Ordas. 2004. Genetics of the timing of vegetative phase transition in a maize population. Plant Breeding 123:585-586.

Sharopova, N., M.D. McMullen, L. Schultz, S. Schroeder, H. Sanchez-Villeda, J. Gardiner, D. Bergstrom, K. Houchins, S. Melia-Hancock, T. Musket, N. Duru, M. Polacco, K. Edwards, T. Ruff, J.C. Register, C. Brouwer, R. Thompson, R. Velasco, E. Chin, M. Lee, W. Woodman-Clikeman, M.J. Long, E. Liscum, K. Cone, G. Davis, and E.H. Coe. 2002. Development and mapping of SSR markers for maize. Plant Molecular Biology 48:463-481.

Schwarz, S., A.V. Grande, N. Bujdoso, H. Saedler, and P. Huijser. 2008. The microRNA regulated SBP-box genes SPL9 and SPL15 control shoot maturation in Arabidopsis. Plant Molecular Biology 67:183-195.

Tamura, K., J. Dudley, M. Nei, and S. Kumar. 2007. MEGA4: Molecular evolutionary genetics analysis (MEGA) software version 4.0. Molecular Biology and Evolution 24:1596-1599.

Wang, D., J. Shi, S.R. Carlson, P.B. Cregan, R.W. Ward, and B.W. Diers. 2003. A low-cost, high-throughput polyacrylamide gel electrophoresis system for genotyping with microsatellite DNA markers. Crop Science 43:1828-1832.

Wang, J.W., R. Schwab, B. Czech, E. Mica, and D. Weigel. 2008. Dual effects of miR156-targeted SPL genes and CYP78A5/KLUH on plastochron length and organ size in Arabidopsis thaliana. Plant Cell 20:1231-1243.

Wu, G., and R.S. Poethig. 2006. Temporal regulation of shoot development in Arabidopsis thaliana by miR156 and its target SPL3. Development 133:3539-3547.

Wu, G., M.Y. Park, S.R. Conway, J.W. Wang, D. Weigel, and R.S. Poethig. 2009. The Sequential Action of miR156 and miR172 Regulates Developmental Timing in Arabidopsis. Cell 138:750-759.

Table 3.1: Leaf identity phenotypes of parental lines and progeny recombinant inbred populations.

	First Leaf with Macrohairs	Last Leaf with Juvenile Wax
B73	5.5	7
B73: *gl15*	3.75	3
Mo17	4.5	7
Mo17: gl15	2.5	3
266 IBM RI lines	Mean=5.91 Range 3.44-8.33	Mean=6.12 Range 4.33-8.56
NC61	7.75	11
NC61: *gl15*	4.5	4
W23	2.75	5
W23: *gl15*	2.5	4
166 NW RI lines	Mean=6.1 Range 3.75-9.67	Mean=8.9 Range 5.0-13.0

Table 3.2. Fit model analysis of FLH and LLW in NWRIL population by QTL markers identified in the IBMs population. R^2 = the proportion of total phenotypic variance explained by a model including the *nc134 (gl15)*, *umc2092* and *umc1396* markers and their interactions. Additive effect refers to the contribution of the NC61 allele.

	Year 2005				Year 2006			
Trait	**R^2**	**Effect test**	**P value**	**Additive effect**	**R^2**	**Effect test**	**P value**	**Additive effect**
First leaf with macrohairs (FLH05)	**0.57 (p<0.0001)**	**nc134 (chr.9)**	**<0.0001**	**0.92**	**0.46 (p<0.0001)**	**nc134 (chr.9)**	**<0.0001**	**0.87**
		umc2092 (chr.7)	**0.05**	**0.36**		**umc2092 (chr.7)**	**0.03**	**0.28**
		umc1396 (chr.1)	**0.04**	**0.14**		**umc1396*nc134**	**<0.01**	**/**
		umc1396*nc134	**<0.01**	**/**		**nc134*umc1704**	**0.04**	**/**
Last leaf with juvenile Wax (LLW05)	**0.45 (p<0.0001)**	**nc134 (chr.9)**	**<0.0001**	**0.60**	**0.31 (p<0.0001)**	**nc134 (chr.9)**	**<0.0001**	**0.92**
		umc2092 (chr.7)	**0.02**	**0.30**		**umc1704 (chr.2)**	**<0.01**	**-0.46**
		umc1396*nc134	**<0.01**	**/**				

Table 3.3: Heritability of the early (W23) and late (NC61) *Glossy15* alleles in the phenotypic tails of NC61 X W23 RI population. X^2 test of allelic deviation for H_0: allelic distribution of *Gl15* marker in the NWRILs population is 0.5.

	Observed	Expected	chi square	P value
Early NWRI tail	41	22.5	30.4	<0.001
	4	22.5		
Late NWRI tail	42	25.5	21.4	<0.001
	9	25.5		

Table 3.4. Phenotypic comparisons of IBM recombinants of *umc1691* and *umc1688* with their "near-isogenic" lines, which harbors same alleles at other major QTL positions.

	1.06	2.09	7.02	umc1691	umc1688	LLW	FLH
MO087	M	B	M	M	B	5.07	5.24
MO092	M	B	M	M	B	4.83	5.11
Average 7 selected IBM	M	B	M	M	M	6.10	5.96
Average 14 selected IBM	M	B	M	B	B	5.34	5.24
MO134	B	B	B	M	B	6.22	4.83
MO250	B	B	B	M	B	6.76	6.81
Average 23 selected IBM	B	B	B	B	B	5.75	5.63
Average 17 selected IBM	B	B	B	M	M	6.52	6.35
MO136	M	B	B	M	B	6.15	4.87
MO292	M	B	B	M	B	5.83	5.48
Average 17 selected IBM	M	B	B	B	B	5.62	5.58
Average 16 selected IBM	M	B	B	M	M	6.18	6.09
MO276	M	M	B	M	B	6.81	6.65
Average 10 selected IBM	M	M	B	B	B	5.90	5.50
Average 19 selected IBM	M	M	B	M	M	6.72	6.45
MO184	B	M	B	M	B	6.52	6.57
Average 19 selected IBM	B	M	B	B	B	6.15	5.80
Average 26 selected IBM	B	M	B	M	M	6.73	6.52

Table 3.5: Variance components for FLH and LLW in the IBM and NWRIL populations.

	IBMs-response FLH		IBMs-response LLW		NWRILs-response FLH		NWRILs-response LLW	
Effect	**Var proportion**	**p>F**	**Var proportion**	**p>F**	**Var proportion**	**p>F**	**Var proportion**	**p>F**
Genotype	**74.39%**	**<0.0001**	**75.54%**	**<0.0001**	**86.01%**	**<0.0001**	**27.81%**	**<0.0001**
Year	**0.69%**	**0.005**	**10.58%**	**<0.0001**	**1.03%**	**0.0004**	**42.35%**	**<0.0001**
Residual	**24.92%**	**/**	**13.88%**	**/**	**12.95%**	**/**	**29.83%**	**/**

Table 3.6: Primers used in this chapter.

Primers	Sequences
qGl15F	GTCACACGAACCCTGTCCATAT
qGl15R	CCCCTCGTTGATTCTGCTACC
SBP5F	GTCCACGACAAGCATACTGGTAAC
SBP5R	TGCTTCACCATGAACTCGTCTG
ActinF	TTGGTATGGAGGCTGCTGGA
ActinR	TATCCACATCTGTTGGAAAGTGCTG
Gl15_1440+	CCTGCTCAGAGATCTTTCGCTTTCCTTAC
Gl15_4504-	CACGGCGCAGGGACGATGGATG
Gl15_150+	GGAGACATGAGAGAGTTTCATATCC
Gl15_1660-	GCAGTTTAGACGATACCAGCTGAG
Gl15-1900-	TGGCATTGCTCCTCCATCGT
Gl15_2014+	CCGCCACCCAGCAGTTCTTT
Gl15_2880+	CTGCCGCGTCAAATGCTTCAGATGA
Gl15_2933-	CAACACGAACTCCTCCTTGCTCAAG
Gl15_3373+	GACAAGGAGCTCCAGTCGCA
Gl15_4000R2-	ACGACAGGAAAGGCTCAGCAGC
Gl15_3500-	CAGCCGCTGAAGAGTTCATGAA

Figure 3.1: Logarithm of Odds (LOD) plots indicating quantitative trait loci (QTLs). QTLs are marked by chromosome locations and zoomed by mapmaker. Hatch marks indicate relative positions of markers; yellow arrows indicate physical positions of identified leaf identity factors; B73 (B) or Mo17 (M) indicate alleles that contributing to positive allelic effect for leaf identity traits in the IBM population.

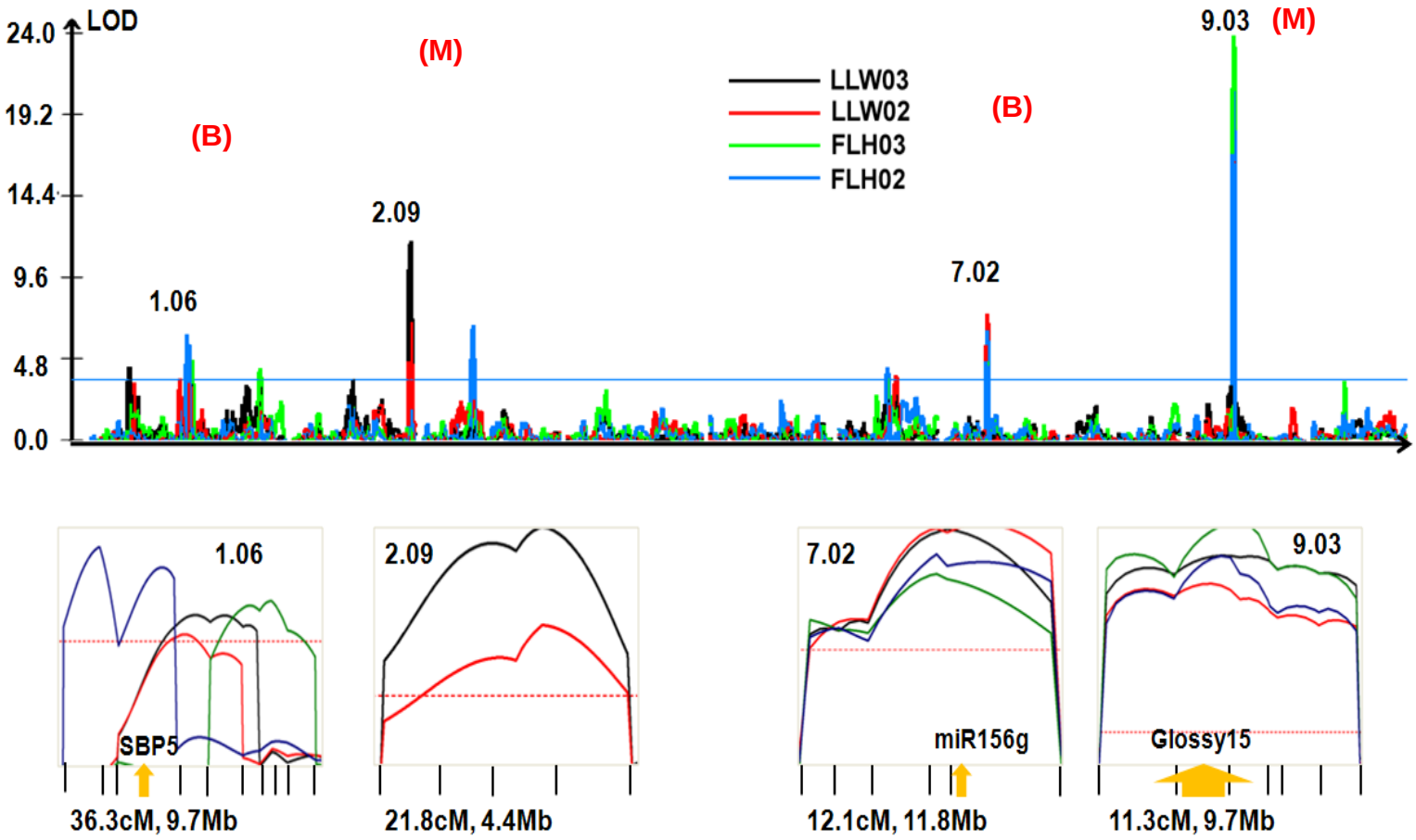


Figure 3.2: Phylogenetic trees of SPL proteins in Arabidopsis, rice and maize. Colored gene names indicate SPL genes with miR156 binding sites from Arabidopsis (green), rice (orange), or maize (red).

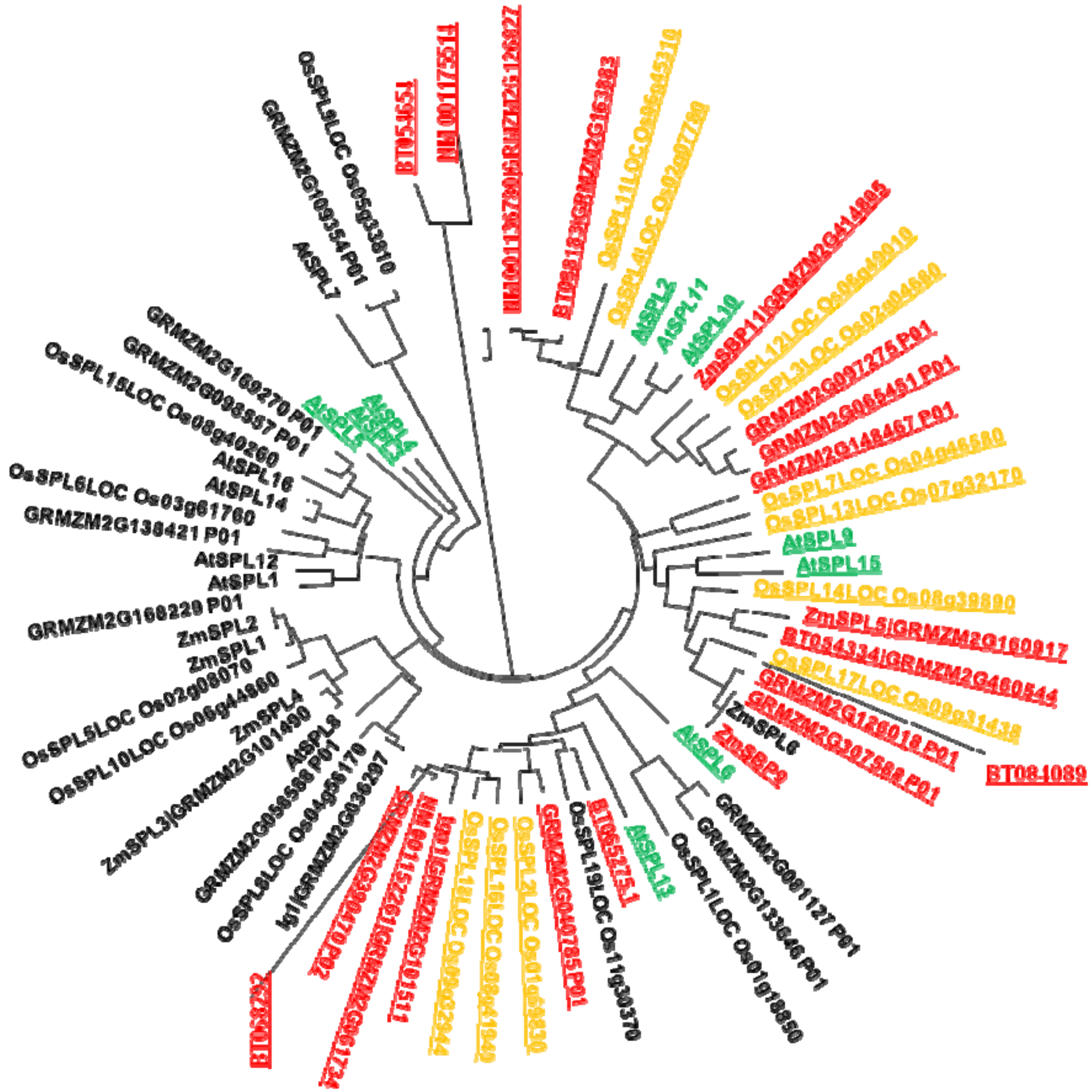


Figure 3.3: *Glossy15* gene structure among parental inbred lines. Triangles represent insertions, while parentheses represent deletions. Start and stop codons and the *miR172* binding site are marked with vertical arrows, the positions primers that amplify polymorphic regions are indicated as horizontal arrows below the Mo17 sequence cartoon.

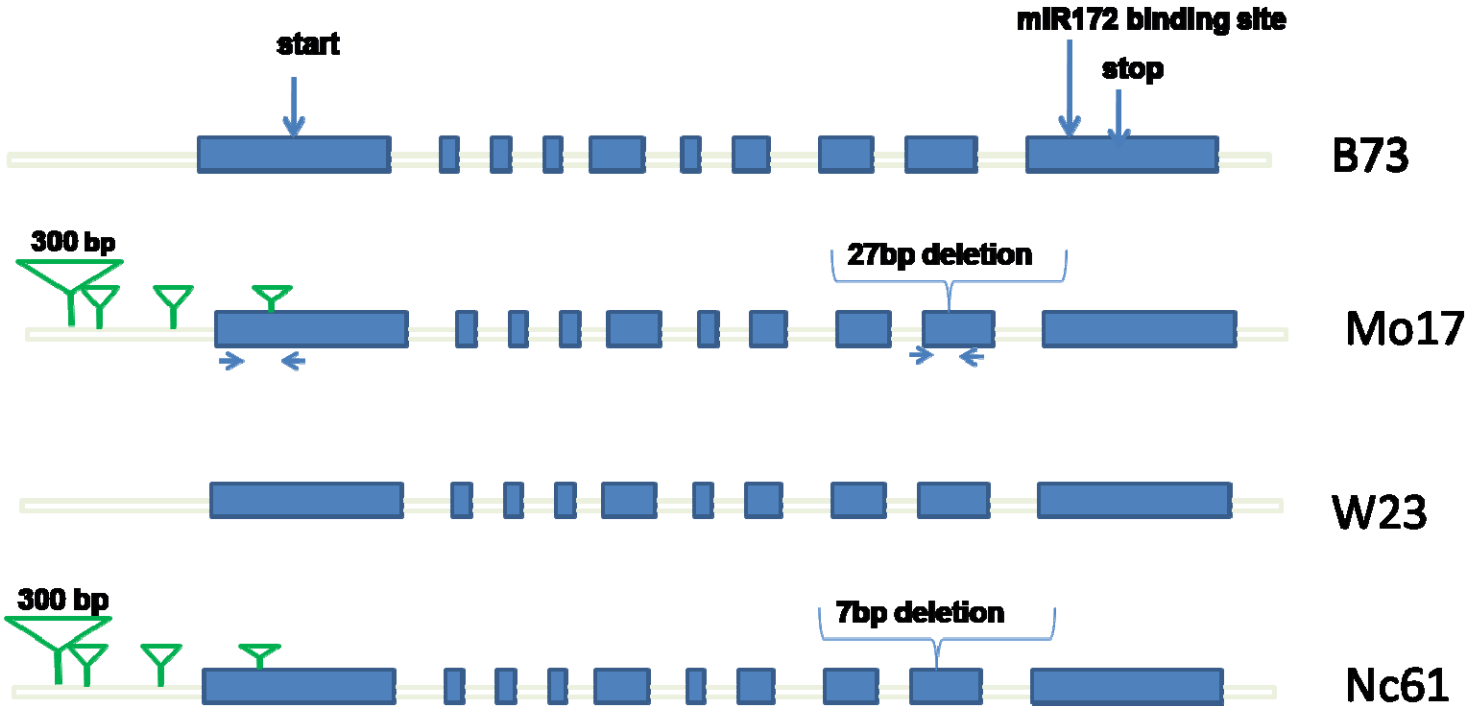


Figure 3.4: Relative expression of *Glossy15*, Zm*SBP5*, *miR156* and *miR172* in B73 and Mo17 during juvenile to adult leaf transition.

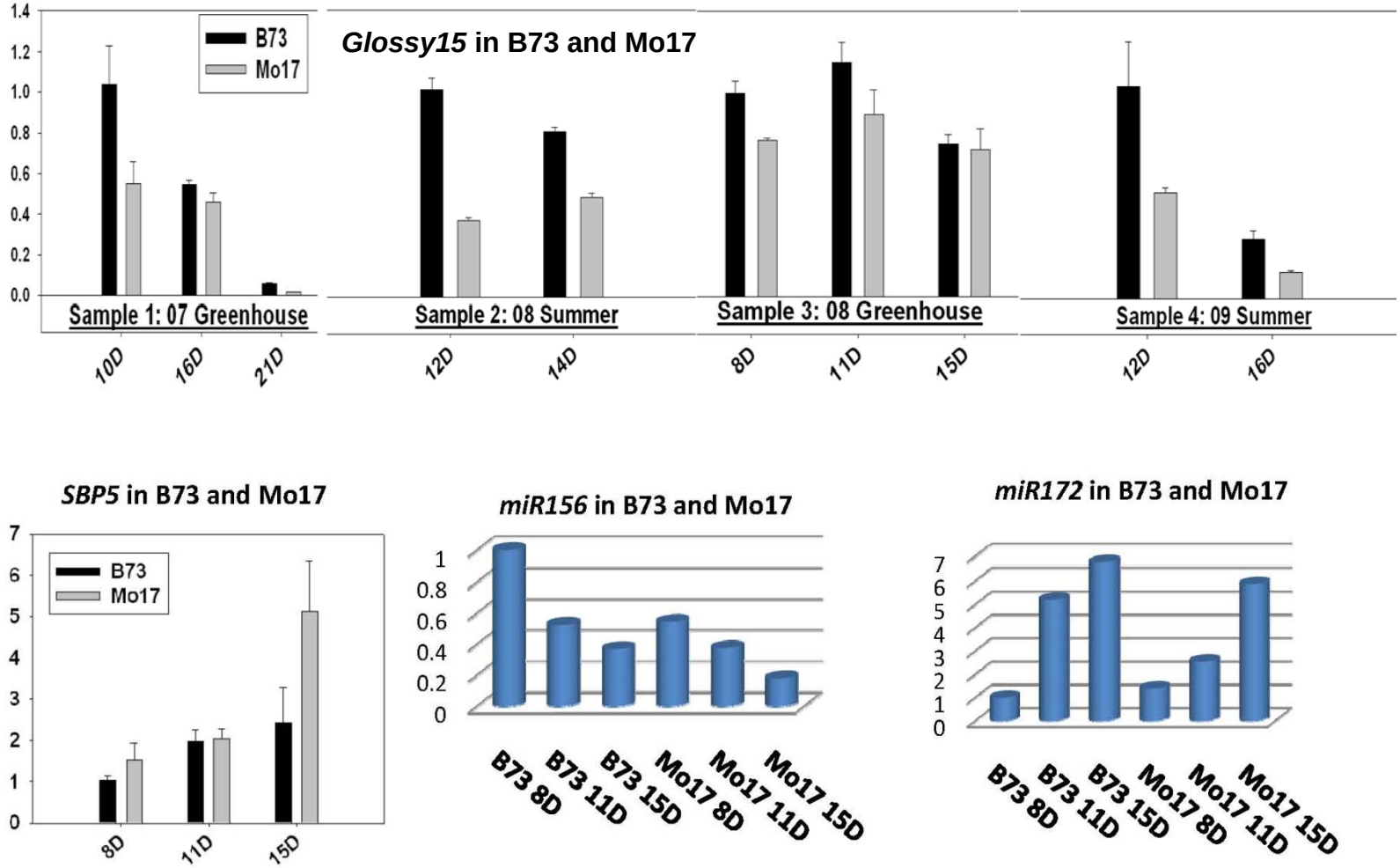


Figure 3.5: Relative expression of *Glossy15, SBP5, miR172* and *miR156* during the transition of juvenile to adult leaf identity in W23 and NC61.

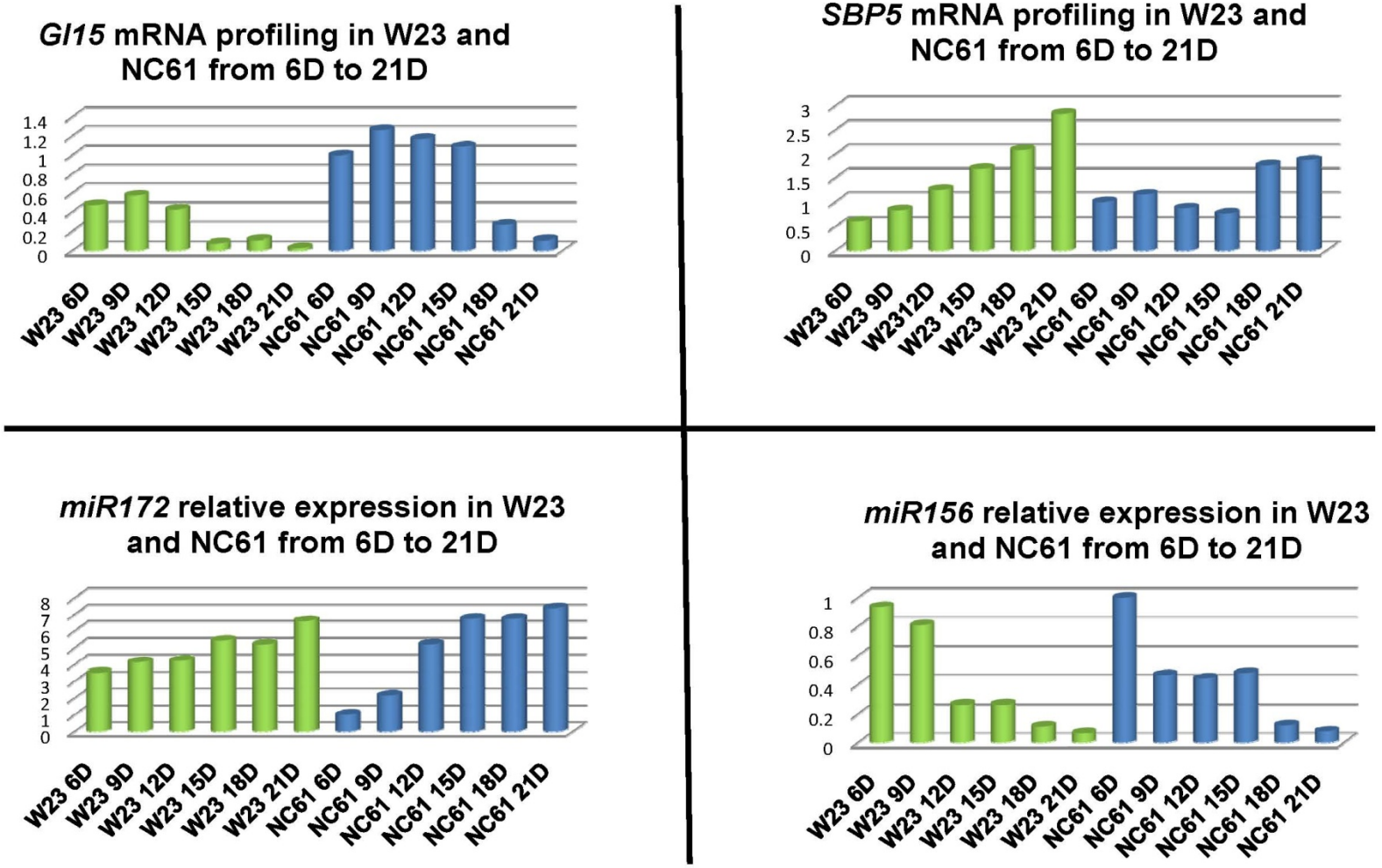
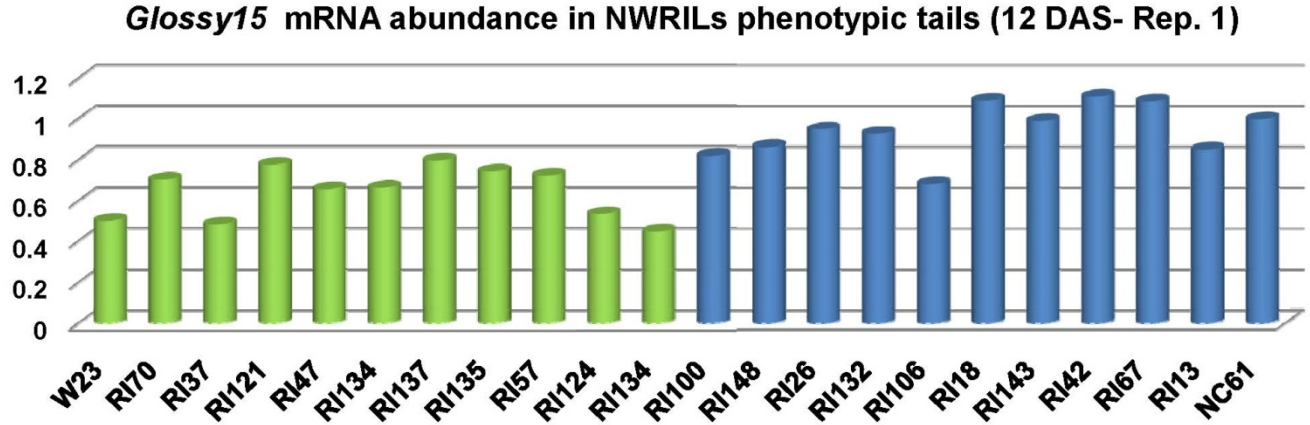
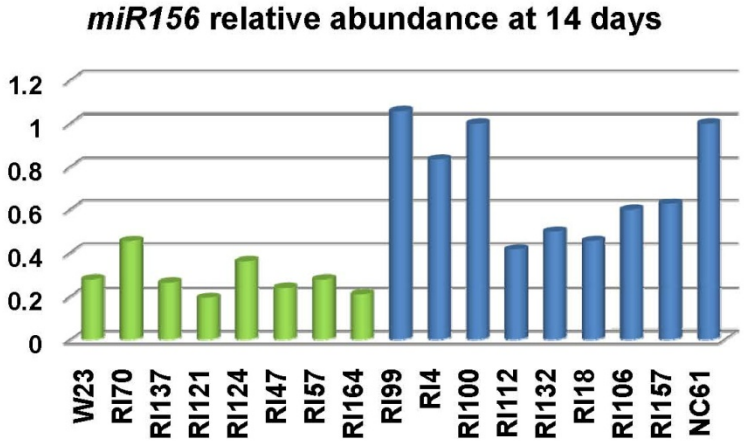
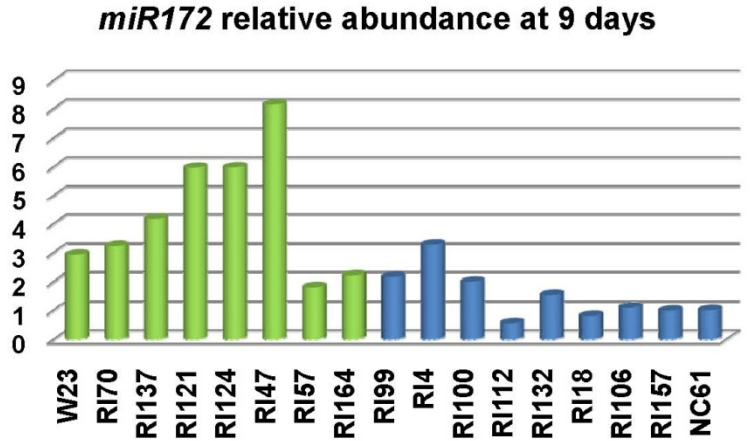


Figure 3.6: Relative expression of *Glossy15* mRNA, *miR156* and *miR172* in phenotypic distribution tails of NWRILs.







Chapter 4:

Sequence and expression variation of *Glossy15* and *miR156* among diverse maize inbred lines

Abstract

The number of leaves expression juvenile leaf identity varies widely among maize inbred lines, ranging from leaf 6 to leaf 13 in the 25 founder lines of the Nested Association Mapping (NAM) population. *Glossy15* exhibits a high degree of allelic diversity among the NAM founder lines, with more sequence variation in regions outside the conserved AP2 domain, especially in the promoter, 5'UTR, 3'UTR and near the stop codon. These polymorphisms could be grouped into two major clades driven largely by sequence variation in the *Glossy15* promoter. Statistical analyses did not identify any individual sequence variants within *Glossy15* that were strongly associated with phenotypic variation for leaf identity traits: early and late juvenile to adult transition lines exist in both *Glossy15* phylogenetic groups. A survey of both *Glossy15* and *miR156* expression during shoot development of the 26 NAM founders revealed a trend toward greater *Glossy15* mRNA and *miR156* expression with later onset of adult leaf identity, but a subset of six mostly tropical-derived inbreds exhibited late vegetative phase despite relatively low *Gl15* and *miR156* expression. The relative levels and rate of decline for *Gl15* expression during shoot development suggested variation in activities for both upstream regulators (e.g. *miR172, SPLs*) and downstream targets of *Gl15* (e.g. genes for wax synthesis and macrohair initiation also are important contributors to observed phenotypic differences for leaf identity traits among the NAM founder lines.

Introduction

Maize leaf identity traits differ between lower juvenile leaves and upper adult leaves. While macrohairs and glossy leaves are adult leaf traits, the coverage of bluish wax on leaves and stems are features of juvenile leaves. The transition from juvenile to adult leaf identity is a defining feature of vegetative phase change. In maize, two vegetative phase change genes are molecularly characterized based on mutants that accelerate or delay the juvenile to adult leaf identities transition. *Glossy15* encodes an AP2 domain transcription factor that is required to maintain juvenile leaf identity in all tested genetic backgrounds (Moose and Sisco, 1994 ; Moose and Sisco, 1996, and transgenic plants that overexpress *Glossy15* show delayed transition to adult leaf identity (Lauter et al., 2005). The function of *Glossy15* is downregulated by *miR172* through complementary binding (Lauter et al., 2005). Another gene for vegetative phase change is *miR156b/c*, which was isolated from the *Cg1* mutant through positional cloning and T-DNA insertion analysis (Chuck et al., 2007). Plants that overexpress *miR156b/c* produce juvenile leaf traits through the inflorescence and have extensively formed tillers (Chuck et al., 2007). In both Arabidopsis and maize, *miR156* delays vegetative phase change by targeting Squamosa Promoter Binding Like proteins (SPLs) (Wu and Poethig, 2006, Chuck et al., 2007, Wu et al., 2009).

In addition to the strong phenotypic effects arising from mutations or transgenic overexpressing lines, *Glossy15* also underlies important QTL for the onset of adult and duration of juvenile leaf identity in two maize recombinant inbred mapping populations (Chapter 3). DNA sequence analysis of *Glossy15* among the parents of these populations found two different alleles, one shared by B73 and W23, and another

divergent allele that is very similar between NC61 and Mo17, which is also present in the original *Gl15* sequence from the inbred line W64A. Furthermore, expression variation of *Glossy15* and *miR156* also underlies the phenotypic variation for the timing of vegetative phase change, where stronger *Glossy15* and *miR156* expression correlate with a late transition from juvenile to adult leaf identity (Chapter 3). Based on observed expression differences among parental lines and their progeny, and QTL effects associated with these two alleles, it appears that the *Gl15* allele in Mo17 and NC61 has greater activity in maintaining juvenile leaf identity compare to the *Gl15* allele present in W23 and B73. We reasoned that surveying sequence polymorphisms and expression variation of both *Gl15* and *miR156* in a broad collection of maize inbreds may reveal additional functional insights about these genes.

Core sets of maize inbred lines that capture the maximum proportion of allelic diversity observed in larger germplasm collections have been identified through marker analysis, which greatly reduces the number of lines required to achieve adequate sampling of alleles (Liu et al., 2003; Yan et al., 2009). In one study, 94 microsatellite markers were used to capture 2039 alleles in 260 temperate lines that represent much of the genetic diversity for important public temperate and some tropical germplasm sources, and a set of 25 core inbreds were identified to represent 80% of the allelic variation found among the original 260 lines (Liu et al., 2003). Single nucleotide polymorphisms (SNPs) may also be used to estimate genetic diversity, although their information content is about ten-fold lower compared to SSRs (Yu et al., 2009). A recent study to estimate relationships among inbreds using 1229 SNP markers generated1794 haplotypes within 327 loci, which confirmed the results of Liu et al. (2003), where the 25

core inbreds plus B73 and Mo17 captured 74.6% of all haplotypes (Yan et al., 2009). Thus, the 27 core inbred lines are appropriate to identify the majority of allelic variants that may be present in maize. We sequenced a genomic region spanning the entire *Gl15* transcription unit from these 27 inbreds, assayed the expression of *Gl15* and *miR156* in each of these lines during early shoot development, and investigated associations between DNA and RNA expression differences with variation in leaf identity phenotypes.

Materials and Methods

Leaf identity measurements

Maize inbreds were grown in Urbana summer nurseries at 2005, 2006, 2007 and 2008; leaf identity phenotypes were measured on three replicate plants each year. First Leaf Glossy (FLGL) and First Leaf macroHair (FLH) were measured and approximated to the nearest quarter leaf and averaged; Last Leaf Waxy (LLW) was recorded as the last whole leaf with visible juvenile wax at the tip of the leaf blade and averaged.

DNA sampling and extraction

For each inbred, 20 leaf punches from 10 individual plants were taken (2X10=20) and frozen at -80°C prior to DNA extraction. Samples were dipped into liquid nitrogen and ground in Genogrinder at 4000 strokes/minute for one minute. DNA extraction was performed by DNA extraction solutions from 5 PRIME (cell lysis solution and protein precipitation solution). First, 300 µl cell lysis solution was added to DNA samples followed by 10 seconds grinding in the Genogrinder. After 65°C water bath for 1 hour,

100 µl protein precipitation buffer was added and samples were left on ice for at least 1 hour. Following centrifugation, the supernatant was added into an equal amount of isopropanol, and precipitated DNA was removed from solution with pipette tips and transferred into 75% ethanol. After washing twice with 75% ethanol overnight, the DNA was dissolved in water.

Sequencing Glossy15

Gl15 primers were designed based on available *Glossy15* sequence from W64A and the B73 genome. *Gl15* sequences were amplified by primers Gl15_1440+ and Gl15_3434-, Gl15-3373+ and Gl15-4000R_2- and by primers Gl15_150+ and Gl15_1660- using EXPAND LONG TEMPLATE PCR SYSTEM from Roche. Components and thermo cycles of PCR are same as described in Chapter 3. *Glossy15* was sequenced directly from PCR products with multiple sequencing primers (for primer sequences, see primer tables in chapter 2 and chapter 3).

Sequence analysis and phylogenetic trees

Glossy15 sequences from diversity inbred lines were aligned using ClustalW within the Vector NTI software package; regions with sequence variation were identified and recorded (Table 4.1). Associations between individual sequence variants and phenotypic variation were investigated using single-factor analysis using the fit model function in the JMP4.04 software package, and TASSEL, which was developed by Ed Buckler's lab. Neighbor-joining phylogenetic and molecular evolutionary analyses were conducted using *MEGA* version 4 (Tamura et al., 2007).

RNA sampling, RNA isolation and mRNA/miRNA profiling

Three shoot apices from each line were dissected and the basal 1.5 centimeters was used for RNA isolation. RNA isolation and mRNA/miRNA profiling followed the same procedures as described in chapter 3.

Results

Variability for leaf identity traits in the maize 25 core diversity inbreds

The three leaf identity traits (FLH, FLGL and LLW) that were measured in each of the maize 25 diversity inbreds vary continuously. Macrohairs, a marker for adult leaf identity, could initially appear as late as leaf 8 in NC61, or as early as leaf three in CML69, CML228 and W23, which is comparable to the phenotype of *gl15* mutant plants (Table 2.2). The coverage of juvenile wax disappears as early as leaf five in W23 and could last as long as leaf 12 in NC61 (Fig. 4.1). The onset of adult traits FLH and FLGL usually correlate very well, but FLGL could be more than 2 leaves later than FLH (CML228). The number of transition leaves that show both juvenile and adult traits ranges from less than two (B73, NC358, Hp301) to more than five (IL14H, Oh43).

Glossy15 sequence polymorphisms

Based on the sequence differences between B73, Mo17, W23 and NC61 (Fig. 3.3), we initially focused our sequencing effort in two *Glossy15* regions. The first region was the promoter, because of the 300 bp insertion in Mo17 and NC61 (Fig. 3.3). The second region was detected by marker *umc1688*, 100 bp upstream of the *miR172* binding site (Fig 3.3). This region bears sequence similarities to *miR172* binding

sequences in B73 and W23 (16 out of 21 nucleotides are complementary to *miR172*), but was missing in Mo17.

The promoter region basically has two alleles (Fig. 4.2), with one allele being amplified as a1.1 kb fragment and the other a 1.5 kb fragment. The two alleles distribute randomly among the 25 diversity inbreds with respect to the timing of vegetative phase transition. For example, among the six earliest transition lines, CML69 and W23 have the 1.1 kb allele, while M37W, CML322, CML52 and CML228 have the 1.5 kb allele. At the pseudo *miR172* binding site, further sequencing of the diversity inbreds reveals this variation occurs as a simple sequence repeat (SSR) of AGC that is highly variable (Fig. 4.3). Sequencing of B73 and Mo17 cDNAs reveals that two of the AGC repeat sequences are within an exon. Relative to the B73 allele that is the most common (19 of 28 genotypes), five genotypes harbor a deletion of a single glutamine residue deletion (NC61, Oh43, P39, CML103 and IL14H), two genotypes possess an insertion of a single glutamine (Nc350, Tx303) and two genotypes (W64A and Mo17) harbor a nine amino acid deletion. Most of the inbred lines that possess changes within this SSR relative to B73 exhibit relatively late vegetative phase transition, except NC350 and Mo17. On the other hand, among those inbred lines with the same allele as B73 and W23, three (Mo18W, Hp301, CML247) also show late onset of adult leaf. The above results indicate that neither the *GI15* promoter variant nor the pseudo *miR172* binding site correlates with leaf identity phenotypes.

More Glossy15 sequence variations

Further sequencing was conducted on the entire *Glossy15* gene, which includes the 1.5 kb promoter and 600 bp of 3' flanking sequence. The results were summarized in Table 4.1. The haplotype patterns indicate prior recombination events among the major variants in some of the lines. For example, MS71, M37W, CML322 and CML277 share the same haplotype throughout the gene, except that in MS71, the promoter region lacks the 300 bp insertion. Based on sequence comparisons, historical recombination could have happened between positions 580 and 1265 in the MS71 *Glossy15* (Table 4.1).

We tested if any of the sequenced variation could correlate with leaf identity phenotypes in the 25 diversity inbred lines by 1) single marker analysis (basic T test) and 2) association analysis. Neither method gave a significant correlation ($p<0.05$) of any tested sequence variation. From the sequences, we noticed several amino acid changes in the coding region, including one conserved amino acid substitution in the AP2 domain (L/V), but again, the substitution doesn't always correlate with early or late leaf identity transition.

A phylogenetic tree of *Glossy15* sequences was constructed, which consisted of two major subgroups defined by the series of insertions within the promoter region. Relatively subtle variants determined the relationships among *Gl15* sequences from the other inbred lines, as indicated by the similarity values in the tree. Some of the branches within the tree reflect known aspects of demography or pedigree. For example, both Mo17 and W64A share the common CI 187-2 parent and are the only inbreds to contain the nine amino acid deletion.

Glossy15 mRNA profiling in maize diversity inbreds

In chapter 3, we showed that *Glossy15* sequence variation underlies the leaf identity QTL on Chr. 9.07 in IBMRIL and NWRIL mapping populations. But we were unable to show the correlation of DNA level variation and the leaf identity variation in a wider collection of maize diversity inbreds. We then tested whether variability in *Glossy15* mRNA profiles variation could be correlated with leaf identity phenotypes in the diversity inbreds.

Shoot apical meristems were sampled at 10, 14 and 19 days after sowing (DAS). As shown in Fig. 3.5, *Glossy15* has the highest expression at 9 DAS-12 DAS in both W23 and NC61, and starts to decrease at 15 DAS in W23, and by 18 DAS in NC61. Because the W23 and NC61 lines are extreme for the differences in the timing of the transition from juvenile to adult leaf identity (Fig. 4.1), we hypothesized that at 10 DAS, *Glossy15* mRNA should represent the highest level in all lines and at 19 DAS, *Glossy15* mRNA should significantly decrease. The results of *Glossy15* mRNA profiling are summarized in Fig. 4.5. As expected, *Glossy15* mRNA drops from 10 DAS to 19 DAS in all diversity lines. In some late transition lines (Hp301, IL14H, P39, B97 and Ms71), *Glossy15* mRNA remains at high level at 14 DAS, which correlates with their leaf identity phenotypes. But we also see low *Glossy15* mRNA levels at 14 DAS in some of the late lines (Mo18W, CML247, NC358, Ky21 and CML103), which was unexpected. Although *Glossy15* underlies the most significant QTL for leaf identities in two mapping populations and could explain over 30% of phenotypic variation (Chapter 3), there are still other factors that could contribute to the phenotypic variation among the diversity inbreds, such as *miR156*, GA, and downstream genes of *Glossy15*. In this regard, the

pattern of *Gl15* mRNA in the inbred Tzi8 is interesting in that *Gl15* is expressed at relatively low levels at 10 DAS, but does not decrease through 19DAS, becoming the line with the strongest *Gl15* expression at 19DAS. One possible explanation for this pattern is relatively low or late onset of *miR172* expression in Tzi8.

miR156 expression variation among maize diversity inbreds

The *miR156* level also correlates with leaf identity phenotypes, for example, the overexpression of *miR156* in *Corngrass1* mutants could greatly delay the juvenile vegetative leaf identity phenotypes (Chuck et al., 2007); and *miR156* accumulates at lower levels W23 compared to NC61 (Fig. 3.5). The *miR156* expression variation could also exist in maize diversity inbred lines.

As shown in Fig. 3.5 and Fig. 3.6, *miR156* has distinct difference between early transition lines and late transition lines around 12 DAS to 15 DAS, thus, we used shoot apical meristem samples collected at 14 DAS for *miR156* profiling. The result is shown in Fig. 4.6, the X axis of which is ordered by the appearance of first leaf with macrohairs. Earliest juvenile to adult transition lines (CML69, CML228, CML52, M37W, CML322 and Mo17) have lower *miR156* level. As the transition delays in NC350, Tx303, Oh7B, Oh43, Ki3, Ki11, B97, MS71, P39, IL14H, and Hp301, *miR156* level increases from 1.5 to 6-fold compared to Mo17. However, in lines CML103, Tzi8, Ky21, Nc358, CML247 and Mo18W, where the juvenile to adult transition is relatively late, *miR156* level is similar as that in the earliest transition lines. The expression levels of *Glossy15* are low in those lines as well. It is reasonable to deduce that factors other than *miR156*-

SPLs and *miR172-Glossy15* are playing key roles in determining the leaf identity phenotypes in those lines.

Discussion

Glossy15 sequence variation and leaf identity phenotypes

Segregation patterns of markers on *Glossy15* facilitated confirmation of the *Glossy15* genomic region as one of the QTLs controlling leaf identity phenotypes in the IBM population, and correlate with early or late juvenile to adult transition phenotypes in the NWRIL population (Chapter 3). Furthermore, a 6 kb genomic region of *Glossy15*, which includes 1.5 kb promoter and 3' UTR, is sufficient to functionally complement a null *glossy15* mutation (Lauter et al., 2005), and all sequenced *gl15* mutant alleles harbor insertions within the *Gl15* coding region (chapter 2). However, despite extensive sequencing of this 6 kb region and the presence of considerable diversity affecting both coding and non-coding sequences, our analysis of the diversity inbred lines couldn't identify key functional variants within *Gl15* that could be associated with phenotypic differences in the timing of vegetative phase change.

There are a number of possible explanations for the difficulties in identifying functional quantitative trait variation within *Gl15*. Analysis of only 25 diversity lines provides low statistical power to detect significant genotype-phenotype associations. In maize, a collection of more than 300 inbred lines have been used in association mapping in multiple studies, and expanding our analyses to this collection may help identify functionally important changes in *Glossy15* or other genes within the vegetative phase change pathway. Another reason of failing to detect any single variation in the

gene as important is that multiple variations are important for the function of *Glossy15*, each contributing a small effect. As a result, the final gene expression is the overall effect of the multiple variations, as described in Thornsberry et al., 2001. The last reason could be that the QTL on *Glossy15* is on genomic region that is far from the 6 kb *Glossy15*. Regulatory region of genes that is tens of kb upstream the coding region underlying QTLs are common in maize, which were demonstrated by studies on *tb1* (Clark et al., 2006) and *Vgt1* (Salvi et al., 2007). The first two scenarios require obtaining *Glossy15* polymorphism in a lot more inbred lines, and the last scenario requires extensive efforts of fine mapping on a much larger mapping population.

Sequencing the *Glossy15* loci in *zea mays ssp. mays* and three wild zea taxa (Ross-Ibarra et al., 2009), and in maize diversity inbred lines (McMullen et al., 2009, www.maizesequence.org) reveals the genetic diversity of *Glossy15*. Single nucleotide information on *Glossy15* (PZE0992800322-PZE0992802355 in maizesequence.org) covers 10 SNPs from 1856-2120 (after start codon and before AP2 domain) based on AY714877, 3 SNPs from 2127-2900 (first AP2 domain), 0 SNPs in the second AP2 domain and 6 SNPs between the end of AP2 domain and the stop codon. Sequence variation in the diversity inbred lines shows similar results to our data in the aspects of allele frequencies and the type of nucleotide changes. SNPs PZE0992800613 and PZE0992800646 in the AP2 domain result in synonymous amino acids, whereas PZE0992801086 leads to amino acids substitution (L or V).

Our sequencing data provides additional sequence polymorphisms beyond the mentioned SNPs, such as insertions/deletions and SNPs that were not listed in the

maizesequence.org. An example of the additional sequence polymorphism can be found in Fig. 4.3.

Sequences in *zea mays ssp. mays* and three wild zea taxa from 2350-3074 found more sequence variation of *Glossy15* in the landraces than modern maize. Among the 32 SNPs/indels in the landraces, only three are shared with NAM founder lines polymorphism and one of them is PZE0992801086. In 40 landraces, only one bears nucleotide C in this SNP locus; while in 22 *zea mays ssp. mays* lines, 15 of them have nucleotide C. In diversity maize inbred lines, the frequency of C is 0.63 (in both maizesequenc.org and our data) and sorghum sequence (NCBI) has the nucleotide of G. From the above analysis, there is G-C change from sorghum to maize. Notably, comparing sorghum, maize landraces and diversity maize lines found conservative AP2 domains. If the *Gl15* gene carries different functionality between maize and sorghum, the differences has to relate to sequences outside the AP2 domain; conversely, if the *Gl15* gene targets the same set of leaf identity genes in both maize and sorghum, then the most important functional domain is the AP2 domain.

Glossy15 and miR156 expression variation and leaf identity phenotype

Glossy15 and *miR156* expression correlate with parental and recombinant inbred phenotypes in NWRIL population (chapter 3), and correlate with promoted or delayed vegetative phase change in mutants. The genetic network of *miR156-SPLs, miR172-Glossy15* and the interactions between them and other factors such as GA regulate leaf identity phenotypes (chapter 2). *Glossy15* regulates both the transition of wax deposition on leaves and stems, and the appearance of macrohairs. Up to now, no

genes are identified as downstream targets of transcription factor *Glossy15*. For lines which have late leaf identity transition but not more *Glossy15* mRNA or *miR156*, genes directly controlling wax deposition or macrohairs formation might have promoted or depressed binding with *Glossy15*. With this reasoning, those lines are important in studying downstream targets of *Glossy15*.

Conclusion

Glossy15 sequence polymorphism was studied in maize core collection of diversity inbreds, and no obvious variation is correlated with leaf identity phenotypes. Diversity inbreds are divided into two subgroups based on *Glossy15* sequence variations. Although *Glossy15* mRNA and *miR156* have the trend to increase in late leaf identity transition lines, some lines are not following this trend, which might be valuable resources to study *Glossy15* downstream targets. Furthermore, larger inbred population for association analysis or larger mapping population for fine mapping analysis are needed to narrow the *Glossy15* genomic region that control the 30% leaf identity variation.

References

Chuck, G., A.M. Cigan, K. Saeteurn, and S. Hake. 2007. The heterochronic maize mutant *Corngrass1* results from overexpression of a tandem microRNA. Nature Genetics 39:544-549.

Clark, R.M., T.N. Wagler, P. Quijada, and J. Doebley. 2006. A distant upstream enhancer at the maize domestication gene tb1 has pleiotropic effects on plant and inflorescent architecture. Nature Genetics 38:594-597.

Lauter, N., A. Kampani, S. Carlson, M. Goebel, and S.P. Moose. 2005. microRNA172 down-regulates glossy15 to promote vegetative phase change in maize. Proceedings of the National Academy of Sciences of the United States of America 102:9412-9417.

Liu, K.J., M. Goodman, S. Muse, J.S. Smith, E. Buckler, and J. Doebley. 2003. Genetic structure and diversity among maize inbred lines as inferred from DNA microsatellites. Genetics 165:2117-2128.

Lee, M., N. Sharopova, W. D. Beavis, D. Grant, M. Katt et al., 2002 Expanding the genetic map of maize with the intermated B73 × Mo17 (IBM) population. Plant Mol. Biol 48: 453–461.

McMullen, M.D., S. Kresovich, H.S. Villeda, P. Bradbury, H.H. Li, Q. Sun, S. Flint-Garcia, J. Thornsberry, C. Acharya, C. Bottoms, P. Brown, C. Browne, M. Eller, K. Guill, C. Harjes, D. Kroon, N. Lepak, S.E. Mitchell, B. Peterson, G. Pressoir, S. Romero, M.O. Rosas, S. Salvo, H. Yates, M. Hanson, E. Jones, S. Smith, J.C. Glaubitz, M. Goodman, D. Ware, J.B. Holland, and E.S. Buckler. 2009. Genetic Properties of the Maize Nested Association Mapping Population. Science 325:737-740.

Moose, S.P., and P.H. Sisco. 1994. Glossy15 Controls the Epidermal Juvenile-to-Adult Phase-Transition in Maize. Plant Cell 6:1343-1355.

Moose, S.P., and P.H. Sisco. 1996. Glossy15, an APETALA2-like gene from maize that regulates leaf epidermal cell identity. Genes & Development 10:3018-3027.

Ross-Ibarra, J., M. Tenaillon, and B.S. Gaut. 2009. Historical Divergence and Gene Flow in the Genus Zea. Genetics 181:1397-1409.

Thornsberry, J.M., M.M. Goodman, J. Doeboley, S. Kresovich, D. Nielsen and E.S. Buckler. 2001. Dwarf8 polymorphism accociate with variation in flowering time. Nature Genetics 28: 286-289.

Wu, G., and R.S. Poethig. 2006. Temporal regulation of shoot development in Arabidopsis thaliana by miR156 and its target SPL3. Development 133:3539-3547.

Wu, G., M.Y. Park, S.R. Conway, J.W. Wang, D. Weigel, and R.S. Poethig. 2009. The Sequential Action of miR156 and miR172 Regulates Developmental Timing in Arabidopsis. Cell 138:750-759.

Yan, J.B., T. Shah, M.L. Warburton, E.S. Buckler, M.D. McMullen, and J. Crouch. 2009. Genetic characterization and linkage disequilibrium estimation of a global Maize collection using SNP markers. Plos One 4:-.

Yu, J.M., Z. Zhang, C. Zhu, D.A. Tabanao, G. Pressoir, et al. 2009 Simulation appraisal of the adequacy of number of background markers for relationship estimation in association mapping. The Plant Genome 2: 63–77.

Salvi, S., G. Sponza, M. Morgante, D. Tomes, X. Niu, K.A. Fengler et al., 2007. Coserved noncoding genomic sequences associated with a flowering-time quantitative trait locus in maize. PNAS 104: 11376-11381.

Table 4.1. *Glossy15* sequence variation in maize NC61, W23, W64A and diversity inbred lines.

	300bp ins	509	1265	1305	1440	1560	1680	1760 (Mo 891)	1765	1783	1810	1860 (aa)	1900 (aa)	1918 (aa)	1930 (aa)	1980	2000	2010 (aa)	2060-2070 (aa) (Mo1 992)	2610 (aa)	2630 (aa)	2660 (aa)	2710 (aa)	3225 (aa)	3240 (aa)	4400	4460
B73	No	+		GA	A		A	BGA	A	C				A	V	E		E ins	SSSSRRPFA	D	S			GS	Y	G	
CML69	No	+		GA	A		A	BGA	A	C				A	V	E		E ins	SSSSRRPFA	D	S			GC	Y	G	
W23	No	+		GA	A		A	BGA	A	C				A	V	E		E ins	SSSSRRPFA	D	S			GS	Y	G	
NC350	No	+		GA	A		A	BGA	A	C				A	V	E			SSSSSRRPPA	D	P	QQ ins	NA	NA	Y	G	
Oh7B	No	+		GA	A		A	BGA	A	C				A	V	E	V	E ins	SSSSRRPFA	D	S			GS	Y	C	
Ki11	No	+		GA	A		A	BGA	A	C				A	V	E		E ins	SSSSRRPFA	D	S			GS	Y	G	
B97	No	+		GA	A		A	BGA	A	C				A	V	E		E ins	SSSSRRPFA	D	S			GS	Y	G	
Ky21	No	+	NA	NA	NA	NA	NA	NA	NA	NA	NA	NA	NA	NA	NA	E		E ins	SSSSRRPFA	D	S			GS	Y	G	
Tzi8	No	+		GA	A		A	BGA	A	C				A	V	E		E ins	SSSSRRPFA	D	S			GS	Y	G	
CML247	No	+		GA	A		A	BGA	A	C				A	V	E		E ins	SSSSRRPFA	D	S			GS	A	G	
Hp301	No	+		GA	A		A	BGA	A	C				A	V	E		E ins	SSSSRRPFA	D	S			GS	A	C	
Mo18W	No	+		GA	A		A	BGA	A	C				A	V	E		E ins	SSSSRRPFA	D	S			GS	Y	G	
Ki3	No			GA	A		A	BGA	A	C				A	V	E		E ins	SSSSRRPFA	D	S			GS	Y	G	
NC358	No			GA	A		A	BGA	A	C				A	V	E		E ins	SSSSRRPFA	D	S			GC	Y	G	
MS71	No	+		GA	A		A	basic	AGCT ins	T	CGAC ns	R ins	R	V	E	R	V	E ins	SSSSRRPFA	D	S			GS	Y	G	1 bp del
M37W	+			GA	A		A	basic	AGCT ins	T	CGAC ns	R ins	R	V	E	R	V	E ins	SSSSRRPFA	D	S		G	GS	Y	G	
CML322	+			GA	A		A	basic	AGCT ins	T	CGAC ns	R ins	R	V	E	R	V	E ins	SSSSRRPFA	D	S			GS	A	C	
CML277	+			GA	A		A	basic	AGCT ins	T	CGAC ns	R ins	R	V	E	R	V	E ins	SSSSRRPFA	D	S			GS	A	C	
Mo17	+	CAA-AG ins	T ins	ACC	C	GGC ns	G ins	GGA	T	T			R	A	V	R	V		ABSENT	G	P	QQ ins		AS	A	C	
Tx303	+		T ins	ACC	C	GGC ns	G ins	GGA	T	T			R	A	V	R	NA		SSSSSSRRPPA	D	S			GS	Y	G	
Oh43	+	16 bp del	T ins	ACC	C	GGC ns	G ins	GGA	T	T			R	A	V	R	V		SSSRRPPF	G	P		G	GT	A	G	GAGC
H11H	+		T ins	ACC	C	GGC ns	G ins	GGA	T	T			R	A	V	R	V		SSSRRPPF	G	P			GT	A	G	GAGC
CML52	+		T ins	ACC	C	GGC ns	G ins	GGA	T	T			R	A	V	R		E ins	SSSSRRPFA	D	S			GS	A	C	
Nc61	+	16 bp del	T ins	ACC	C	GGC ns	G ins	GGA	T	T			R	A	V	R	V		SSSRRPPF	G	P		G	GT	A	G	
W64A	+	CAA-AG ins	T ins	ACC	C	GGC ns	G ins	GGA	T	T			R	A	V	R	V		ABSENT	G	P	QQ ins		GC	A	C	
CML103	+		NA	NA	NA	NA	NA	NA	NA	NA	NA	NA	NA	NA	NA	NA	NA		SSSRRPPF	G	P			GS	A	C	TG
CML228	+		NA	NA	NA	NA	NA	NA	NA	NA	NA	NA	NA	NA	NA	NA	NA	E ins	SSSSRRPFA	D	S			GS	A	C	
P39	+		NA	NA	NA	NA	NA	NA	NA	NA	NA	NA	NA	NA	NA	NA	NA		NA	NA				GS	Y	NA	

Figure 4.1: Leaf identity traits vary continuously among maize core diversity inbred lines. The onset of adult traits is reflected by Fist Leaf with macroHairs (FLH) and Fist Leaf with adult Glossy (FLGL); the duration of juvenile leaf traits is represented by Last Leaf with juvenile Wax (LLW).

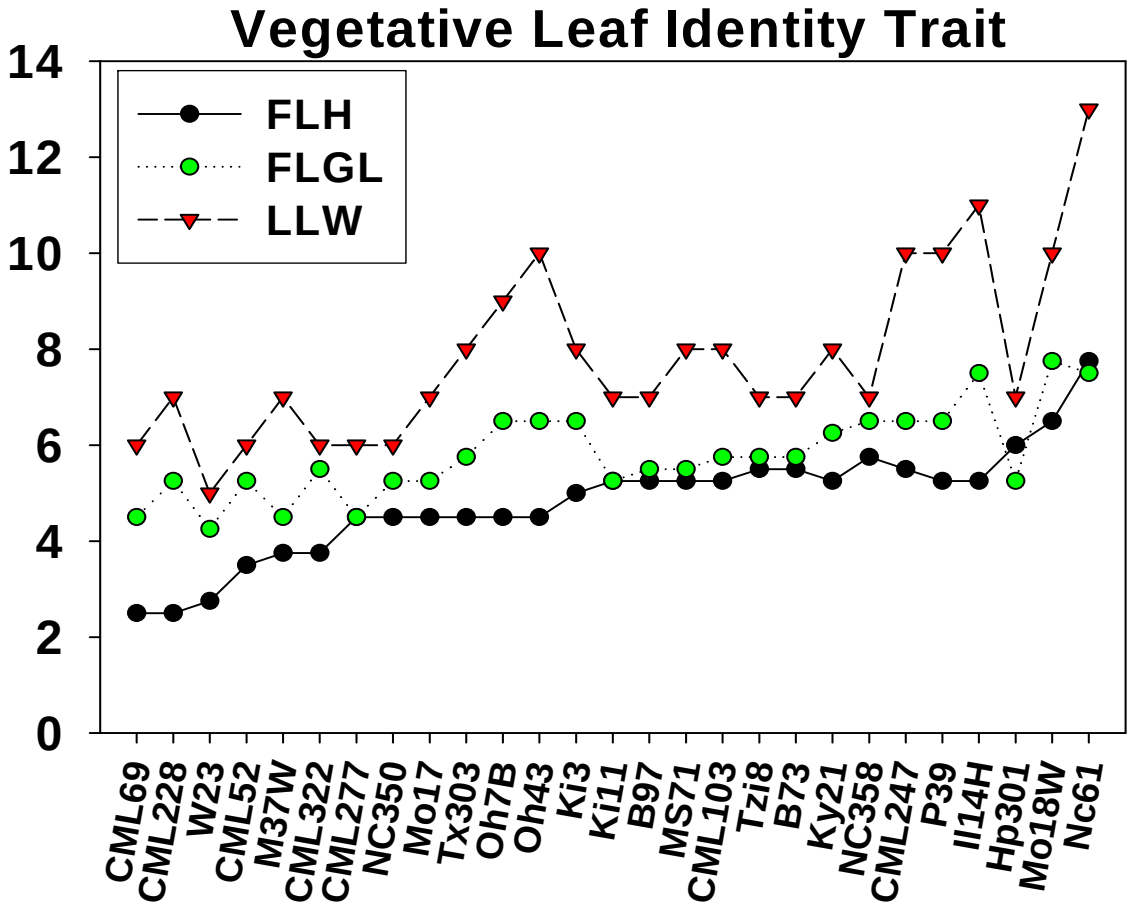


Figure 4.2: Two versions of *Glossy15* promoter exist in maize diversity inbreds.

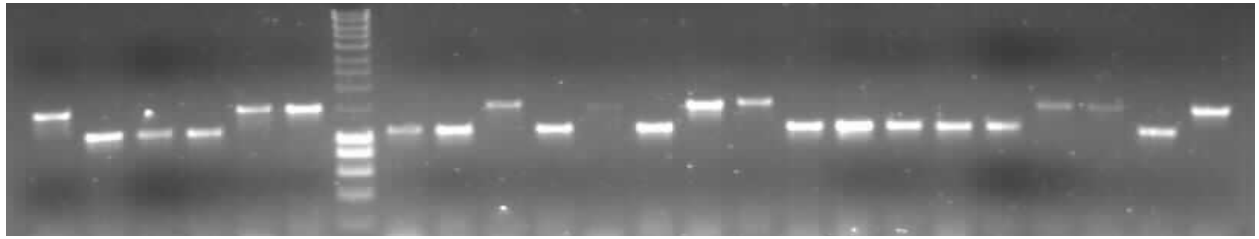


Figure 4.3: *Glossy15* simple sequence repeat variation at pseudo *miR172* target site in maize NC61, W23, W64A and diversity inbred lines.

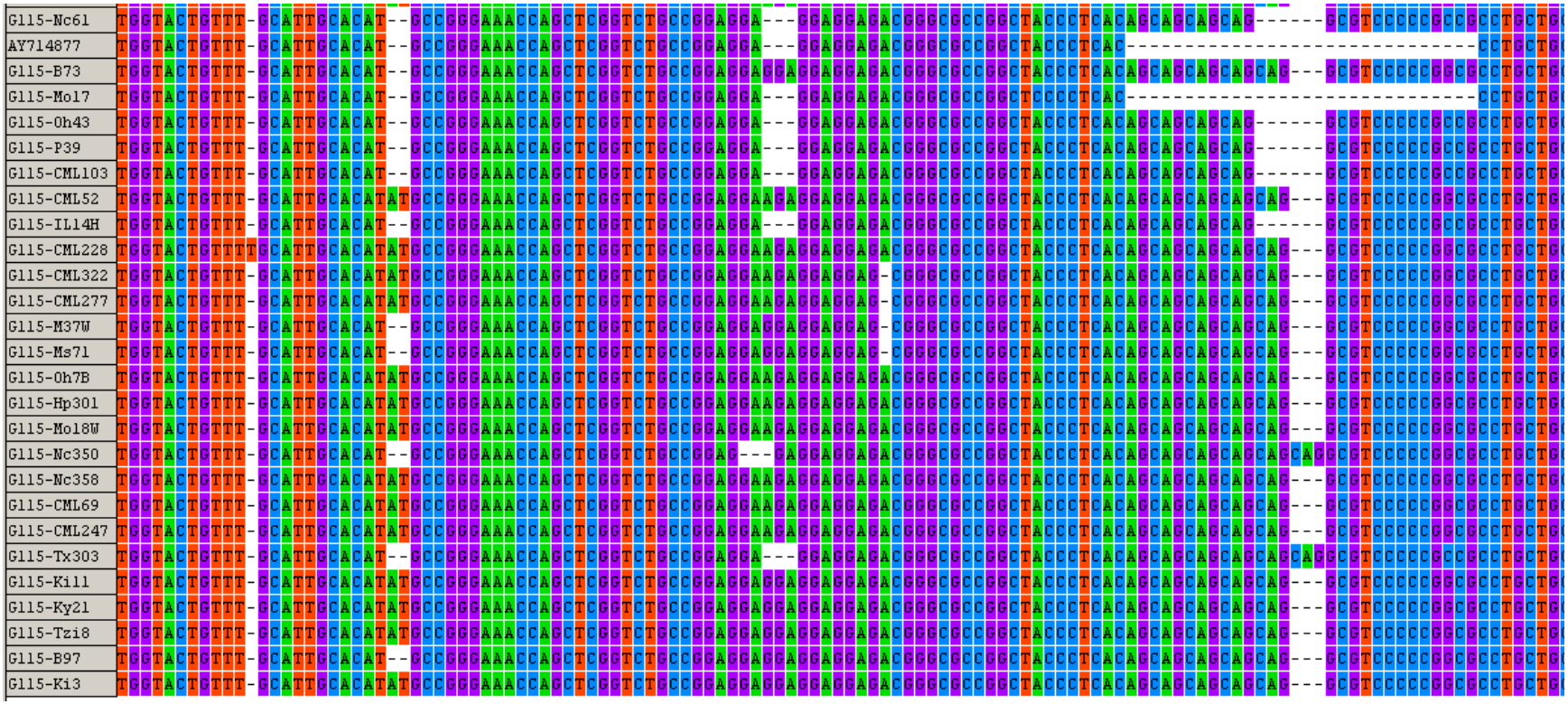


Figure 4.4: Phylogenetic distance of maize inbreds based on *Glossy15* sequence variation.

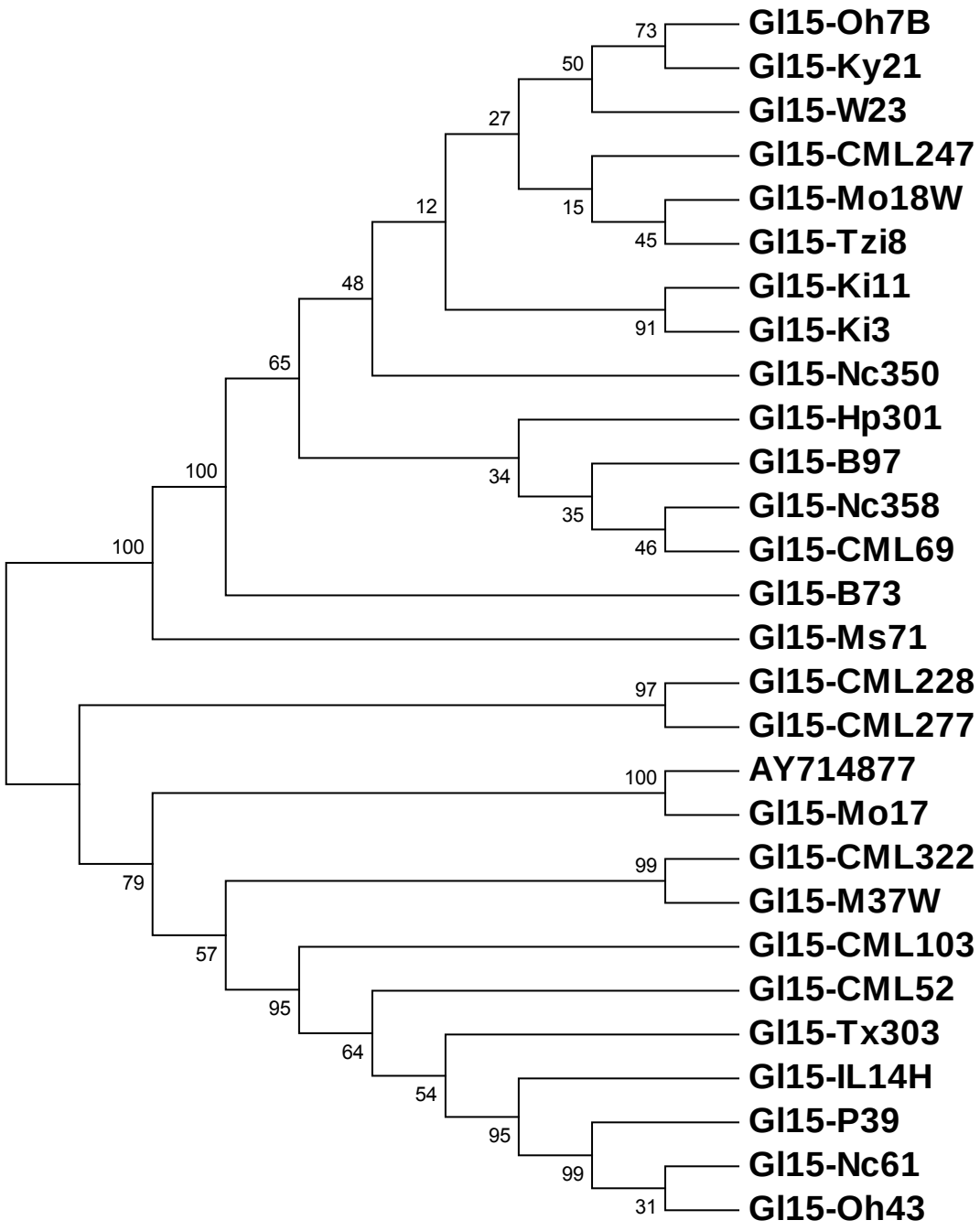


Figure 4.5: *Glossy15* mRNA profiling during vegetative phase change in maize diversity inbred lines.

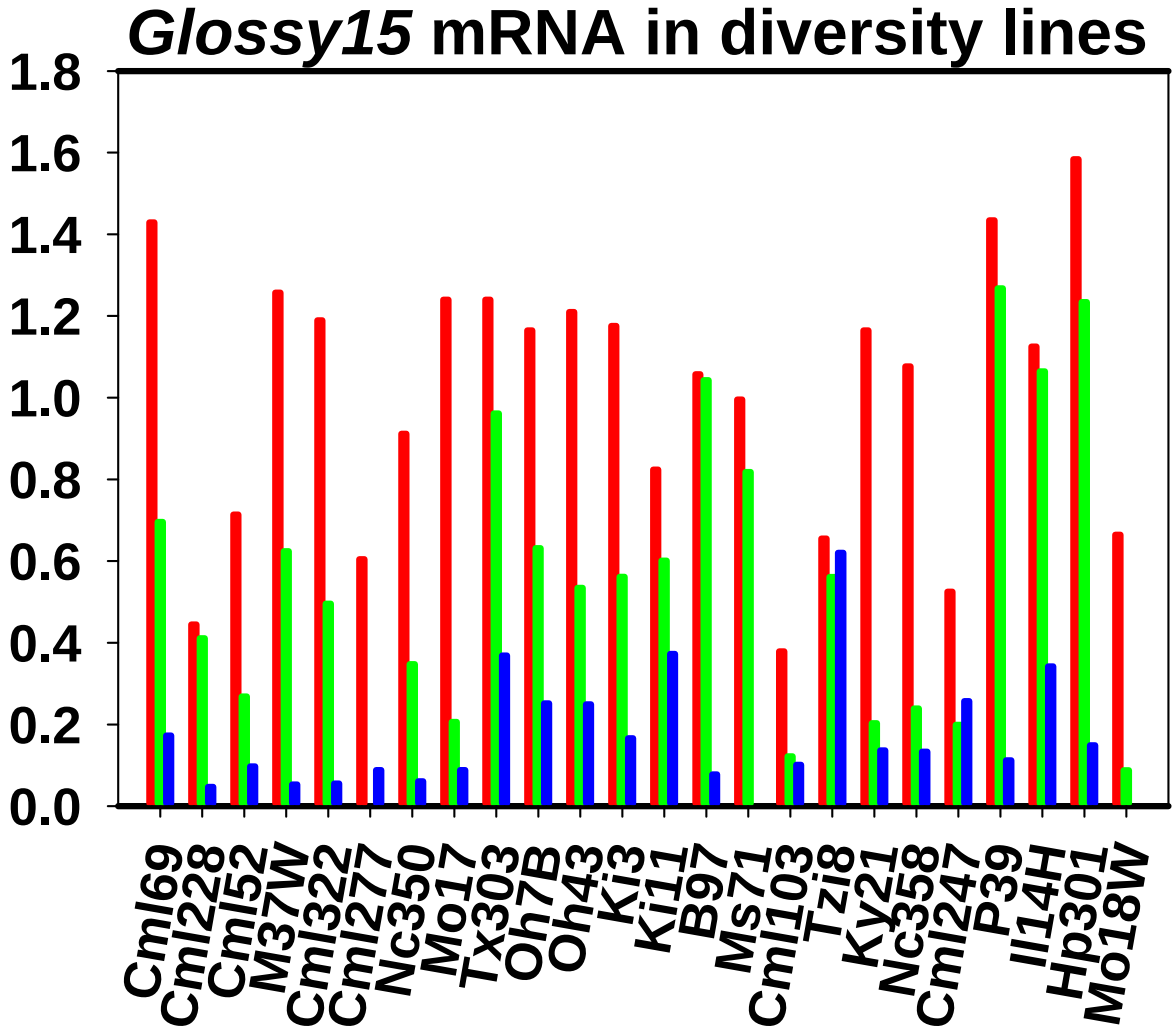
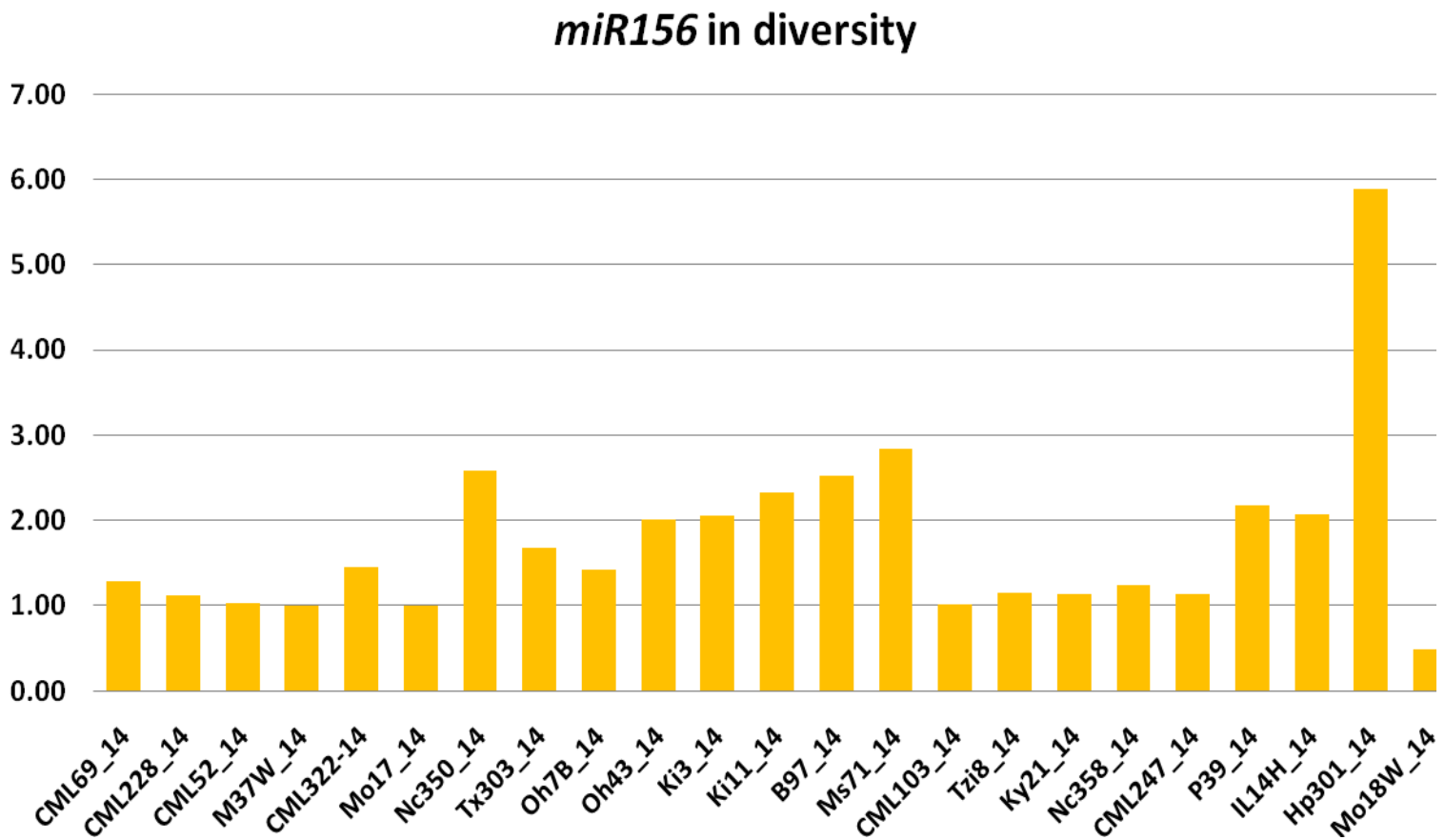


Figure 4.6: *miR156* profiling in maize diversity inbred lines at 14 days after planting.



Chapter 5:

Transcriptome profiling comparisons of *gl15* mutant and wildtype shoot apices reveals potential downstream target genes of *Glossy15*

Abstract

Maize leaf identity genes are identified based on altered leaf identity traits in mutants. Mutations in maize "glossy" genes result in glossy seedling leaves and stems that impact epicuticular wax production; the *macrohairless1* mutation controls macrohair initiation in adult leaves; and the *Corn rootworm sensitive1* (*Crs1*) locus affects the differential reactions of juvenile and adult epidermal cells with histochemical stains. To identify genes that appear to be under the control of *Glossy15* and hence potentially associated with leaf identity traits*,* a microarray experiment was designed to compare mRNA expression profiles from maize shoot apices of *glossy15* mutant and wildtype. Using the Maize Oligonucleotide Array with 57,000 oligonucleotide probes, a set of 113 genes were identified as showing statistically significant differential expression, among which 33 showed greater than four-fold differences in relative expression between wild-type and *gl15*. Several of the differentially-expressed genes have predicted functions in epicuticular wax production, including an Acyl CoA reductase gene (MZ00002722), and in subsequent validation experiments showed expression patterns that are highly correlated with the expression of *Glossy15*. Chemical components between juvenile and adult leaves, and between leaf five from wildtype and *gl15* mutant plants, reveal the functional positioning of *Glossy15* within the wax biosynthesis pathway, which are further supported by microarray and qPCR results. Our study demonstrates that

Glossy15 appears to determine the components of juvenile and adult waxes by activating aldehyde reductase and suppressing aldehyde decarbonylase.

Introduction

The most visually obvious trait that distinguishes juvenile from adult leaf identity in maize is the production of leaf epicuticular waxes. Juvenile leaves exhibit a blue-gray coating of epicuticular wax that is lost upon transition to the adult phase. Adult leaves thus appear shiny or "glossy". A total of 18 distinct genetic loci have been identified where mutations interfere with juvenile epicuticular wax production, leading to a glossy seedling leaf phenotype (reviewed in Schnable et al., 1994). For wax biosynthesis, fatty acid precursors (18 carbons in length, C_{18}) are sequentially elongated in 2-carbon steps to very long chain fatty acids ($>C_{24}$) that can subsequently be reduced to aldehydes then alcohols, decarbonylated to alkanes, or conjugated to alcohols to form wax esters (reviewed in Avato, 1987; Samuels et al., 2008). Maize juvenile leaves produce a greater amount of wax relative to adult leaves, which consists nearly entirely of the C_{32} primary alcohol dotriacontanol (Bianchi et al., 1984; Blaker and Greyson, 1988). In contrast, adult leaf wax is a complex mixture of alkanes and esters. Many of the maize *glossy* mutants can be placed at defined steps within the wax biosynthetic pathway, and at least five of these genes have been cloned, including *Glossy15*.

Glossy1 encodes a putative membrane-bound decarbonylase (Sturaro et al., 2005). *Gl1* expression is not restricted to juvenile developmental stage, pointing to the fact that this gene has a broader function, which could be seen by the pleiotropic effect brought by the *glossy1* mutation, such as cutin structure and trichome size (Sturaro et

al., 2005). *Glossy8* is a beta-keto acyl reductase/elongase, whose expression is mainly in juvenile seedlings, but also present in other developmental tissues (Xu et al., 1997; Xu et al., 2002). *Glossy2* is homologous to the Arabidopsis CER2 acyltransferase, which is required for the C_{30}-C_{32} elongation step, *Glossy2* expresses mainly in juvenile leaves as well (Tacke et al., 1995). Therefore, the expression pattern of *Glossy8* and *Glossy2* indicates they are potentially interacting with *Glossy15*. *Glossy4* was recently cloned, this gene shares 60% similarity to Arabidopsis CUT1 gene (Liu et al., 2009), which encodes a condensing enzyme involved in the synthesis of very- long-chain fatty acids (Miller et al., 1999).

A distinguishing feature of maize adult leaves is the formation of a number of specialized cell types, the most prominent being the visible macrohairs. The *macrohairless1 (mhl1)* mutation specifically blocks macrohair initiation in the leaf blade (Moose et al., 2004). Double mutant analysis with *dwarf1* and *gl15*, which maps only 5 cM from *mhl1*, demonstrated that *mhl1* acts downstream of these genes, suggesting that the *MHL1* gene product is likely to be repressed by *Gl15* and stimulated by GAs.

Juvenile and adult maize leaves also differ in the staining reaction of epidermal cells with toluidine blue. Juvenile epidermal cells stain purple, whereas adult cells stain blue. These staining differences are believed to reflect biochemical differences in cell wall composition, most likely resulting from the higher degree of transesterification among glucoarabinoxylans, hydroxycinnamic acids, and ferulic acid in adult compared to juvenile leaves (Moose, 1995). Genetic screens conducted by the Moose laboratory have identified the *epidermal cell wall1(ecw1)* mutation, which causes adult leaf epidermal cells to stain violet instead of aqua with toluidine blue without altering the

expression of leaf waxes or hairs. A second transposon-induced allele of *ecw1* has been characterized by Guri Johal's laboratory at Purdue University, which they have named *Corn rootworm sensitive1* (*Crs1*) because of the associated phenotype of increase susceptibility to leaf feeding by insects such as the corn rootworm beetle (*Diabrotica* spp.).

In a study that characterize transcriptome differences between maize juvenile and adult leaves, authors compared and analyzed differentially expressed genes in juvenile leaf 4, adult leaf 9 and rejuvenated leaf 3 or 4 (Strable et al., 2008). The largest class of juvenile induced genes was associated with photosynthesis, an example of which is Cab48. Phase change or leaf wax related genes are also identified, such as CUT1, CER5 and one of the SPL genes (Strable et al., 2008). Mutation of CUT1 and CER5 both result in glossy, waxless plants in Arabidopsis. SPL genes are also involved in phase change and appear to promote adult traits, their activity is repressed during the juvenile phase by *miR156* (Wu and Poethig, 2006, Chuck et al., 2007 and Wu et al., 2009).

In order to identify genes whose expression is specifically affected by *Glossy15*, which could be involved in determining leaf identity traits. A microarray experiment was designed to compare RNA expression profiles from the *glossy15-H* null mutation and the wildtype at nine days after sowing (DAS). Some differentially expressed genes were further analyzed with qRT-PCR in *glossy15* null mutation, wildtype and *Glossy15* transgenic plant samples.

Materials and Methods

Microarray hybridization and data acquisition

For microarray analysis, 10 shoot apices were pooled and used for RNA extraction and cDNA synthesis. RNA extraction followed the method described in Chapter 2.

Two-color microarray experiments were carried out using the Maize Oligonucleotide Array which contains 57,000 70-mer oligonucleotide probes printed over 2 slides, and 1,500ng total RNA as starting material, according to Maize Oligonucleotide Array Project protocols (www.maizearray.org, University of Arizona). Two biological replications and a dye-swap were conducted. RNA samples were amplified and labeled using the Amino Allyl MessageAmp™ II aRNA Amplification kit (Ambion, Austin, TX). Reverse transcription using T7 oligo(dT) primer was followed by in-vitro transcription with 5-(3-aminoallyl)-UTP, which produced amplified amino allyl modified antisense RNA (aRNA). NHS ester cyanine-3 and -5 dyes (GE Healthcare Bio-Sciences Corp., Piscataway, NJ) were then coupled to the amino allyl modified UTP residues in the aRNA to produce dye labeled aRNA. After purification, the targets were hybridized to the microarrays overnight at 42°C, and then washed. Microarrays were scanned with a Genepix 4000B scanner (Molecular Devices Corporation, Sunnyvale, CA) at 2 settings to enhance the detection of both weakly and strongly expressed genes. The slide images were quantified with Genepix Pro software, version 6.0 (Molecular Devices Corporation). Spots below background, or flagged as “bad” by Genepix Pro, for which spot fluorescence cannot be distinguished from the background, were ignored in all pre-processing and analysis steps.

Microarray data analysis

Intensity-dependent and space-dependent biases were minimized with replication and dye swap. Analyses were done with the Bioconductor package (VanHoute et al., 2010) in the R computing environment (http://www.r-project.org). After background subtraction from each array, spot quality weighting, with good spots of 1 and flagged spots of 0.1, were implemented in the *limma* software package. The expression values were normalized within each array using global loess, and between arrays using scalars estimated by the *limma* package. The normalized data for each slide/dye combination were median-centered so that expression measures would be comparable across slides. A least squares method was used for the linear fit model. Corrected data sets were examined graphically by MA-plots, where the average log2 of expression intensity A (corrected intensity Cy5 + corrected intensity Cy3)/2) was plotted against the log2 of expression difference M (corrected intensity Cy5 – corrected intensity Cy3). We call a gene significantly differentially expressed if its *p*-value is below a significance threshold of 0.01 according to the model distribution, A is greater than 7, and M is less than -1 or over greater than 1 for the data set

Quantitative real time PCR

Two biological replicate samples of shoot apical meristems were collected from *glossy15-H* null mutant, wildtype and *Glossy15*-TG plants at 9 DAS. RNA extraction and cDNA synthesis followed method in Chapter 2. The sequences of the oligonucloetide from the Maize Oligonucleotide Array (MZxxxxxxxx) were BLAST searched against the maize EST assembly TC19 (ZmB73_4a.53_working_cdna), and realtime PCR primers

were then designed based on EST sequences. Realtime PCR followed 94°C for 15 secs and melting and extension at 60°C for 1 min for all genes.

Results

gl15 mutation influences wax genes and cell wall genes

Using our criteria for significant differentially expressed genes, 153 probes are detected as differentially expressed between the wildtype and *gl15-H* null mutation (Fig. 5.1), among which 87 probes have increased and 66 have decreased relative expression levels in the *gl15* null mutation (Table 5.1). Thirty-three genes showed at least four-fold differences between the wildtype and *gl15* mutant shoot apex. Based on their annotated functions, ten genes associated with either cell wall or wax biosynthesis pathways were downregulatedin *gl15-H* compared to wildtype; conversely, five such genes were upregulated in *gl15-H* (Table 5.1).

Notably, *Glossy15* shows a six-fold decrease in relative expression in the *gl15-H* mutant, which is expected. Two wax genes, *Glossy4* that encodes a maize homology of the Arabidopsis CUT1 gene and a putative fatty acyl CoA reductase (MZ00002722), show similar decreases in *gl15-H* (Table 5.1), suggesting *Glossy15* activates the transcription of these two genes in shoot apical meristems. Another gene associated with wax production, a maize homolog of CER1 from Arabidopsis (MZ00027664)), shows eight-fold upregulation in the *glossy15* mutant samples. Another gene of note that is also strongly upregulated (six to eight-fold) in the *gl15-H* mutant encodes the rust resistance protein gene RP-1D.

qPCR validation of microarray genes

The differential expression of multiple genes with predicted functions in the wax biosynthesis pathway from this microarray analysis were investigated further using qRT-PCR. We chose several genes for qPCR validation, including *Glossy4* (CUT1 homolog), MZ00002722 (Acyl CoA reductase), MZ00000261, MZ00027664 (putative CER1), *Glossy2* and *Glossy8*. Even though we did not detect either *Glossy2* or *Glossy8* as differentially expressed through our microarray data, they are important in wax biosynthesis in maize. We also included *Gl15-TG* samples in this experiment, as true *Gl15* target genes might be expected to show increased expression in *Gl15-TG* relative to wild-type, although at this stage both the wildtype and *Gl15-TG* plants are in juvenile stage. As expected, qPCR results of most of the tested genes were consistent with microarray data. For the two Glossy genes, *Glossy2* shows decreased level in *gl15* mutant and *Glossy*8 barely changes between wild type and *gl15* mutant. This result matches very well with previous RNA gel blot analyses, where *Glossy8* was not influenced by *gl15* (S. Moose, unpublished). The qPCR results fail to validate the putative differential expression of CER1 transcript.

Discussion

Proposed model of wax synthesis in juvenile and adult tissues

Plant epicuticular waxes are composed of Very Long Chain Fatty Acids (VLCFA), which are elongated through sequential addition of C2 moieties from malonyl–coenzyme A (CoA) to preexisting C16 or C18 fatty acids. In Arabidopsis, there are two wax biosynthesis pathways: the acyl reduction pathway and the decarbonylation

pathway. Both of the two pathways begin by reducing VLCFAs into aldehydes through fatty acyl CoA reductase. Then the aldehydes can enter either the acyl reduction pathway where aldehyde reductase produces primary alcohols with an even number of carbons, or they enter the decarbonylation pathway where one carbon is removed by aldehyde decarbonylase to produce odd-numbered carbon alkanes (Millar et al., 1999).

Studies of Arabidopsis and maize mutants with defects in wax production, as well as the cloning of their gene products, have placed some of these genes into the wax biosynthesis pathway. For example, *glossy4* and *glossy2* mutation in maize accumulate C_{30} carbons, while in wild-type C_{32} prevails, indicating these two genes are involved in the elongation of C_{30} VLCFAs to C_{32} (Bianchi et al., 1979). The *glossy1* and *glossy8* mutants have drastically reduced overall amount of the all wax compounds, except esters, indicating these two genes sit at the very early stage of VLCFA elongation (Bianchi et al., 1979).

The biochemical composition of juvenile and adult wax was analyzed earlier using gas chromatography-mass spectrometry by Dr. Moose in his Ph.D. dissertation (Moose, 1995), and the results are shown again here for reference in Fig. 5.3. In wild-type W64A, leaf 5 represents a juvenile leaf and leaf 10 represents an adult leaf. The same leaf positions were analyzed from the gl15 mutant, but leaf five has adult identity. This analysis confirmed prior results (Blaker and Greyson, 1988) that juvenile leaves have a major peak of C_{32} alcohols, whereas adult leaf 10 of wild-type has major peaks of C_{27}, C_{29} and C_{31} alkanes and decreased C_{32} alcohols. Leaf five in the *gl15* mutant has a wax composition similar to leaf 10 in wildtype, and unlike other glossy mutants, *gl15* mutant has little reduction in total amount of wax (Moose, 1995).

Combining the microarray results, we propose a model as to how *Glossy15* conditions the changes in juvenile versus adult leaf waxes that is consistent with the biochemical and gene expression changes observed in the epicuticular wax synthesis pathway (Fig. 5.4).

Because the aldehyde reductase and aldehyde decarbonylase are the enzymes that control whether the chemically unstable aldehydes are converted to primary alcohols or odd chain alkanes, we propose that *Glossy15* mainly activates a C_{32} aldehyde reductase and also may inhibit the activity of aldehyde decarbonylase. When *Glossy15* is present in juvenile tissues and shoot apical meristems before 15 DAS, aldehyde reductase is activated and synthesizes C_{32} primary alcohols. At the same time, aldehyde decarbonylase is either inhibited by *Gl15* or the flux of C_{32} fatty acid precursors through the reduction pathway is so strong that alkanes do not accumulate (Fig. 5.4). In the adult leaf, the activities of both *Glossy15* and aldehyde reductase drop significantly, leading to a dramatic decrease in the amount of C_{32} primary alcohols. If *Gl15* suppresses aldehyde decarbonylase, then the transition to adult leaf identity would cause a rise in its activity and subsequent conversion of aldehydes to alkanes. Alternatively, lower levels of aldehyde reductase may increase the availability of aldehyde precursors available to enter the decarbonylation pathway. Another consequence from declining aldehyde reductase activity is the greater accumulation of aldehydes, which appears to have a negative feedback effect on fatty acyl CoA reductase and enzymes responsible for C_{30} to C_{32} elongation (*Glossy2, Glossy4*) and leads to the increased production of shorter chain (C27 and C29) alkanes. However, genes acting further upstream in the production of epicuticular waxes (e.g., *Glossy1* and

Glossy8) do not appear to be influenced by either the *gl15* mutation or vegetative phase change (Fig. 5.4).

Rust resistance gene RP1-D is repressed by Glossy15

The differential responses to common rust disease between juvenile and adult leaves are well-studied. For example, in the *Corngrass1* mutant where the juvenile to adult transition is severely delayed, the resistance to common rust is also delayed, which means juvenile leaves are more susceptible to the disease compared to adult leaves (Abedon and Tracy, 1996). Pataky and Campana (2007) demonstrated that in a survey of disease reactions among sweet corn hybrids, those containing the *Rp1-D* gene show reduced common rust severity when the frequency of virulent isolates is less than 40%. A possible explanation for the changes in rust susceptibility between juvenile and adult leaves may be found in our microarray data, which indicated that *Rp1-D* expression is 6-8 fold higher in *gl15* mutants compared to the wild-type, indicating *Rp1-D* is more strongly expressed in adult leaves. .

Future research

While our proposed model explains very well how *Glossy15* conditions juvenile leaf identities, future research should focus on identifying the C_{32} aldehyde reductase gene in maize. An interesting glossy mutant in this respect is *glossy5*, a supposed duplicate gene with *glossy20*, because only the double mutation *gl5, gl20* shows glossy phenotypes (Schnable et al., 1994). While in wild-type maize plant, the dominant primary alcohols are C_{32}, in the *glossy5* mutant, C_{24}, C_{26} and C_{28} primary alcohols

accumulate. This altered wax composition indicates the functional *Glossy5* gene is responsible for the conversion of C_{30} and C_{32} aldehyde into C_{30} and C_{32} primary alcohols (Bianchi et al., 1978), a function of C_{32} aldehyde reductase. *Gl5* in maize has been mapped to short arm of Chromosome 4 (196.0, IBM 2008 neighbors 4), between markers *tasselseed5* (*ts5*) and *benzoxazinone synthesis7* (*bx7*) (Maizegdb.com). The physical distance between the *mmp111* and *bx7* markers flanking *Gl5* is approximately 240 kb (Wei et al., 2009), which following a blast2go online analysis (blast2go.org) harbors 5-6 predicted proteins beyond transposons and retrotransposons. Populations segregating for *gl5, gl20* and *gl15* in the common B73 background are available in Moose lab. It should be possible to design additional markers and use them to genotype these populations to identify co-segregation between the predicted proteins within the interval and the *gl5* mutant.

References

Abedon, B.G., and W.F. Tracy. 1996. Corngrass1 of maize (Zea mays L) delays development of adult plant resistance to common rust (Puccinia sorghi Schw) and European corn borer (Ostrinia nubilalis hubner). Journal of Heredity 87:219-223.

Avato, P. 1987. Chemical genetics of epicuticular wax formation in maize. Plant Physiol. Biochem. 25: 179-190.

Bianchi, G., P. Avato and F. Salamini. 1978. Glossy mutants of maize. VIII. Accumulation of fatty aldehydes in surface waxes of gl5 maize seedlings. Biochemical genetics 16: 1015-1021.

Bianchi, G, P. Avato and F. Salamini. 1979. Glossy mutants of maize. IX. Chemistry of *Glossy4, Glossy8, Glossy15* and *Glossy18* surface waxes. Heredity 42 (3), 391-395.

Bianchi, G., Avato, P. and F. Salamini. 1984. Surface waxes from grain, leaves, and husks of maize (Zea mays L.). Cereal Chem. 61: 45-47.

Blaker, T.W. and R.I. Greyson. 1988. Developmental variation of leaf surface wax of maize, *Zea mays*. Can. J. Bot. 66: 839-846.

Chuck, G., R. Meeley, E. Irish, H. Sakai, and S. Hake. 2007. The maize tasselseed4 microRNA controls sex determination and meristem cell fate by targeting Tasselseed6/indeterminate spikelet1. Nature Genetics 39:1517-1521.

Evans, M.M.S., H.J. Passas, and R.S. Poethig. 1994. Heterochronic Effects of Glossy15 Mutations on Epidermal-Cell Identity in Maize. Development 120:1971-1981.

Lauter, N., A. Kampani, S. Carlson, M. Goebel, and S.P. Moose. 2005. microRNA172 down-regulates glossy15 to promote vegetative phase change in maize. Proceedings of the National Academy of Sciences of the United States of America 102:9412-9417.

Liu, S.Z., C.R. Dietrich, and P.S. Schnable. 2009. DLA-Based Strategies for Cloning Insertion Mutants: Cloning the gl4 Locus of Maize Using Mu Transposon Tagged Alleles. Genetics 183:1215-1225.

Millar, A.A., S. Clemens, S. Zachgo, E.M. Giblin, D.C. Taylor, and L. Kunst. 1999. CUT1, an arabidopsis gene required for cuticular wax biosynthesis and pollen fertility, encodes a very-long-chain fatty acid condensing enzyme. Plant Cell 11:825-838.

Moose, S.P., and P.H. Sisco. 1994. Glossy15 Controls the Epidermal Juvenile-to-Adult Phase-Transition in Maize. Plant Cell 6:1343-1355.

Moose, S.P., and P.H. Sisco. 1996. Glossy15, an APETALA2-like gene from maize that regulates leaf epidermal cell identity. Genes & Development 10:3018-3027.

Moose, S.P. 1995. Molecular genetic analysis of the maize *Glossy15* gene and the control of juvenile versus adult leaf identity. Ph.D. dissertation, North Carolina State University.

Moose, S.P., N. Lauter, and S.R. Carlson. 2004. The maize macrohairless1 locus specifically promotes leaf blade macrohair initiation and responds to factors regulating leaf identity. Genetics 166:1451-1461.

Nole-Wilson, S., and B.A. Krizek. 2001. DNA binding properties of the Arabidopsis floral development protein AINTEGUMENTA (vol 28, pg 4076, 2000). Nucleic Acids Research 29:U6-U6.

Pataky, J.K., and M.A. Campana. 2007. Reduction in common rust severity conferred by the Rp1D gene in sweet corn hybrids infected by mixtures of Rp1D-virulent and avirulent Puccinia sorghi. Plant Disease 91:1484-1488.
Samuels, L., Kunst, L. and R. Jetter. 2008. Sealing plant surfaces: cuticular wax formation by epidermal cells. Annu. Rev. Plant Biol. 59: 683-707.
Schnable, PS, PS Stinard, TJ Wen, S Heinen, D Weber, L Zhang, JD Hansen, BJ Nikolau. 1994. The genetics of cuticular wax biosynthesis. Maydica 39:279-287.
Strable, J., L. Borsuk, D. Nettleton, P.S. Schnable, and E.E. Irish. 2008. Microarray analysis of vegetative phase change in maize. Plant Journal 56:1045-1057.
Sturaro, M., Hartings, H., Schmelzer, E., Velasco, R., Salamini, F. and M. Motto. 2005. Cloning and characterization of GLOSSY1, a maize gene involved in cuticle membrane and wax production. Plant Physiol. 138: 478-489.
Tacke, E., C. Korfhage, D. Michel, M. Maddaloni, M. Motto, S. Lanzini, F. Salamini, and H.P. Doring. 1995. Transposon tagging of the maize Glossy2 locus with the transposable element En/Spm. Plant Journal 8:907-917.
Van Houte, B.P.P., T.W. Binsl, H. Hettling, and J. Heringa. 2010. CGHnormaliter: a Bioconductor package for normalization of array CGH data with many CNAs. Bioinformatics 26:1366-1367.
Wei, F.S., J.W. Zhang, S.G. Zhou, R.F. He, M. Schaeffer, K. Collura, D. Kudrna, B.P. Faga, M. Wissotski, W. Golser, S.M. Rock, T.A. Graves, R.S. Fulton, E. Coe, P.S. Schnable, D.C. Schwartz, D. Ware, S.W. Clifton, R.K. Wilson, and R.A. Wing. 2009. The Physical and Genetic Framework of the Maize B73 Genome. Plos Genetics 5:-.
Wu, G., and R.S. Poethig. 2006. Temporal regulation of shoot development in Arabidopsis thaliana by miR156 and its target SPL3. Development 133:3539-3547.
Wu, G., M.Y. Park, S.R. Conway, J.W. Wang, D. Weigel, and R.S. Poethig. 2009. The Sequential Action of miR156 and miR172 Regulates Developmental Timing in Arabidopsis. Cell 138:750-759.
Xu, X., C.R. Dietrich, M. Delledonne, Y. Xia, T.J. Wen, D.S. Robertson, B.J. Nikolau, and P.S. Schnable. 1997. Sequence analysis of the cloned glossy8 gene of maize suggests that it may code for a beta-ketoacyl reductase required for the biosynthesis of cuticular waxes. Plant Physiol 115:501-10.
Xu, X., Dietrich, C.R., Lessire, R., Nikolau, B.J. and P.S. Schnable. 2002. The endoplasmic reticulum-associated maize GL8 protein is a component of the acyl-coenzyme A elongase involved in the production of cuticular waxes. Plant Physiol. 115: 501-510.

Table 5.1: Differentially expressed genes in *gl15-H* mutant compared to wildtype at 9 DAS shoot apical meristems (P<0.01, M>1 or <-1, A>7.0). Yellow lighted genes with at least 4 fold difference between wildtype and *gl15* mutant.

ID	TC19	Putative_Annotation	M	A	P.Value
MZ00034210	TC458530	cellulose synthase-5 {Zea mays;}	-5.2	7.6	0.0064
MZ00024269	TC468573	proline-rich protein	-4.6	10.9	0.0000
MZ00027625	TC484956	probable cinnamoyl-CoA reductase	-4.2	6.9	0.0066
MZ00040420	CF627793	CSLE1	-3.8	8.5	0.0001
MZ00036403	TC468573	proline-rich protein	-3.6	13.6	0.0001
MZ00030588	TC474238	putative fatty acid condensing enzyme CUT1	-3.5	7.5	0.0002
MZ00020354	TC476311	putative UDP-glucoronosyl and UDP-glucosyl transferase	-3.2	7.6	0.0028
MZ00050768	TC532803	esterase/lipase/thioesterase family protein	-2.9	8.4	0.0075
MZ00041611	TC504542	Nonspecific lipid-transfer protein precursor (LTP)	-2.8	13.2	0.0007
MZ00008140	CD947371	similar to polyprotein	-2.8	7.0	0.0032
MZ00002722	TC505652	putative fatty acyl coA reductase	-2.7	7.6	0.0009
MZ00032386	TC458385	APETALA2-like protein Glossy15 - maize	-2.6	8.7	0.0000
MZ00027767	TC459165	naringenin 3-dioxygenase	-2.4	8.3	0.0020
MZ00041613	TC506799	Nonspecific lipid-transfer protein precursor (LTP)	-2.4	10.9	0.0038
MZ00027768	TC468741	naringenin 3-dioxygenase (EC 1.14.11.9)	-2.3	7.4	0.0002
MZ00036806	TC459398	OSJNBa0006B20.16	-2.2	12.8	0.0015
MZ00022573	TC476414	hypothetical protein F14F8_120 - Arabidopsis thaliana	-2.1	7.3	0.0004
MZ00006202	TC510496	putative cell death associated protein	-2.0	9.4	0.0053
MZ00049111	TC472557	homeodomain protein-like	-2.0	7.6	0.0061
MZ00024057	TC480419	lipid transfer protein-like protein	-2.0	7.0	0.0021
MZ00049288	EE042770	receptor kinase-like protein - Arabidopsis thaliana	-2.0	7.0	0.0076
MZ00000358	AI372191	probable trypsin inhibitor	-1.9	8.4	0.0053
MZ00004710	TC461136	nodulin-like protein	-1.9	7.3	0.0001
MZ00002048	TC545348	putative formylglycinamide ribonucleotide amidotransferase	-1.9	7.9	0.0061
MZ00040577	TC475157	globulin-1	-1.8	8.3	0.0007

Table 5.1 (Continued):

ID	TC19	Putative_Annotation	M	A	P.Value
MZ00002817	FL431912	Putative AMP-binding protein	-1.7	7.0	0.0043
MZ00018473	TC458214	putative laccase	-1.7	8.2	0.0087
MZ00013928	TC460500	probable trypsin inhibitor - maize {Zea mays;}	-1.7	11.6	0.0099
MZ00024150	TC527539	NADP-dependent malic enzyme, chloroplast precursor	-1.7	11.4	0.0060
MZ00041757	TC524834	putative low molecular mass early light-induced protein,chloroplast precursor (ELIP)	-1.7	11.3	0.0034
MZ00049141	TC461903	putative bHLH transcription factor	-1.7	7.1	0.0022
MZ00014004	TC513453	Probable U3 small nucleolar RNA-associated protein 11	-1.7	7.8	0.0030
MZ00016604	TC540927	U2 snRNP auxiliary factor, small subunit	-1.6	8.3	0.0082
MZ00049993	TC463832	Proline-rich protein APG isolog	-1.6	7.9	0.0051
MZ00020437	TC467040	O-methyltransferase ZRP4 (EC 2.1.1.-) (OMT)	-1.6	8.0	0.0014
MZ00021224	TC526373	flagelliform silk protein	-1.6	9.3	0.0081
MZ00042848	TC501209	ABA- and ripening-inducible-like protein	-1.5	9.0	0.0023
MZ00027338	TC514383	abscisic stress ripening protein homolog	-1.5	8.7	0.0033
MZ00043234	CF009470	profilin 2	-1.5	7.2	0.0077
MZ00040565	NP003964	phospholipid transfer protein 6B6	-1.5	13.8	0.0063
MZ00007760	TC524443	heat shock factor RHSF5	-1.4	7.6	0.0091
MZ00023087	TC473930	contains EST C73720(E20258) hypothetical protein	-1.4	9.4	0.0074
MZ00026446	TC494593	putative actin interacting protein	-1.4	8.2	0.0037
MZ00052439	TC494030	expansin-like protein	-1.4	7.7	0.0032
MZ00030461	TC459159	similar to Arabidopsis thaliana chromosome 2, T8P21.12 unknown protein	-1.3	7.4	0.0021
MZ00027606	TC471141	similar to Arabidopsis thaliana chromosome 2 ,At2g41250	-1.3	7.7	0.0094
MZ00025920	TC484161	one helix protein	-1.3	12.2	0.0033
MZ00037309	BM501448	putative calcium-dependent protein kinase	-1.3	7.3	0.0039
MZ00033732	TC461077	At3g16370/MYA6_18	-1.3	7.8	0.0025
MZ00028093	TC460389	putative salicylate-induced glucosyltransferase	-1.3	8.1	0.0050

Table 5.1 (Continued):

ID	TC19	Putative_Annotation	M	A	P.Value
MZ00004156	BG837741	beta glucanase	-1.3	8.4	0.0093
MZ00015084	TC494279	putative NPH3 family protein (with alternative splicing)	-1.2	7.5	0.0057
MZ00046720	TC501625	putative formin-like protein	-1.2	7.4	0.0056
MZ00017814	TC474349	putative alcohol dehydrogenase	-1.2	8.5	0.0089
MZ00025768	TC532672	glutathione S-transferase GST 20	-1.2	10.1	0.0094
MZ00026554	TC464066	putative carbonate dehydratase	-1.2	8.1	0.0026
MZ00043645	TC479770	heme oxygenase 1	-1.2	11.7	0.0087
MZ00000261	TC500240	probable acyl-CoA synthetase	-1.1	8.2	0.0032
MZ00050051	TC513633	putative geranylgeranyl diphosphate synthase	-1.1	7.8	0.0094
MZ00029735	TC524967	beta-adaptin-like protein A	-1.1	7.7	0.0058
MZ00035433	TC488238	protein phosphatase 2C homolog F11C18.60	-1.1	7.0	0.0091
MZ00047690	TC482658	probable prolylcarboxypeptidase	-1.1	7.7	0.0045
MZ00007895	EE020545	putative PTH-2, resistance gene (PTO kinase) homologs	-1.1	8.1	0.0064
MZ00044906	TC494622	zinc finger transcription factor-like protein	-1.1	7.8	0.0077
MZ00054898	TC479477	putative GTP-binding protein	-1.0	7.2	0.0053
MZ00019925	TC462901	OSJNBa0064H22.28	-1.0	10.3	0.0046
MZ00020779	TC462121	polygalacturonase-inhibitor protein	-1.0	9.5	0.0049
MZ00020791	AW519861	RING zinc finger protein hypothetical protein	-1.0	7.6	0.0089
MZ00050046	TC510062	putative protein serine/threonine kinase	1.0	8.0	0.0070
MZ00033481	TC466519	putative CR4	1.0	9.7	0.0039
MZ00013755	TC541397	thioredoxin H	1.0	12.2	0.0041
MZ00018613	TC463613	putative MtN3	1.0	11.4	0.0083
MZ00011836	TC521002	fiber protein-like	1.1	7.5	0.0063
MZ00043114	TC547783	HMG-like nucleosome/chromatin assembly factor D	1.1	12.4	0.0096
MZ00023347	BE050639	hypothetical protein T22H22.2	1.1	7.2	0.0093
MZ00015482	TC482531	origin recognition complex subunit 1	1.1	9.7	0.0092

Table 5.1 (Continued):

ID	TC19	Putative_Annotation	M	A	P.Value
MZ00007679	CD447327	mutant 19 kDa S15P alpha-zein	1.1	7.5	0.0039
MZ00028014	TC501994	contains similarity to chromosome condensation protein gene_id:K12B20.9	1.2	8.9	0.0078
MZ00019196	TC516472	senescence-associated protein 5	1.2	10.5	0.0045
MZ00013802	TC534289	putative microtubial binding protein	1.2	7.5	0.0049
MZ00004059	TC473287	putative ribonucleoprotein	1.3	7.4	0.0081
MZ00007806	TC461964	putative sorbitol transporter	1.3	7.3	0.0047
MZ00001659	TC472784	putative myb/SANT domain protein	1.3	7.1	0.0057
MZ00034829	TC543849	NAD(P)H-quinone oxidoreductase chain 6	1.3	7.0	0.0071
MZ00036653	TC460127	probable germin protein 4 - rice	1.4	12.8	0.0093
MZ00004216	TC505725	DNA-binding protein-like protein	1.4	7.7	0.0055
MZ00005879	BQ538366	putative CBL-interacting protein kinase 23	1.4	7.0	0.0072
MZ00047936	TC459081	putative water stress induced tonoplast intrinsic protein	1.4	7.3	0.0093
MZ00036789	TC523093	probable cinnamoyl-CoA reductase	1.4	11.1	0.0011
MZ00047365	TC476322	putative peroxidase	1.6	8.3	0.0029
MZ00034098	TC530591	putative RING finger 1	1.6	7.6	0.0057
MZ00014560	TC460127	probable germin protein 4	1.6	10.0	0.0024
MZ00048046	TC460911	putative beta-amylase	1.7	7.4	0.0054
MZ00018506	TC499614	probable cinnamoyl-CoA reductase	1.7	8.9	0.0046
MZ00002139	EE187875	OSJNBb0040D15.7	1.8	7.3	0.0048
MZ00048021	FL472315	myosin heavy chain class VIII A2 protein	1.9	7.1	0.0078
MZ00024384	TC490394	probable cinnamoyl-CoA reductase	2.0	9.3	0.0017
MZ00046388	TC482975	putative amino-acid N-acetyltransferase	2.1	7.0	0.0037
MZ00040722	TC529726	opaque 2	2.3	7.0	0.0084
MZ00040944	TC496219	putative adapter protein ATH-55	2.4	8.3	0.0001
MZ00035182	TC477849	probable cinnamoyl-CoA reductase	2.5	11.1	0.0002
MZ00016495	TC530145	permatin precursor	2.6	7.3	0.0039

Table 5.1 (Continued):

ID	TC19	Putative_Annotation	M	A	P.Value
MZ00004101	TC460005	MYB transcription factor	2.6	7.0	0.0096
MZ00041276	TC466300	chitinase (EC 3.2.1.14) A	2.8	7.2	0.0004
MZ00040567	NP004048	rust resistance protein RP1-D homolog {Zea mays;}	2.8	7.4	0.0042
MZ00032651	TC499245	Putative ovule development protein antitegumenta (ANT)	2.9	7.1	0.0098
MZ00036113	BE051184	glucose starvation-induced protein precursor	2.9	7.1	0.0016
MZ00024775	TC512753	pyruvate decarboxylase {Zea mays;}	2.9	7.4	0.0078
MZ00027664	TC493570	putative CER1	3.1	8.7	0.0002
MZ00027248	TC468679	receptor-like protein kinase	3.6	7.6	0.0053
MZ00041127	TC533543	probable submergence induced, nickel-binding protein 2A - rice	5.4	8.9	0.0001
MZ00047300	TC503341	similar to Arabidopsis thaliana chromosome 5, MVP7.2;nodulin-like protein	6.0	7.2	0.0077
MZ00004148	TC511819	unknown protein	6.1	8.7	0.0029

Figure 5.1: Distribution of normalized fluorescent dye intensity for Maize Oligonucleotide Array proges in comparisons of *glossy15-H* and wild type shoot apex RNAs. Red grid lines marked areas with M>1 or <-1 and with A>7.0.

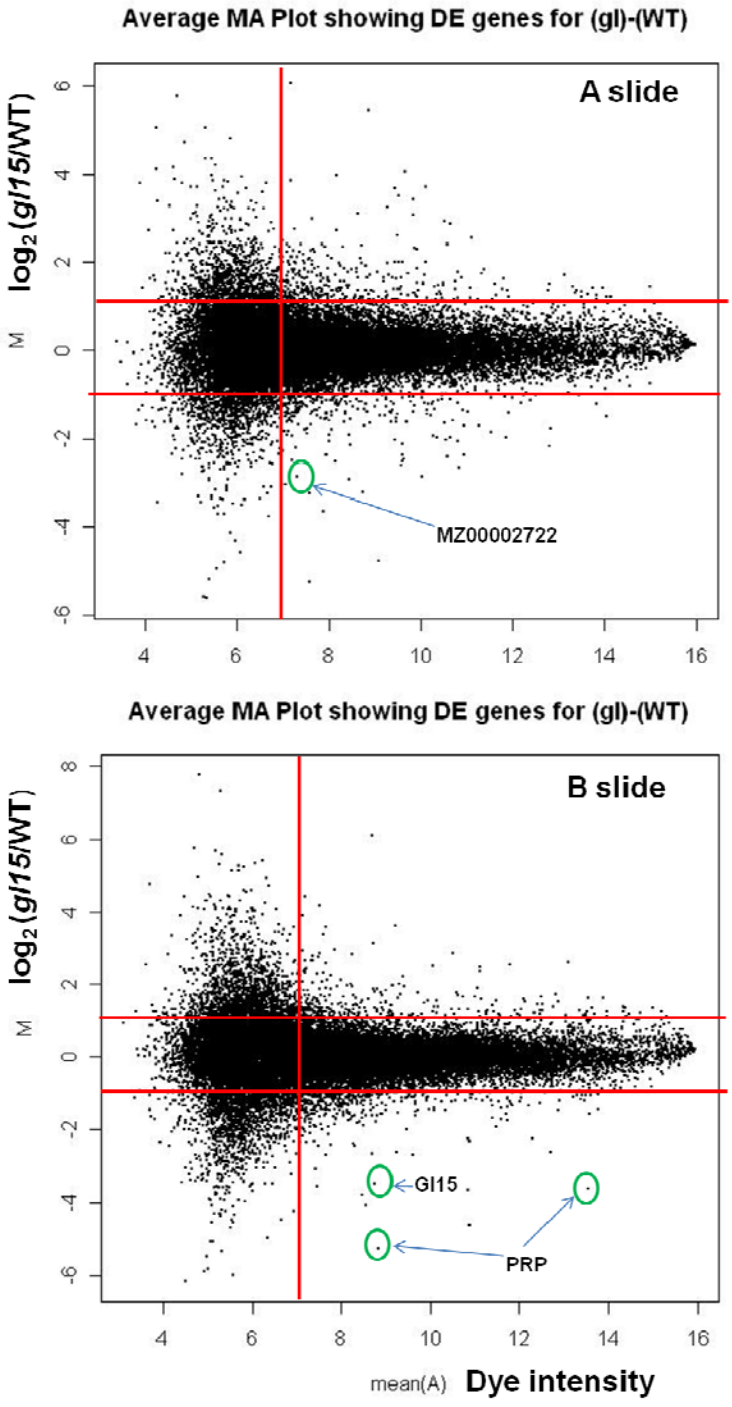


Figure 5.2: qPCR validation of selected differentially expressed genes from microarray comparison of wild-type and *gl15* mutant shoot apex RNAs sampled at 9 DAS.

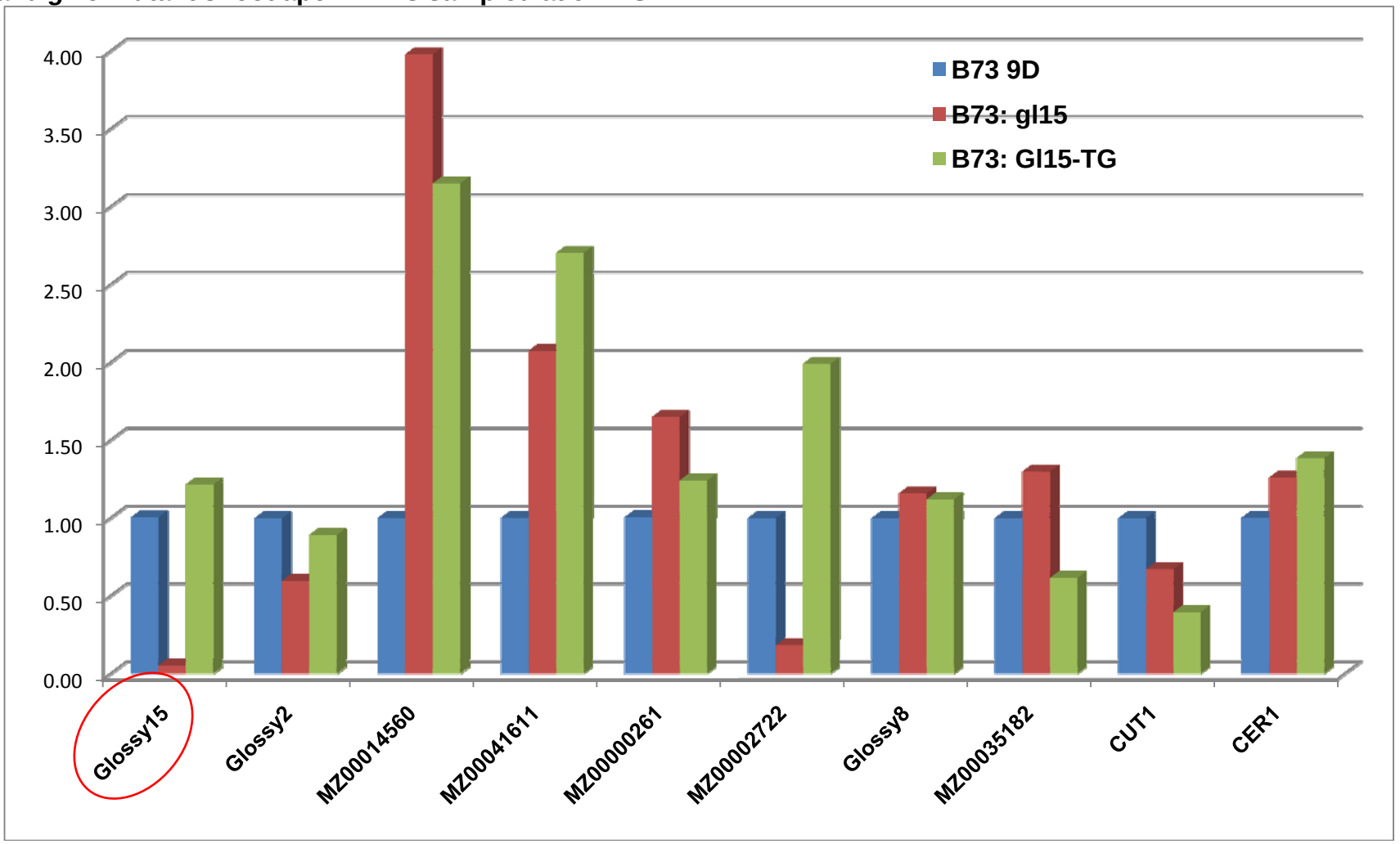


Figure 5.3: Wax composition of leaf 5 and leaf 10 in wildtype and *gl15* mutant (from S. Moose, 1995). Leaf 5 in wildtype W64A is a juvenile leaf and leaf 10 is an adult leaf.

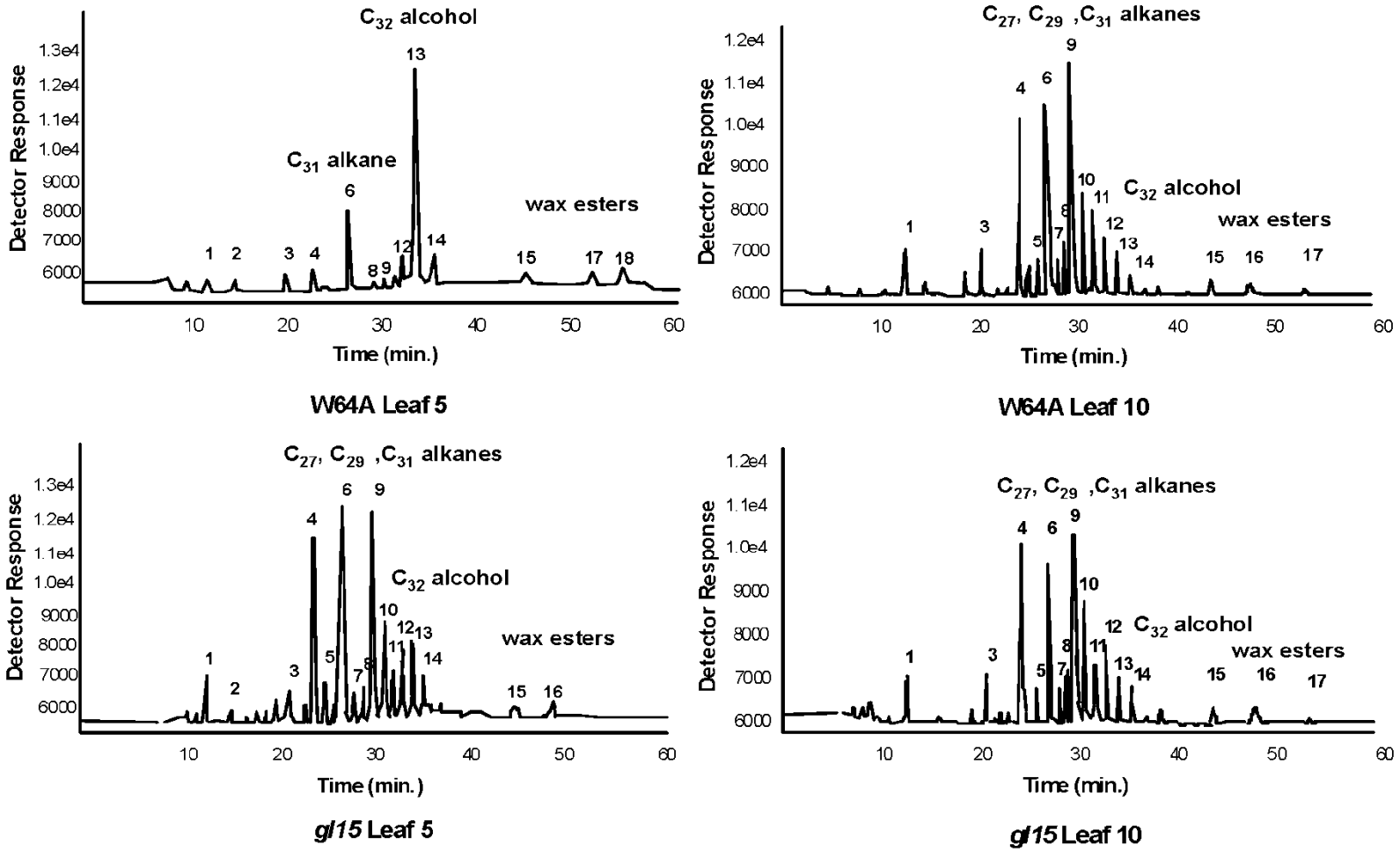
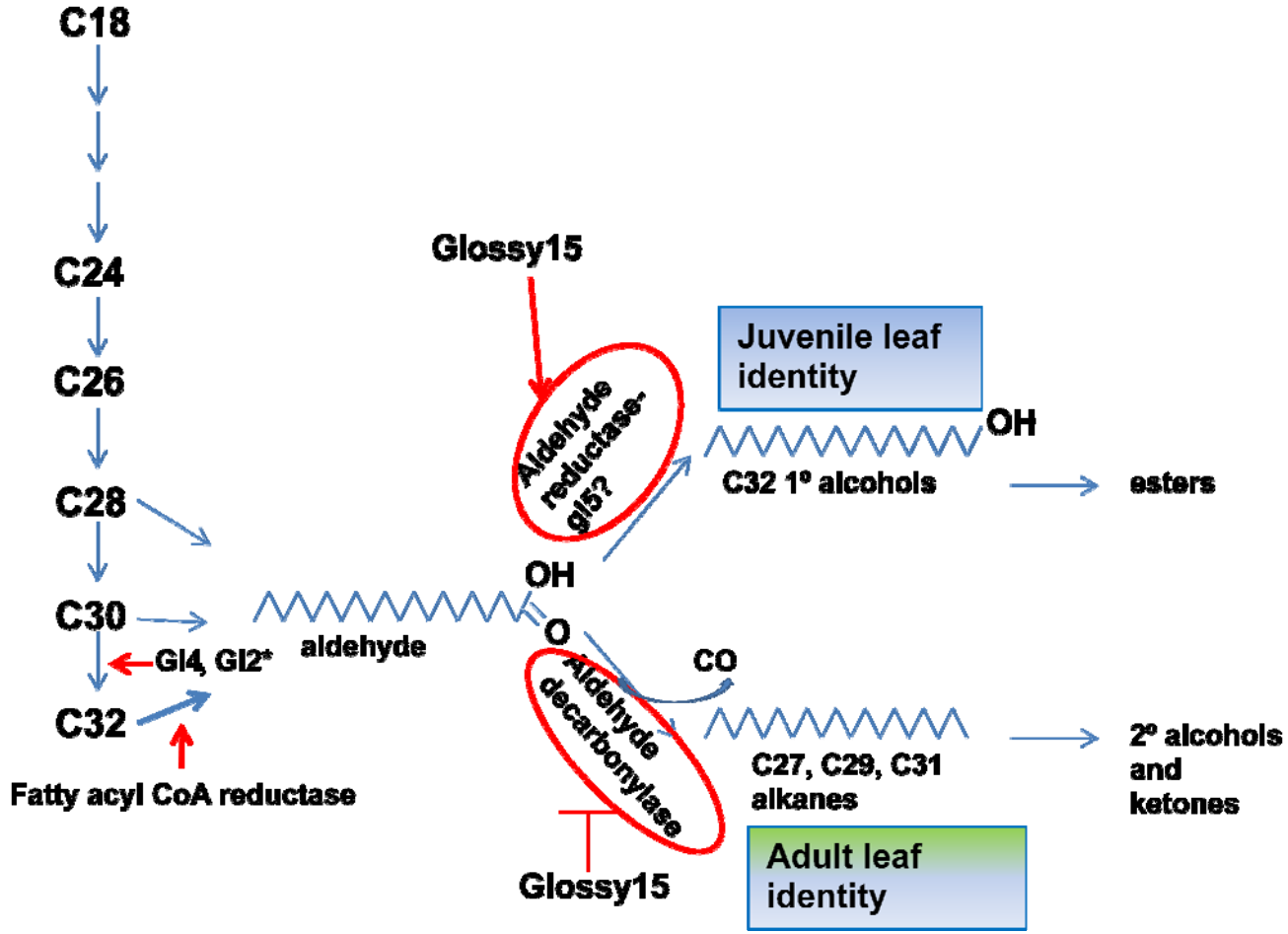


Figure 5.4: Proposed model of how *Glossy15* conditions juvenile versus adult leaf waxes: *Glossy15* could activate aldehyde reductase and repress aldehyde decarbonylase.



*Bianchi et al., 1979.